

SUPPORTING INFORMATION FOR:
**One-Step Synthesis of Favipiravir from Selectfluor® and 3-Hydroxy-2-
pyrazinecarboxamide in Ionic Liquid**

Germán Fuentes,^a María F. García,^b Hugo Cerecetto,^{a,b} Guzmán Álvarez,^{c*} Marcos Couto^{a*} and
Angel H. Romero^{a*}

^a*Grupo de Química Orgánica Medicinal, Instituto de Química Biológica, Facultad de Ciencias, Universidad de la República, 11400 Montevideo, Uruguay.*

^b*Area de Radiofarmacia, Centro de Investigaciones Nucleares, Facultad de Ciencias, Universidad de la República, Mataojo 2055, 11400 Montevideo, Uruguay.*

^c*Laboratorio de Moléculas Bioactivas, Departamento de Ciencias Biológicas, CENUR Litoral Norte, Universidad de la República, 60000 Paysandú, Uruguay.*

Table of Contents

1. Summary of Typical Strategies for Synthesis of Favipiravir.....	S2
2. General Considerations and Reaction Procedures.....	S5
2.1. General Information.....	S5
2.2. Synthesis of Intermediates.....	S6
2.3. Optimization Procedure for Favipiravir Synthesis.....	S12
2.4. Effect of Water.....	S14
2.5. Effect of Acid and Base in Aqueous Solution.....	S25
2.6. Effect of Fluorinating Agent.....	S33
2.7. Effect of Metallic Catalyst and Additives.....	S34

2.8. Effect of Energy Source.....	S36
2.9. Fluorination Comparison Under Different Selectfluor® Quantities	S37
2.10. Tautomeric Studies.....	S39
3. Mechanistic Experiments.....	S40
3.1. Reactions with Radical Scavengers.....	S40
4. Mini-Scalable and Gram-scalable Synthesis of Favipiravir.....	S48
5. References.....	S56

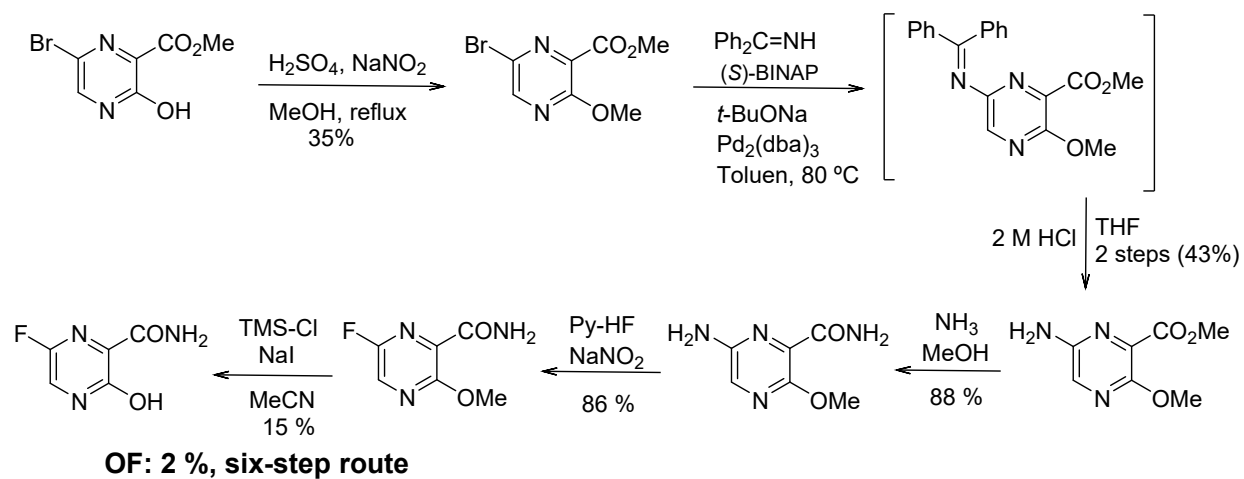
1. Summary of Typical Strategies for Synthesis of Favipiravir

The first strategy-route, developed by FUJIFILM Toyama Chemical Company in 2000, involved seven reaction steps from methyl 3-amino-6-bromopyrazine-2-carboxylate with a poor overall yield of 2 % (**route a** in Scheme 1A, **A** in Scheme 1S)¹⁻⁴ and serious limitation to scale. The second-generation strategy, also was developed by Toyama Company and the strategy consisted of five-step route from 3-hydroxypyrazine-2-carboxamide, which was scalable with a better overall yield of 17%, but two purifications by column chromatography were needed (**route b** in Scheme 1A, **B** in Scheme 1S).^{1,5} A improvements of the second-generation route provided a scalable six-step route to favipiravir in 33% yield with the use of the commercially available aminomalonic acid diamide (**route c** in Scheme 1A, **C** in Scheme S1).^{1,6} However, that second generation strategy involves the formation of a high skin irritant and volatile compound like 3,6-difluoropyrazine-2-carbonitrile, which required of the use of a special equipment for handling. Then, a third-generation route (nine-step route) was developed by Toyama in 2013, focusing on the construction of pyrazine core from simple and inexpensive starting materials such as ethyl diethoxyacetate and amino-acetonitrile with an overall yield of 9 %.^{1,6} Nevertheless, the multiple step-synthetic route (nine step-reaction), lower yield and unpractical isolation of their intermediates became to the third generation in a less attractive synthetic strategy than the second-generation route.

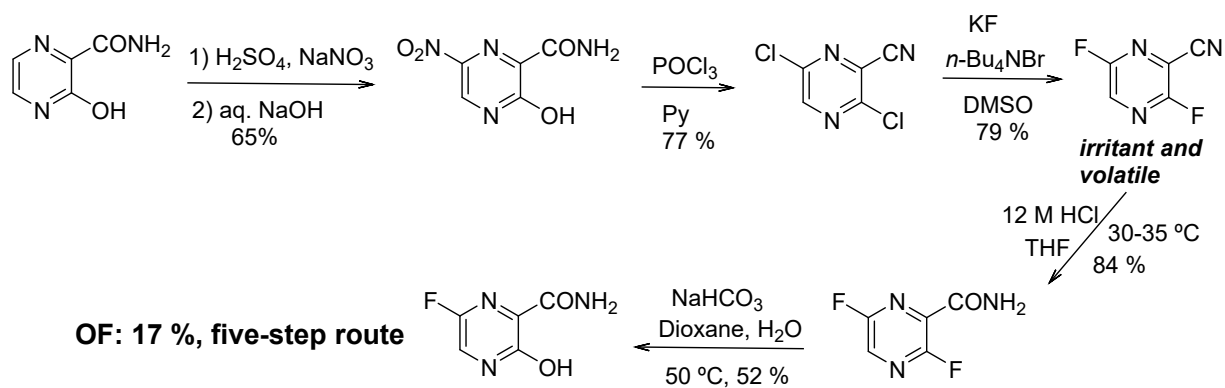
In general, the routes **a**, **b**, and **c**, that were developed between 2000 and 2013, are considered as the main synthetic strategies for the synthesis of favipiravir with scalable industrial production (Scheme 1S).¹ However, they involve multiple steps (five to seven steps) with poor or modest overall reaction yields (2 to 33 %) as well as multiple drawbacks including column

chromatography to purify intermediates, generation of toxic and volatile intermediate (*e.g.* 3,6-difluoropyrazine-2-carbonitrile, Scheme 1S), limitation to scale some reaction step, the use of unfriendly agents (*e.g.* Olha's reagent (pyridine-HF), phosphorous oxychloride) or high-cost catalyst (*e.g.* (*S*)-BINAP)) and the use of class II solvents (*e.g.* acetonitrile, methanol).¹ To minimize the mentioned disadvantages, some new strategies have been developed. Recently, J. Zheng and co-workers disclosed an attractive three-step strategy from 6-nitro-3-hydroxy-2-acetamidepyrazine (**route d**, Scheme 1A) with an overall yield by about 34 %.^{1,7} From the academy, six-step strategies with overall yields from 18 to 22 % have been developed (routes **e** and **f**, Scheme 1A).^{8,9} More advances are directed to the facile preparation of the 6-bromo-3-hydroxy-2-acetamidepyrazine intermediate or toward the facile conversion of 3,6-dichloropyrazine-2-carbonitrile to favipiravir to elude the skin irritant 3,6-fluoropyrazine-2-carbonitrile.¹

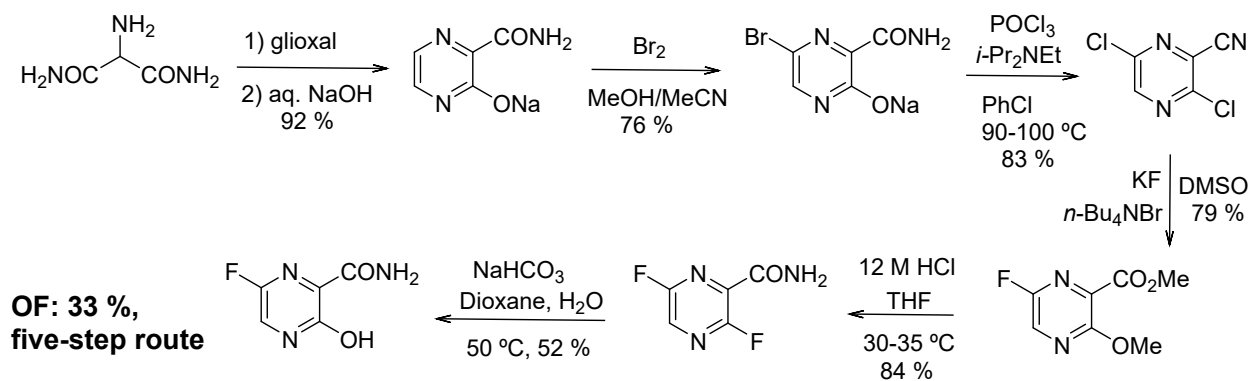
A) First generation Toyoma's strategy



B) Second generation Toyoma's strategy

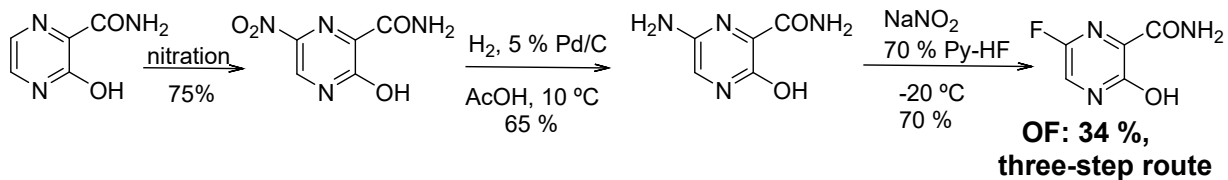


C) Second generation Nippon Soda-Toyoma's strategy

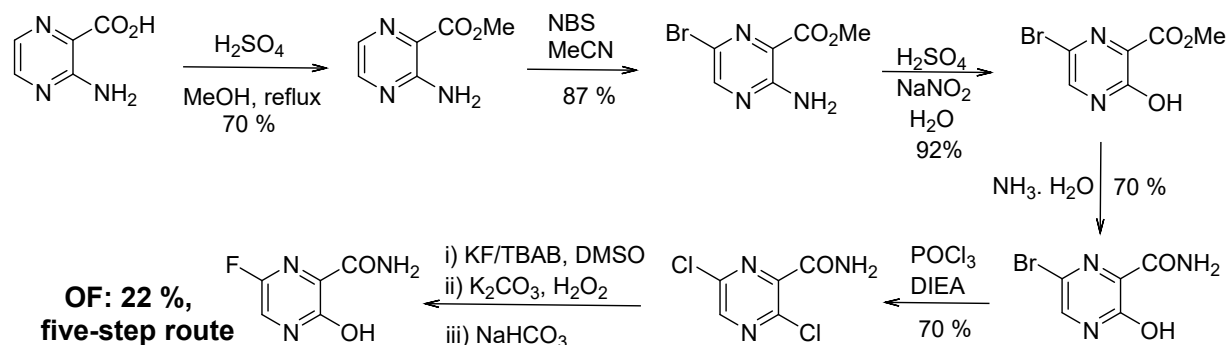


Scheme S1. First (A) and second (B and C) generation strategies for the synthesis of favipiravir.

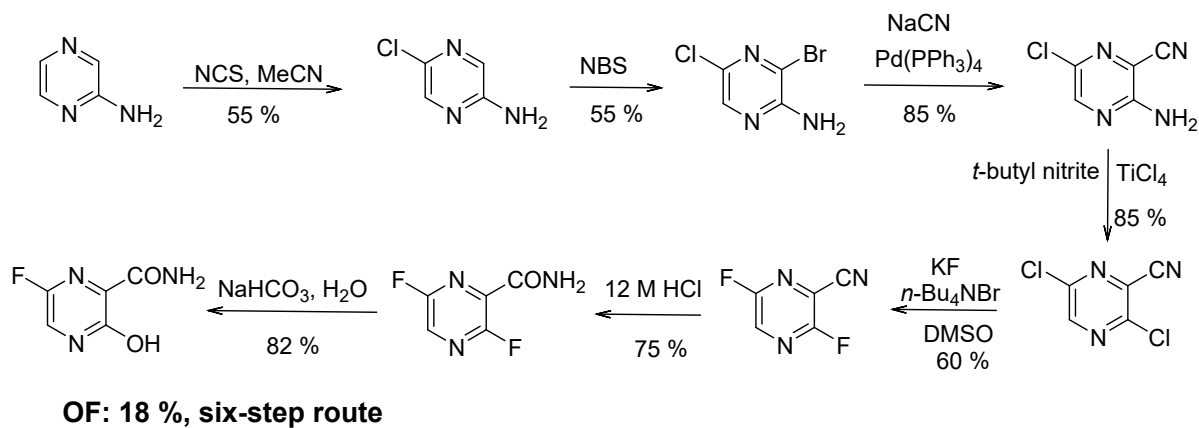
A) Route d of Chart 1 (Liu Feng, 2017)



B) Route d of Chart 1 (Liu Feng, 2017)



C) Route f of Chart 1 (Y. Xie, 2019)



Scheme S2. Detailed synthetic routes **d**, **e** and **f** for the synthesis of favipiravir shown in Scheme 1A.

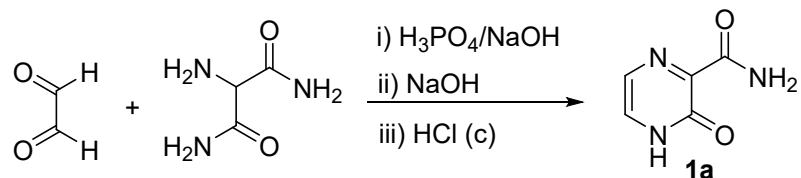
2. General Considerations and Reaction Procedures

2.1. General Information

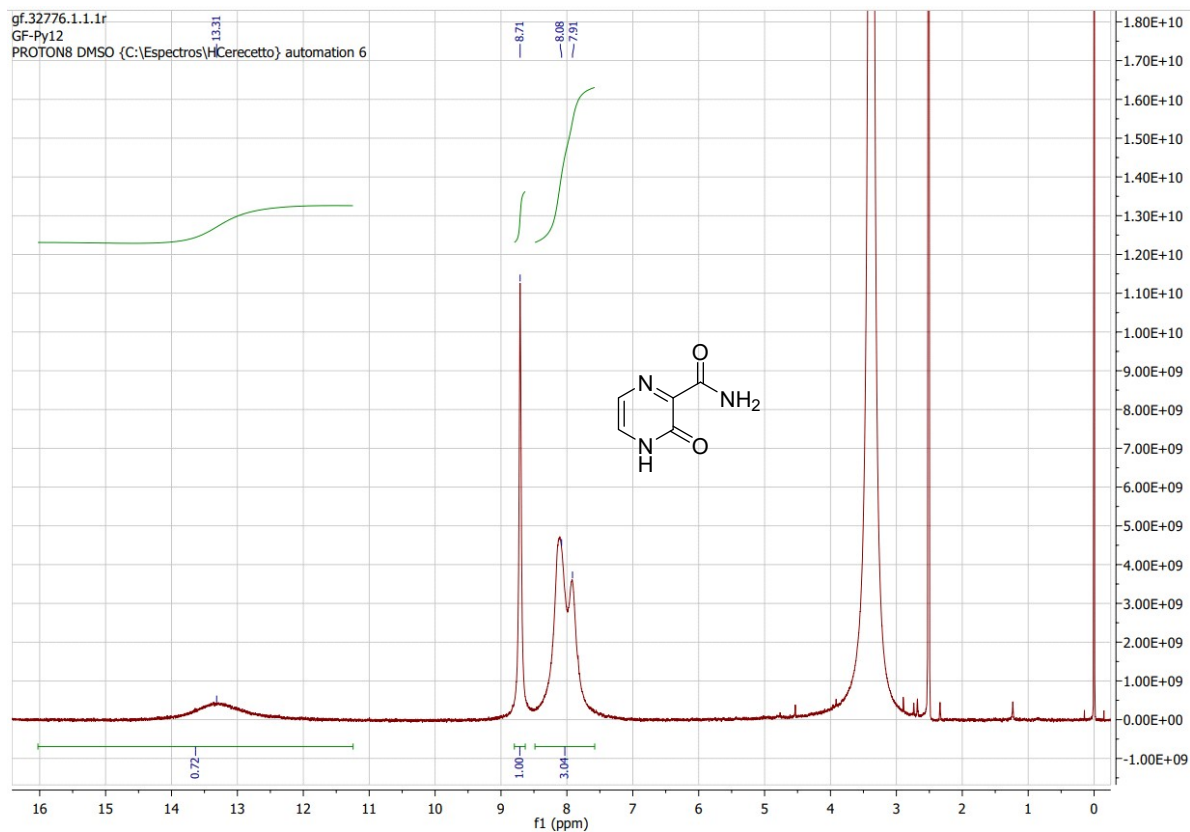
Reagents and solvents were purchased at the highest commercial quality and used without purification. Reactions were monitored by fluorometric measurements taken advantage on the high fluorescence of the favipiravir product.¹⁰ Maximum fluorescence was measured at 430 nm emission band upon 360 excitation band. Conversion percentage was determined from corresponding calibration curve of fluorescence for favipiravir. Fluorescence was recorded on a Thermo Scientific Varioskans Flash Multimode instrument for air-equilibrated solutions at 25 °C. Conversion percentage were corroborated HPLC-UV (Reverse phase-high performance liquid chromatography (RP-HPLC) on an Agilent 1200 Series Infinity Star equipped with GABI detector, a UV detector and a ThermoScientific Hypersil ODS reverse phase C18 column (300 mm × 4.6 × 10 microns). The measurements were performed using an isocratic mode (flow rate 1 mL/min) and mobile phase consisted of a mixture of phosphate buffer 0.05 M, *pH* 5.1 (40 %) and acetonitrile (60 %). The injection volume was 30 µL and, the detection was performed at a wavelength of 340 nm. The reaction yields percent are derived from two separated experiments. NMR spectra were recorded on a 400 MHz NMR-spectrometer (Bruker-400) and calibrated using residual undeuterated solvent as an internal reference (**CDCl₃**: ¹H-NMR: 7.26 ppm, ¹³C-NMR: 77.16 ppm; **DMF-D₇**: ¹H-NMR: 8.04 ppm (CH) and 2.93/2.77 (CH₃), ¹³C-NMR: 166.22 and 34.66/29.58 ppm; **D₂O**: ¹H-NMR: 4.60 ppm; **CD₃OD**: ¹H-NMR: 4.63 (OH) and 3.32 (CH₃) ppm, ¹³C-NMR: 47.60 ppm); **acetone-d₆**: ¹H-NMR: 2.07 ppm, ¹³C-NMR: 205.57 and 28.94 ppm). NMR spectroscopy data was obtained either from 1D-experiments such as ¹H-NMR, ¹³C-NMR, ¹⁹F-NMR or from 2D experiments such as ¹H/¹H-COSY, ¹H/¹³C-HSQC, ¹H/¹³C-HMBC, ¹H/¹⁹F-HETEROCOSY, ¹H/¹⁵N-HMBC. Multiplicity is indicated as follows: s (singlet), d (doublet), t (triplet), m (multiplet), dd (doublet of doublets), brs (broad singlet); chemical shifts were measured in parts per million (δ) and coupling constant (*J*) are given in Hz. The mass spectra (MS) were recorded on a Shimadzu DI-2010 instrument using the electron impact mode (70 eV ionizing voltage). Mass spectra are presented as *m/z* (% rel int.).

2.2. Synthesis of Intermediates

2.2.1. Synthesis of 3-hydroxy-pyrazine-2-carboxamide **1a**¹¹



The starting pyrazine **1a** was prepared following a reported protocol with a few modifications.¹¹ 2-Amino malondiamida (2 g, 17.1 mmol, 1 eq) was added into a phosphate buffer solution (12 mL) constituted by 0.3 g of NaOH (7.5 mmol, 0.44 eq), 0.4 g de H₃PO₄ 85 % (4.1 mmol, 0.24 eq). Subsequently, NaOH (0.76 g, 19 mmol, 1.1 eq) dissolved in water (2 mL) and glioxal 40% (2.64 g, 45.5 mmol, 2.7 eq.) were added to the mixture. The reaction mixture was stirred at room temperature for 1 hour. Then, concentrated hydrochloric acid (0.5 mL) was added, the mixture was heated at 80 °C for 2 h. When the reaction was completed, hydrochloric acid (30 mL, 3 M) was added. The reaction was cooled at room temperature and the resulting precipitate was collected, dried in vacuum to give a beige solid (1.9 g, 80 %). The data matches those previously reported.¹ Rf.: 0.2 (AcOEt). M.p.: 247-250 °C (dec.) (Lit.¹ 251-253 °C). ¹H-NMR (400 MHz, DMSO-*d*₆): δ 7.80-8.30 (m, 3H); 8.71 (s, 1H); 13.36 (s, 1H). ¹³C-NMR (100 MHz, DMSO-*d*₆): δ 167.36; 159.68; 140.10 (CH); 130.24 (CH); 122.02. EI-MS ([M]⁺): 139.04. Found: 139.10.



Fig

ure S1. $^1\text{H-NMR}$ of starting 3-hydroxy-pyrazine-2-carboxamide **1a** in $\text{DMSO-}d_6$.

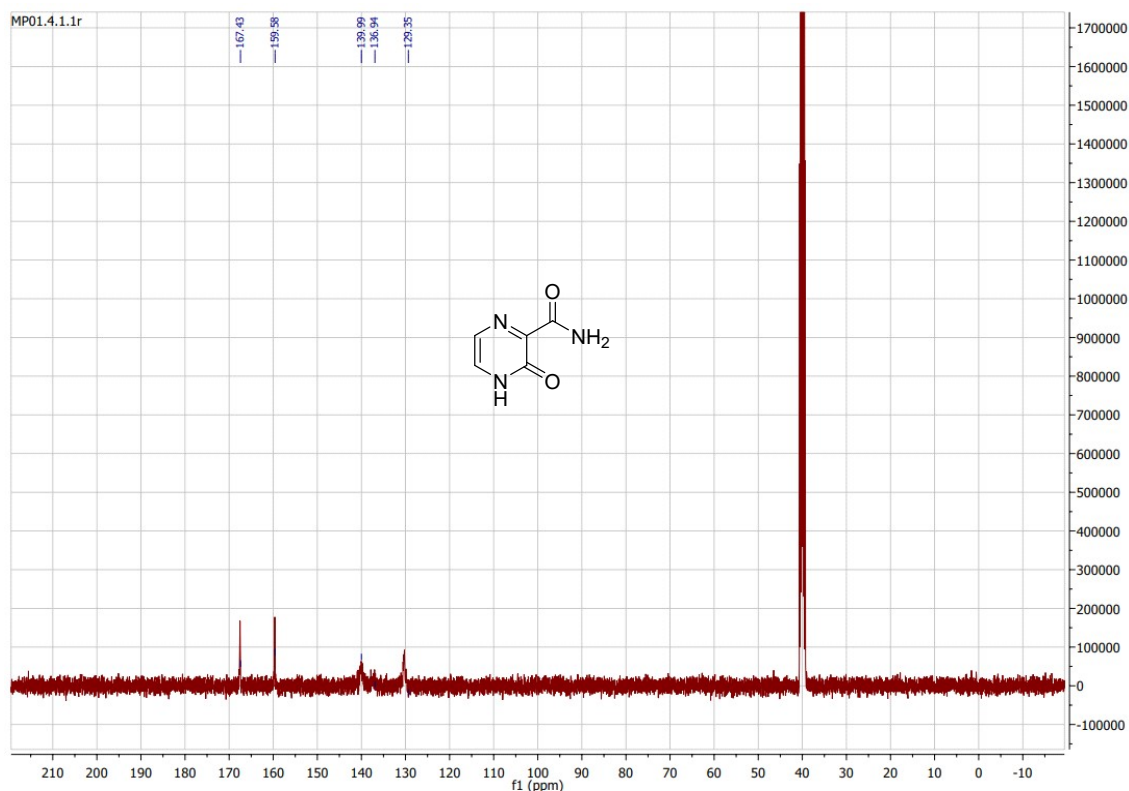


Figure S2. $^{13}\text{C-NMR}$ of starting 3-hydroxy-pyrazine-2-carboxamide **1a** in $\text{DMSO-}d_6$.

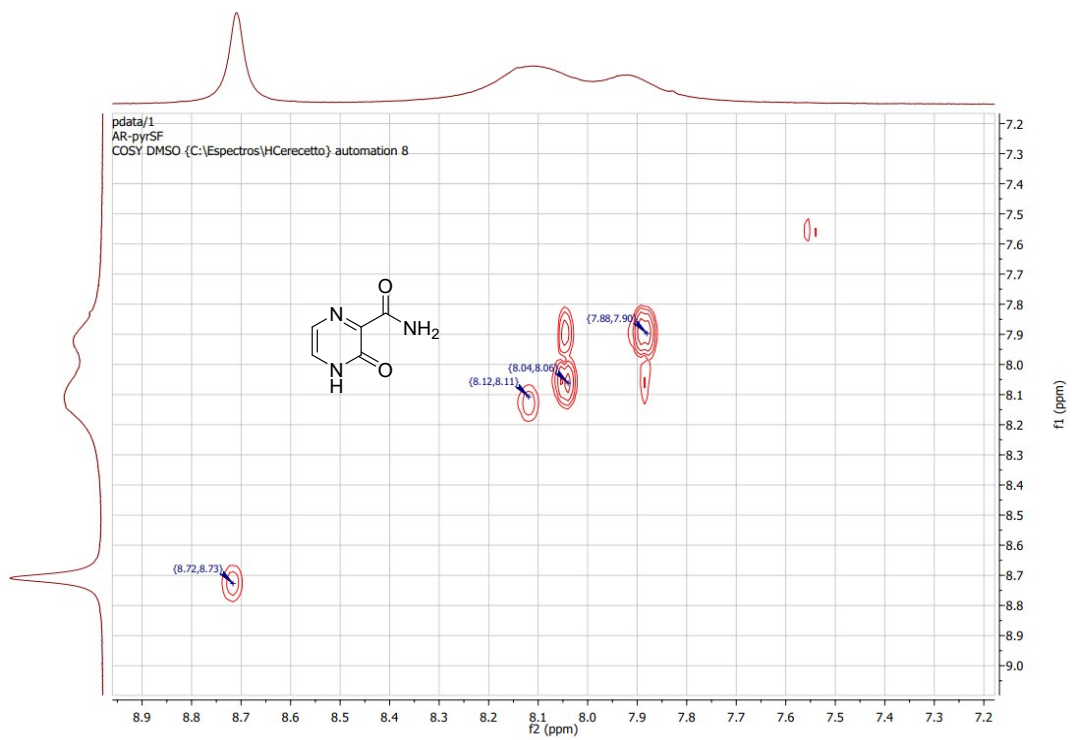


Figure S3. 2D- $^1\text{H}/^1\text{H}$ -COSY of 3-hydroxy-pyrazine-2-carboxamide **1a** in $\text{DMSO-}d_6$.

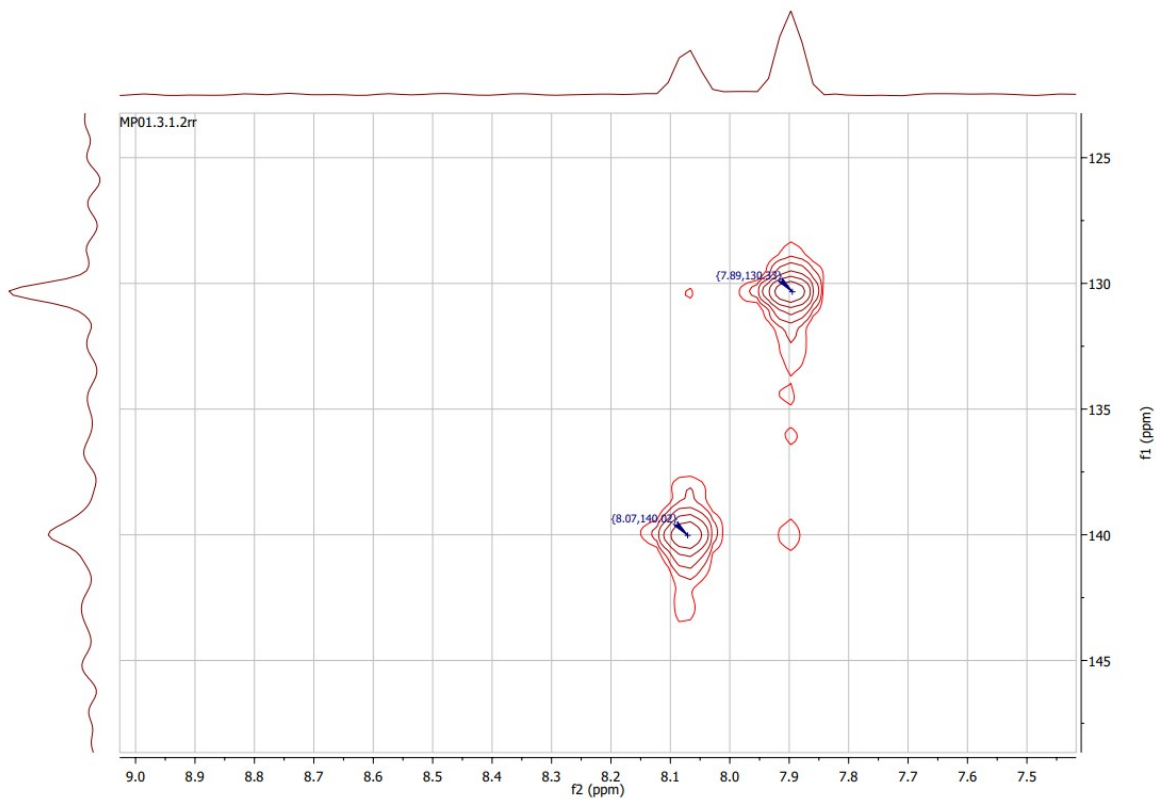
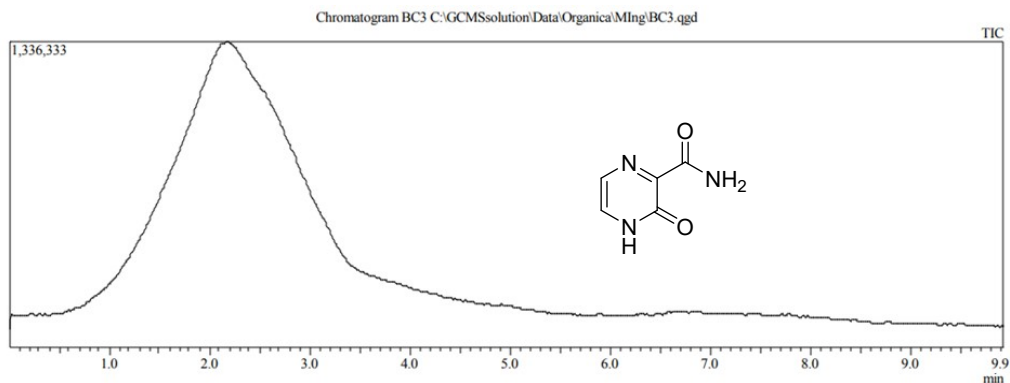
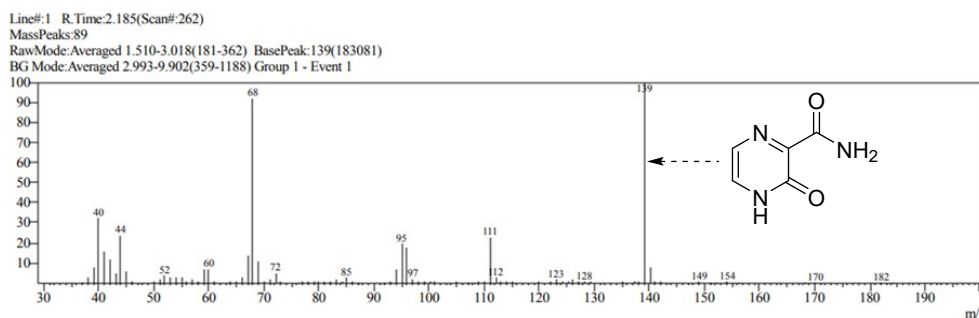


Figure S4. 2D- $^1\text{H}/^{13}\text{C}$ -HSQC of 3-hydroxy-pyrazine-2-carboxamide **1a** in $\text{DMSO-}d_6$.



Spectrum



Mass Tal

Line#:1 R.Time:2.185(Scan#:262)

MassPeaks:89

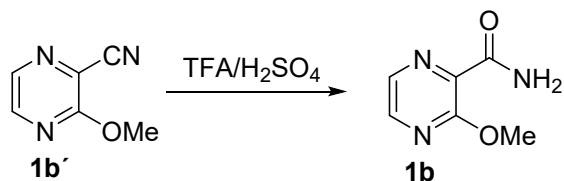
RawMode:Averaged 1.510-3.018(181-362) BasePeak:139(183081)

BG Mode:Averaged 2.993-9.902(359-1188) Group 1 - Event 1

#	m/z	Abs. Int.	Rel. Int.	#	m/z	Abs. Int.	Rel. Int.	#	m/z	Abs. Int.	Rel. Int.
1	37.05	185	0.10	22	61.00	560	0.31	43	86.05	501	0.27
2	38.00	5510	3.01	23	63.95	331	0.18	44	87.00	324	0.18
3	39.00	12955	7.08	24	65.00	1193	0.65	45	92.00	282	0.15
4	40.00	58853	32.15	25	66.00	4403	2.40	46	93.05	672	0.37
5	41.00	28820	15.74	26	67.05	24329	13.29	47	94.00	11920	6.51
6	41.95	20479	11.19	27	68.05	168528	92.05	48	95.00	35247	19.25
7	43.05	8919	4.87	28	69.00	19170	10.47	49	96.00	31254	17.07
8	43.95	43530	23.78	29	70.05	1385	0.76	50	97.05	3526	1.93
9	44.95	9946	5.43	30	71.05	3794	2.07	51	98.05	1624	0.89
10	45.95	549	0.30	31	72.05	9431	5.15	52	99.05	510	0.28
11	50.00	521	0.28	32	73.05	1494	0.82	53	100.05	803	0.44
12	51.00	3420	1.87	33	76.05	285	0.16	54	101.05	425	0.23
13	51.95	6826	3.73	34	77.05	1330	0.73	55	105.00	1161	0.63
14	52.95	4179	2.28	35	78.05	1009	0.55	56	107.10	279	0.15
15	53.95	5212	2.85	36	79.05	868	0.47	57	108.05	253	0.14
16	55.00	5312	2.90	37	80.05	383	0.21	58	109.05	1042	0.57
17	56.00	2043	1.12	38	81.10	1756	0.96	59	110.05	1115	0.61
18	57.00	2686	1.47	39	82.05	1003	0.55	60	111.05	41946	22.91
19	58.05	353	0.19	40	83.10	3796	2.07	61	112.05	4293	2.34
20	59.00	12128	6.62	41	84.05	899	0.49	62	113.05	538	0.29
21	60.00	12747	6.96	42	85.00	4362	2.38	63	114.10	1204	0.66
#	m/z	Abs. Int.	Rel. Int.	#	m/z	Abs. Int.	Rel. Int.	#	m/z	Abs. Int.	Rel. Int.
64	115.10	617	0.34	73	129.15	414	0.23	82	151.15	295	0.16
65	120.00	551	0.30	74	135.15	329	0.18	83	152.15	291	0.16
66	122.05	1550	0.85	75	137.15	398	0.22	84	154.15	490	0.27
67	123.05	2701	1.48	76	138.15	1857	1.01	85	156.15	197	0.11
68	124.10	517	0.28	77	139.10	183081	100.00	86	168.10	199	0.11
69	125.15	555	0.30	78	140.10	14214	7.76	87	170.15	226	0.12
70	126.10	2295	1.25	79	141.10	1350	0.74	88	182.10	202	0.11
71	127.15	449	0.25	80	142.15	332	0.18	89	184.10	232	0.13
72	128.15	1035	0.57	81	149.10	564	0.31				

Figure S5. Chromatogram, EI-MS spectrum and data of 3-hydroxy-pyrazine-2-carboxamide **1a**.

2.2.2. Synthesis of 3-(methoxy)pyrazine-2-carboxamide **1b**



The compound **1b** was prepared following a reported protocol with a few modifications.¹² A solution of 0.3 mmol of 3-methoxypyrazine-2-carbonitrile in a ca. 0.6 mL mixture of TFA-H₂SO₄ (4:1, v/v) was stirred either at room temperature. The progress of the reaction in each case was monitored by TLC analysis. After completion of the reaction, the reaction mixture was poured into ice-cold water. Then, reaction mixture was extracted with dichlorometane, and purified by a flash chromatography. The resulting solution was dried in vacuum to give a white solid (0.034 g, 85 %). Rf.: 0.9 (AcOEt). ¹H-NMR (400 MHz, CDCl₃): δ 8.30 (d, 1H, *J* = 8.0); 8.20 (s, 1H); 4.10 (s, 3H). ¹³C-NMR (100 MHz, CDCl₃): δ 164.95; 159.34; 144.37 (CH); 135.70 (CH); 133.70; 54.58 (CH₃).

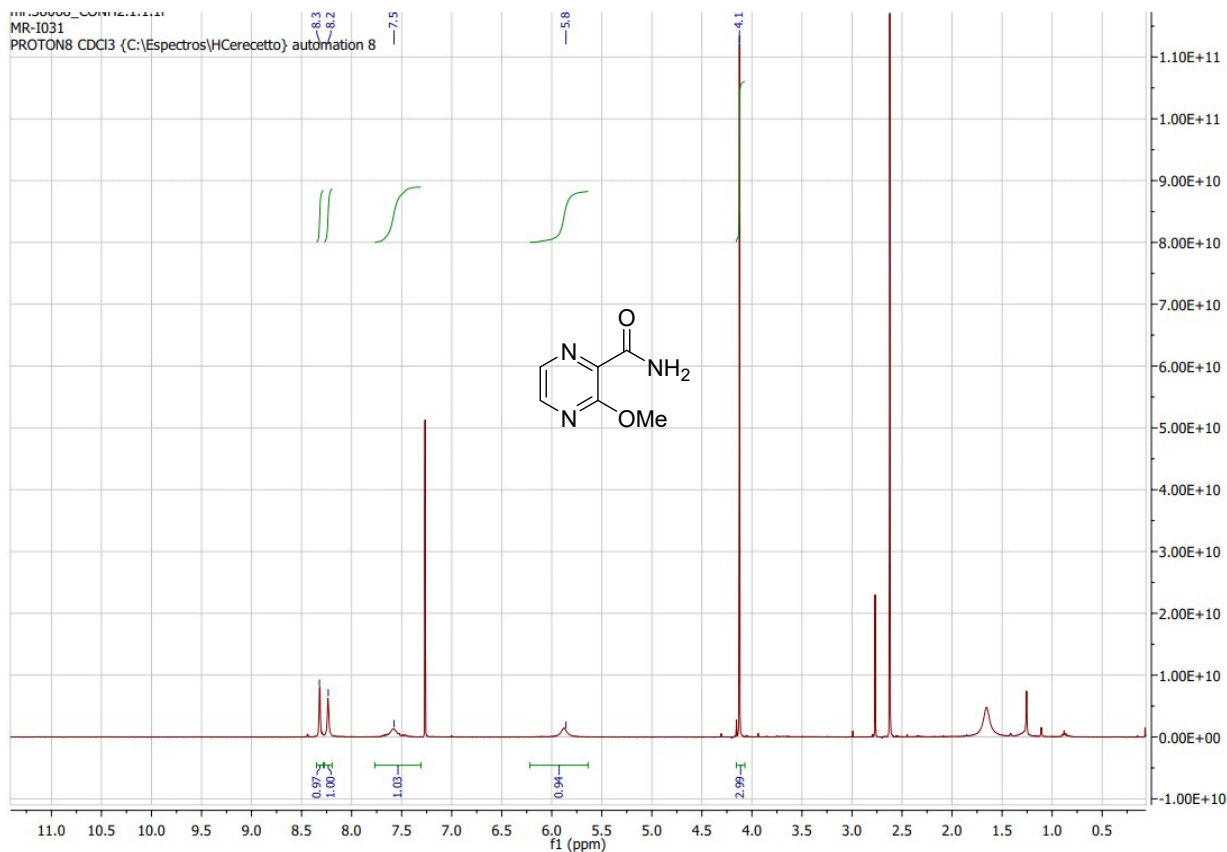


Figure S6. ¹H-NMR of 3-methoxy-pyrazine-2-carboxamide **1b** in CDCl₃.

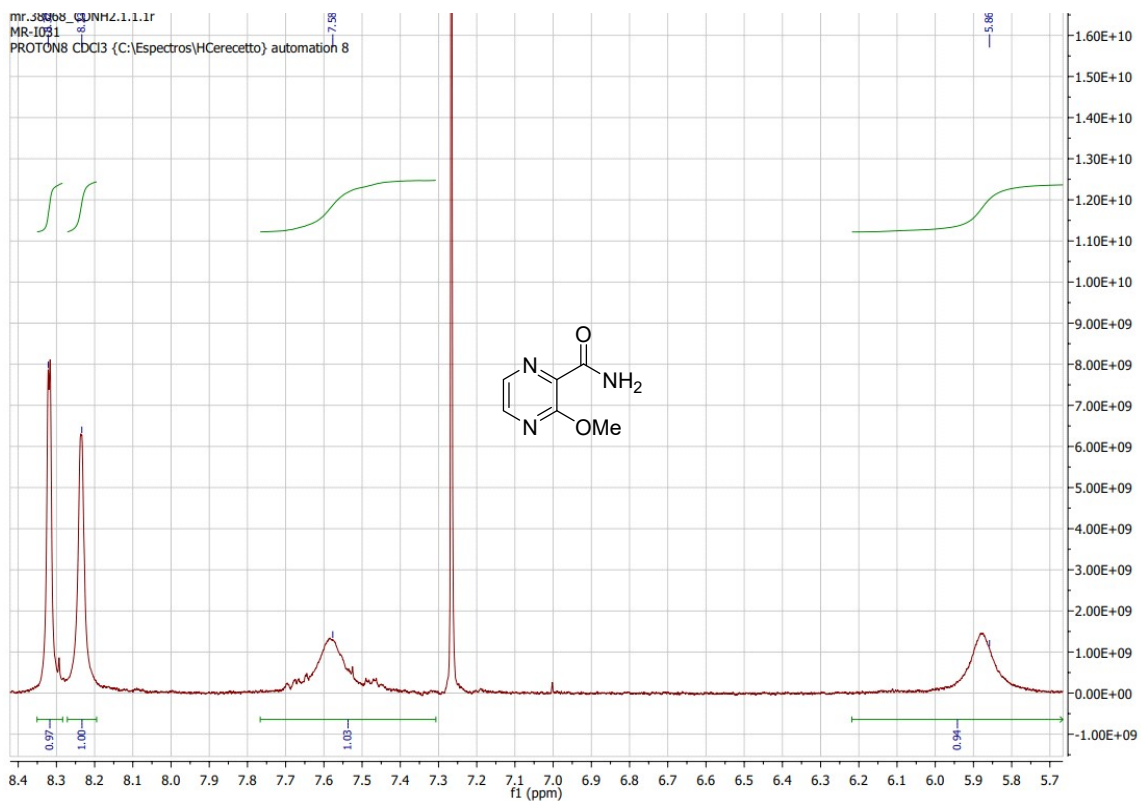


Figure S7. Ampliation of ^1H -NMR of 3-methoxy-pyrazine-2-carboxamide **1b** in CDCl_3 .

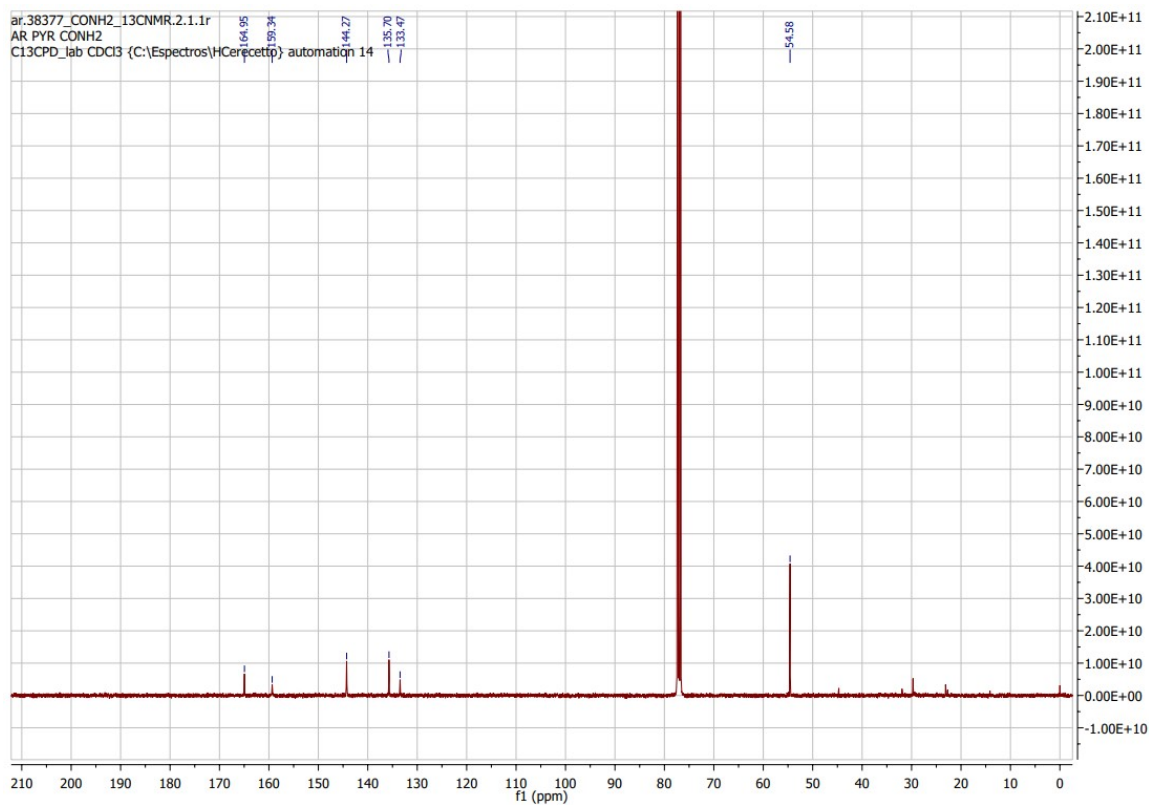


Figure S8a. ^{13}C -NMR of 3-methoxy-pyrazine-2-carboxamide **1b** in CDCl_3 .

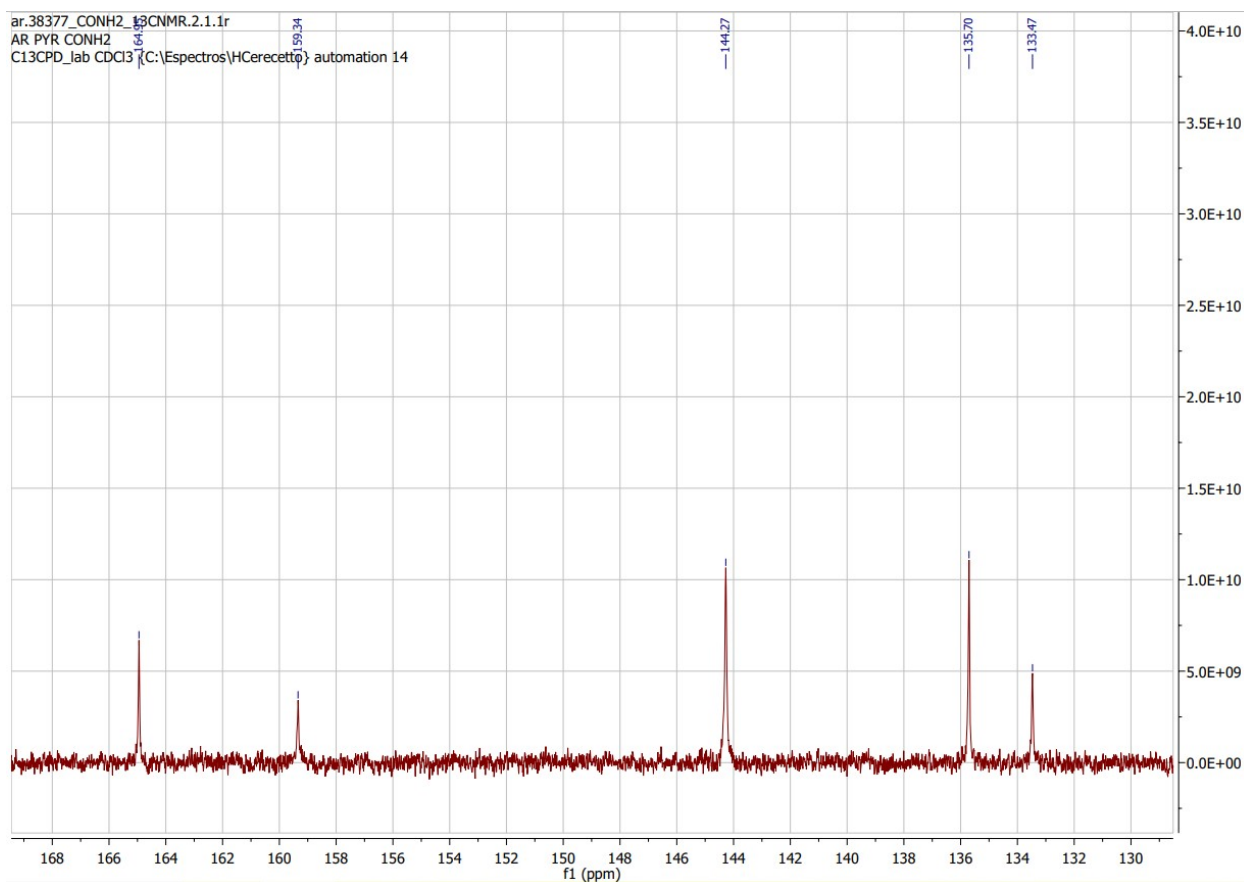


Figure S8b. Ampliation of ^{13}C -NMR of 3-methoxy-pyrazine-2-carboxamide **1b**.

2.3. Optimization Procedure for Favipiravir Synthesis

3-Hydroxy-pyrazine-2-carboxamide (20 mg, 1 eq., 0.14 mmol) and fluorinating agent (0.8-2.4 eq., 0.12-0.28 mmol) were added in a sealed tube in presence of the corresponding solvent, then the reaction mixture was stirred at 50-100 °C for 4-24 h. Selectfluor®, NFSI, *N*-fluoro-2,6-dichloropyridinium, *N*-fluoro-2,4,6-trimethylpyridinium and silver (II) difluoride were employed as fluorinating agent. Different solvents such as DCE, DMF, THF, dioxane, toluene, ethanol, methanol, water, DCE-DMF and some ionic liquids (ILs) such BF₄-BMIM, PF₆-BMIM and Cl-BMIM were used. Range of temperatures including 50, 70, 80, 90 and 100 °C and reaction time of 4, 8, 12 and 24 h were employed. Reactions were monitored by TLC with a solvent *n*-hexane/ethyl acetate (7/3). Percentage of conversion was determined from fluorometric measurements and HPLC measurements through UV-Vis detection.

2.3.1. Fluorescence Yield Measurement

The organic solvent was evaporated by vacuum and, resulting reaction mixture was diluted with methanol/water (4:1) (5 mL). Resulting solid consisting of Selectfluor®, defluorinated Selectfluor® (H-TEDA-BF₄), starting pyrazine and “self-addition sub-product” **9** (Scheme 4A) and fluoride salt were filtered and resulting solvent was used to prepare stock solutions. Then, 20 μL of this solution was diluted in water (2 mL) to prepare stock solution for fluorescence measurements. In a 96-well microplate, 20 μL of stock solution was added to 180 μL of water and, the fluorescence was recorded at 430 nm upon 360 nm excitation. This condition allowed us to work in the linear range of calibration curve: fluorescence intensities from 30 to 1600 R.F.U. and favipiravir concentrations from 0.098 to 25 μM. With calibration curve of the fluorescence of favipiravir, amount of favipiravir of the reactions were determined and then, their conversion percent to favipiravir were calculated. BF₄-BMIM quenched discretely the fluorescence of the favipiravir. Then, two calibration curves were performed: (i) one of them in presence of BF₄-BMIM and, (ii) other in absence of the IL, being each one of them depending on reaction conditions (Figure S9A-B). Curve B (Figure S9) was employed for determining reaction yields for reaction solution containing BF₄-BMIM, were calibration curve A was used for solution in absence of ILs. Importantly, starting 3-hydroxy-pyrazine-2-carboxamide, Selectfluor® and H-TEDA-BF₄ did not show fluorescence.

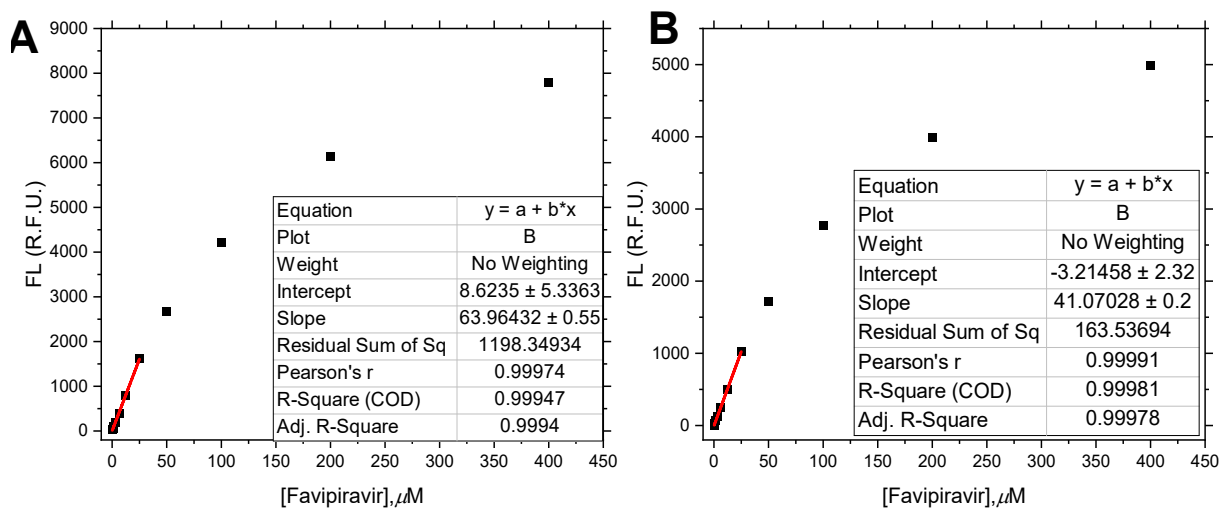


Figure S9. Calibration curves for (A) solution in presence of BF₄-BMIM or absence of BF₄-BMIM (B). Each point was derived from two separated experiments with a SD below 5 %.

2.3.2. *HPLC Yield Measurement*

The organic solvent was evaporated by vacuum and, resulting reaction mixture was diluted with methanol/water (4:1) (5 mL). Resulting solid consisting of Selectfluor®, H-TEDA-BF₄, starting 3-hydroxy-pyrazine-2-carboxamide, fluoride salt and other sub-products, i.e. “self-addition subproduct” **9** (Scheme 4A), were filtered and resulting solvent was used to prepare stock solutions. Stock solution of starting pyrazine also were prepared. Conversion percentages were then determined from HPLC-UV/Vis analysis.

2.4. *Effect of Water*

General procedure: 3-Hydroxy-pyrazine-2-carboxamide or favipiravir (20 mg, 1 eq., 0.141 mmol) and Selectfluor® agent (84 mg, 1.7 eq., 0.238 mmol) were added in a sealed tube in deuterated water. Then, the reaction mixture was stirred at 80 °C for 24 h. Reactions were monitored by TLC with a solvent *n*-hexane/ethyl acetate (7/3). Percentage of conversion was determined from fluorometric and HPLC measurements. Some control experiments in deuterated water such as; (i) favipiravir in presence of Seletfluor and water and, (ii) favipiravir only in presence of water under heating, were performed. It is important to mention that favipiravir and 3-hydroxy-2-pyrazinecarboxamide were inert in aqueous solution in absence of Selectfluor®. Only a smaller traces of hydrolysis-product on carboxamide moiety was detected for favipiravir (blue spectrum in Figures S10-S11), the rest of component was favipiravir.

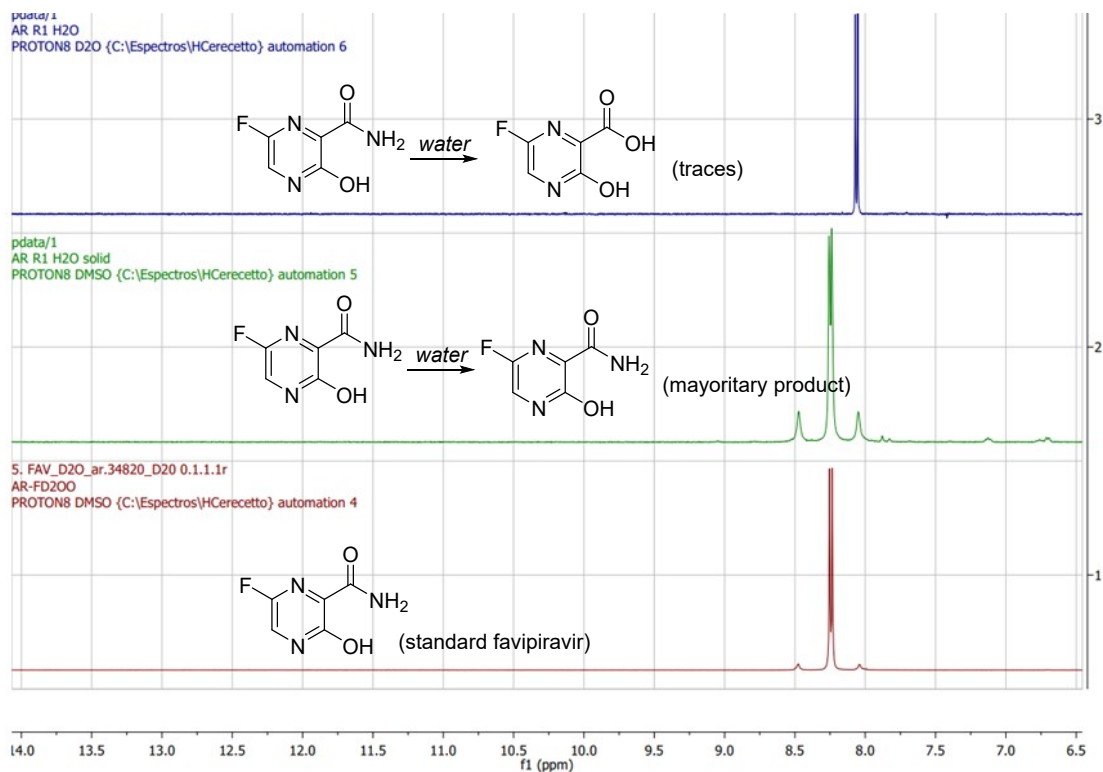


Figure S10. ¹H-NMR of spectra of favipiravir upon water: (A) hydrolysis sub-product (blue spectra) (spectra from trace product); (B) major product (green spectra) and (C) standard favipiravir (red spectra).

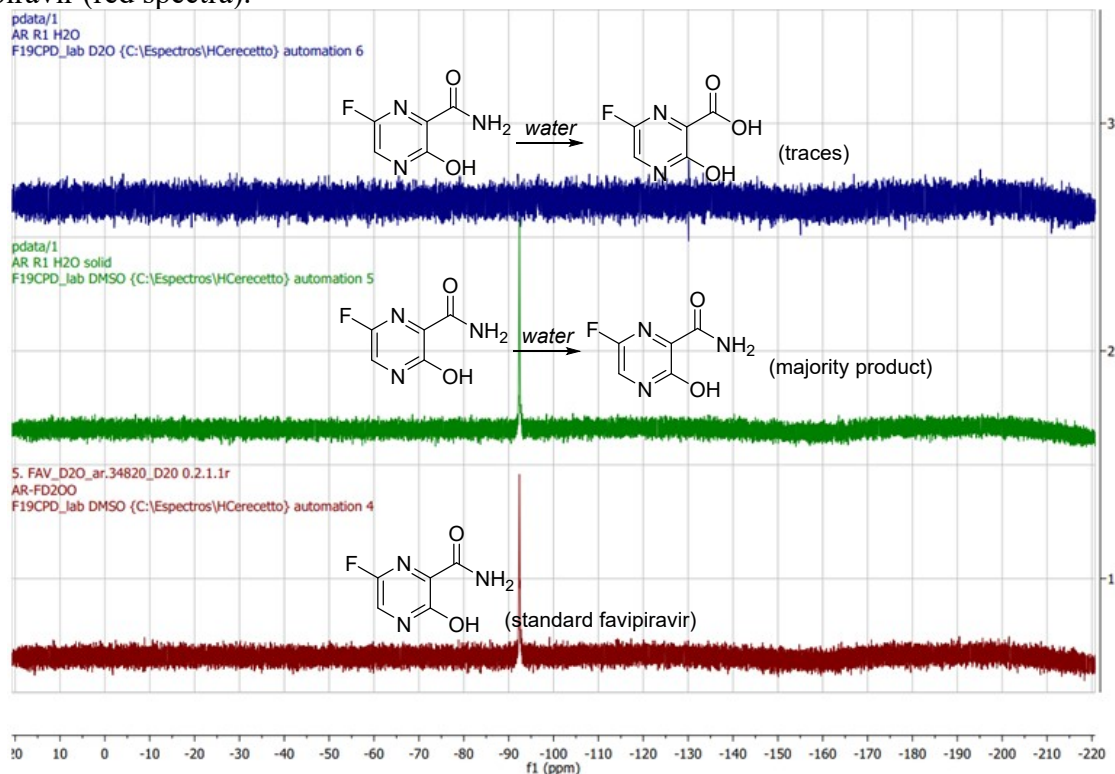


Figure S11. ¹⁹F-NMR spectra of favipiravir upon water: (A) hydrolysis sub-product (trace product, blue spectra); (B) major product (green spectra) and (C) standard favipiravir (red spectra).

From NMR experiments, a complete route was proposed for the decomposition of starting 3-hydroxy-pyrazine-2-carboxamide or favipiravir in presence of Selectfluor® in aqueous solution (Figure S12). Detection of fluoride anion, intermediates **2** (favipiravir), **3**, **4**, **7** and **H-TEDA** cation allowed us to suggest that the decomposition of 3-hydroxy-pyrazine-2-carboxamide was favored by a simultaneous mechanism of nucleophilic addition-electrophilic addition as depicted in Figure S12. Intermediate **4** and **7** also were detected by treatment of favipiravir with Selectfluor® in aqueous solution. This type of mechanism is very common in non-aromatic chemical systems featuring a double bond and, it is favored by the presence of a nucleophile and electrophilic species at same time in the reaction environment.¹⁵⁻¹⁷ The 3-hydroxy-pyrazine-2-carboxamide can present two tautomeric forms in turn to 3-hydroxy moiety: the enolic tautomer (**1-E**) and the ketonic tautomer (**1-K**). This last can be taken as a pseudo-aromatic, which could be more susceptible to simultaneous nucleophilic addition-electrophilic addition mechanism. Previously, we demonstrated that either starting pyrazine or favipiravir were under ketonic tautomeric form in aqueous solution.¹⁸ However, it is possible to suppose that the ketonic form react, whereas non reacting enolic form regenerated the enoli-ketonic equilibrium to form further ketonic tautomer until total consumption of the 3-hydroxy-2-pyrazinecarboxamide. Then, the decomposition initiated with nucleophilic addition of one water molecule at C5 of pyrazine and simultaneous electrophilic addition to fluorine atom of Selectfluor® through C6 to form intermediate **3**. That intermediate was detected and possibly, the favipiravir is formed immediately through a dehydration to give **2-K** (favipiravir under keto-form in aqueous solution). The favipiravir is detected in traces either in ¹H-NMR spectrum (H_{Ar} at 8.25 ppm (d, 8 Hz), Figure S17) or ¹⁹F-NMR (-90.76 ppm, Figure S18). Subsequently, other simultaneous nucleophilic addition-electrophilic addition mechanism occur on favipiravir to give intermediate **4**, which also was detected in traces from ¹⁹F-NMR by a two double doublet (dd) at -143.23 ppm with constants coupling of 40 and 20 Hz (Figure S18, S23 and S24), which is in concordance with structure **4**.¹⁹ Then, intermediate **4** dehydrogenates to intermediate **5**, which suffers other simultaneous nucleophilic addition-electrophilic addition to give intermediate **6**. Subsequently, successive reactions led the final decomposition to compound **7**, oxalic acid (that was not detected from NMR) and fluoride anion (F⁻). Evidences of intermediate **7** were supported from ¹H-NMR (Figure S13, S15, S17, S19 and S20), ¹³C-NMR (Figure S21) and 2D-COSY. The triplet at 7.15 ppm can be attributed to no equivalent NH-protons by intermolecular bonding (**7** in Scheme 12), whereas small peak at 8.28

ppm could be attributed to NH-hemiamidal proton. From ^{13}C -NMR, a good correspondence was found for structure of **7**, having two peak at 118 and 167 ppm, which correspond to the hemiaminal carbon, $\text{C-NH}_2(\text{OH})(\text{CONH}_2)_2$ and carboxamide carbons, respectively. The large intensity at 118 ppm also supports the existence of a hemiaminal carbon. From 2D-spectra, no H-H and C-H correlations were identified from COSY and HSQC and HMBC experiments, respectively, which is in good concordance with the structure of hemiaminal compound **7**. Finally, fluoride anion was analyzed from ^1H -NMR, ^{19}F -NMR (Figure S14, S16, S18 and S22). Then, the 3-hydroxy-2-pyrazinecarboxamide is not compatible for the direct fluorination with Selectfluor® in aqueous solution. Complete spectra for favipiravir and 3-hydroxy-2-pyrazinecarboxamide in presence of Selectfluor® in aqueous solution can be found in Figures S19-S27 and Figure S28-S31, respectively. Interestingly, a partial decomposition of starting material to the intermediate **3** was observed under basic media in aqueous solution with Selectfluor® (Fig. S32-S38), whereas a total decomposition was favored in acidic environment (Fig. S39-S43).

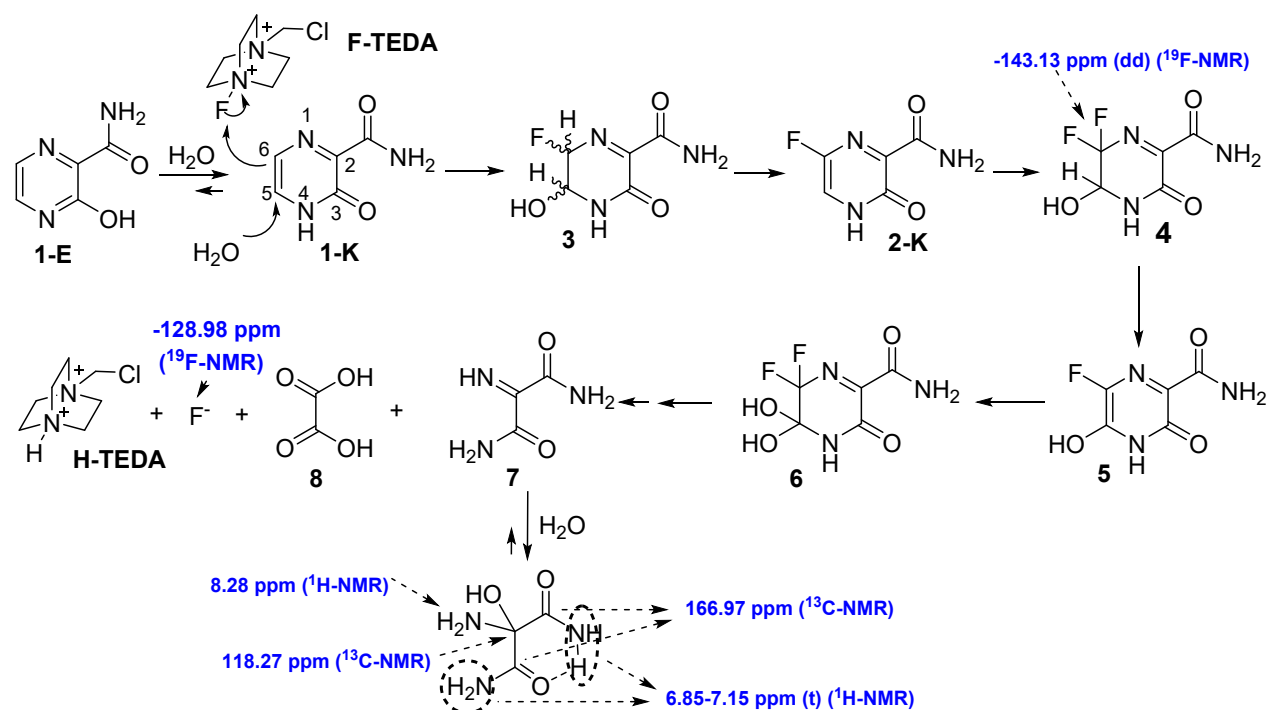


Figure S12. Decomposition of starting pyrazine and favipiravir in presence of Selectfluor® upon water environment.

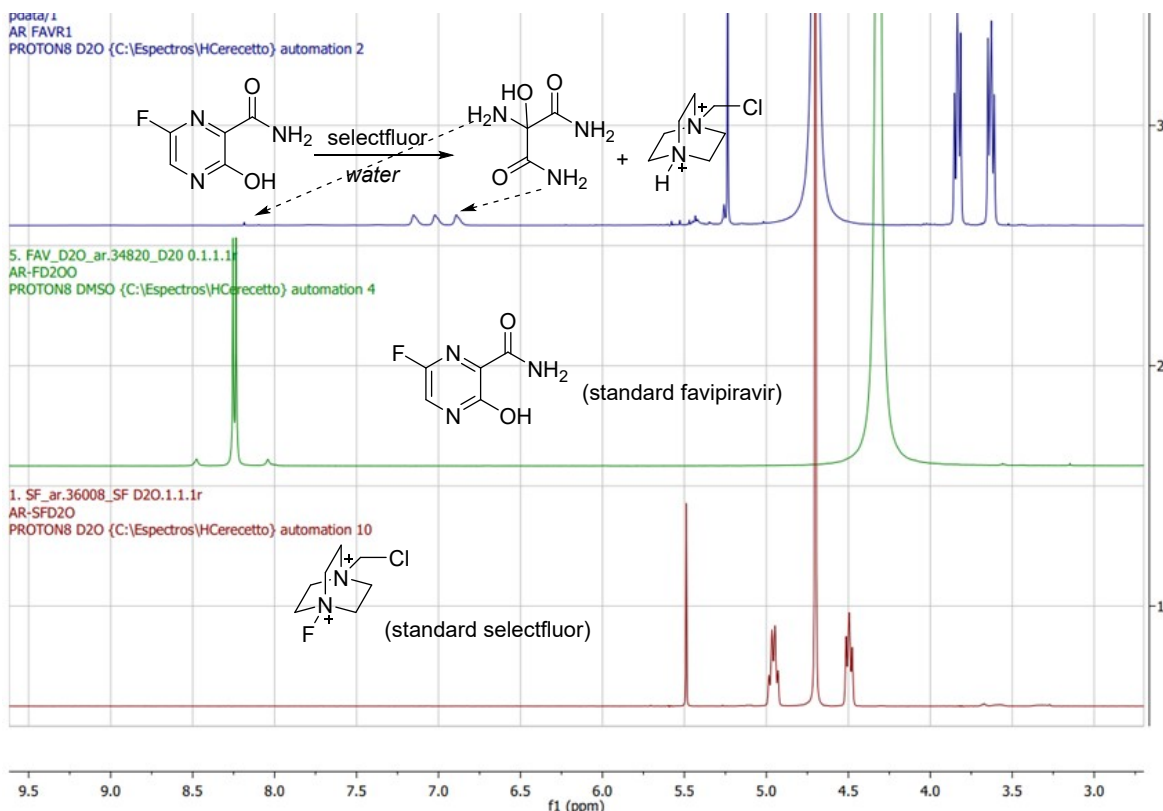


Figure S13. $^1\text{H-NMR}$ of favipiravir reaction in presence of Selectfluor[®] and water: (A) reaction product (blue spectra); standard favipiravir (B) (green spectra) and Selectfluor[®] (C) (red spectra).

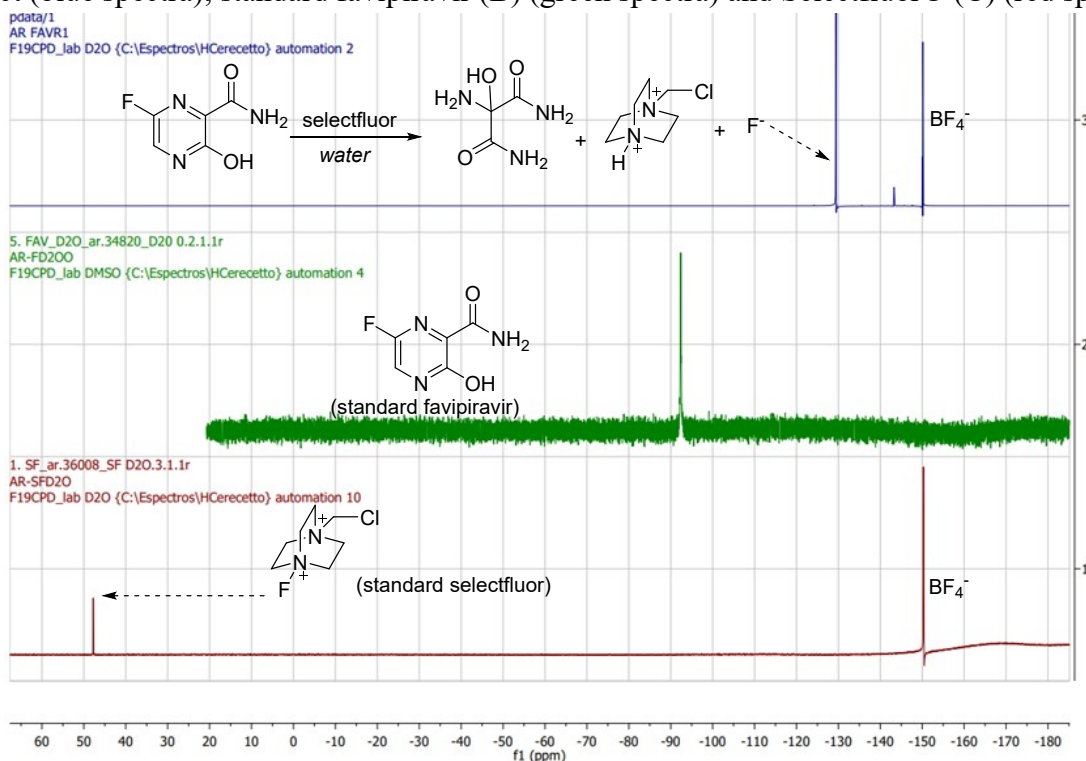


Figure S14. $^{19}\text{F-NMR}$ of favipiravir reaction in presence of Selectfluor[®] and water: (A) reaction product (blue spectra); standard favipiravir (B) (green spectra) and Selectfluor[®] (C) (red spectra).

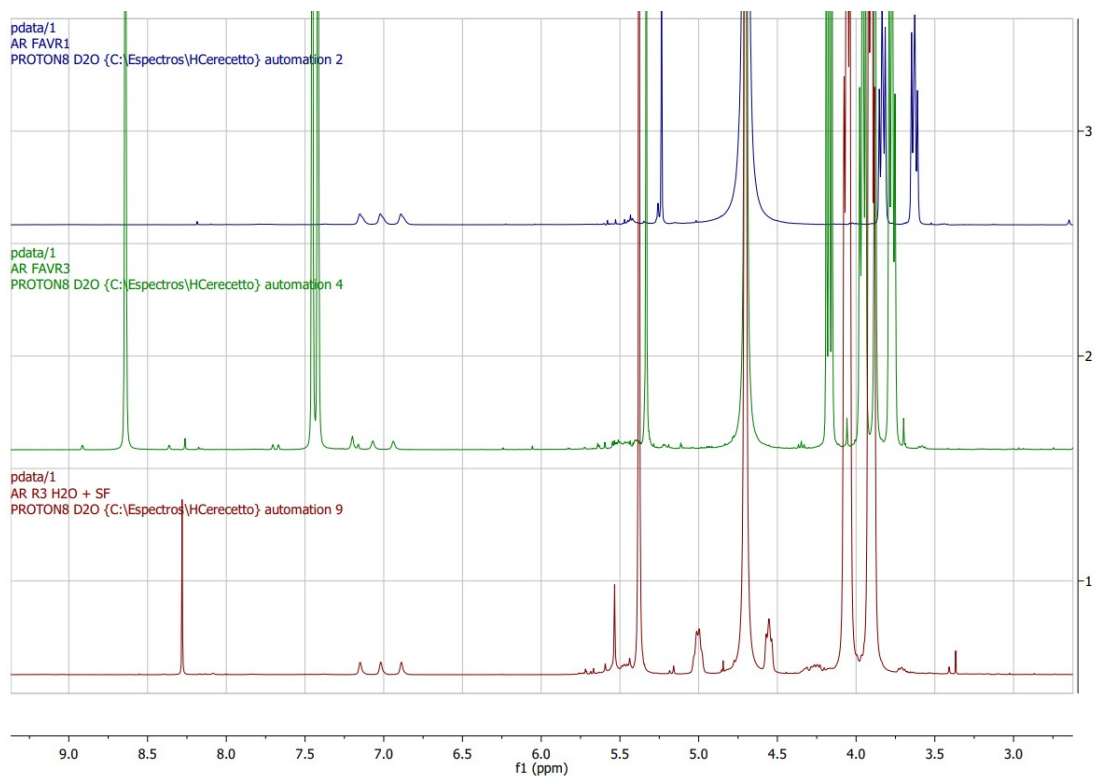


Figure S15. ^1H -NMR of favipiravir reaction in presence of Selectfluor $^{\text{®}}$ and H_2O : (A) at 80°C (blue spectrum); (B) at 80°C in $\text{BF}_4\text{-BMIM}$ (green spectrum) and, (C) at room-temperature (red spectra).

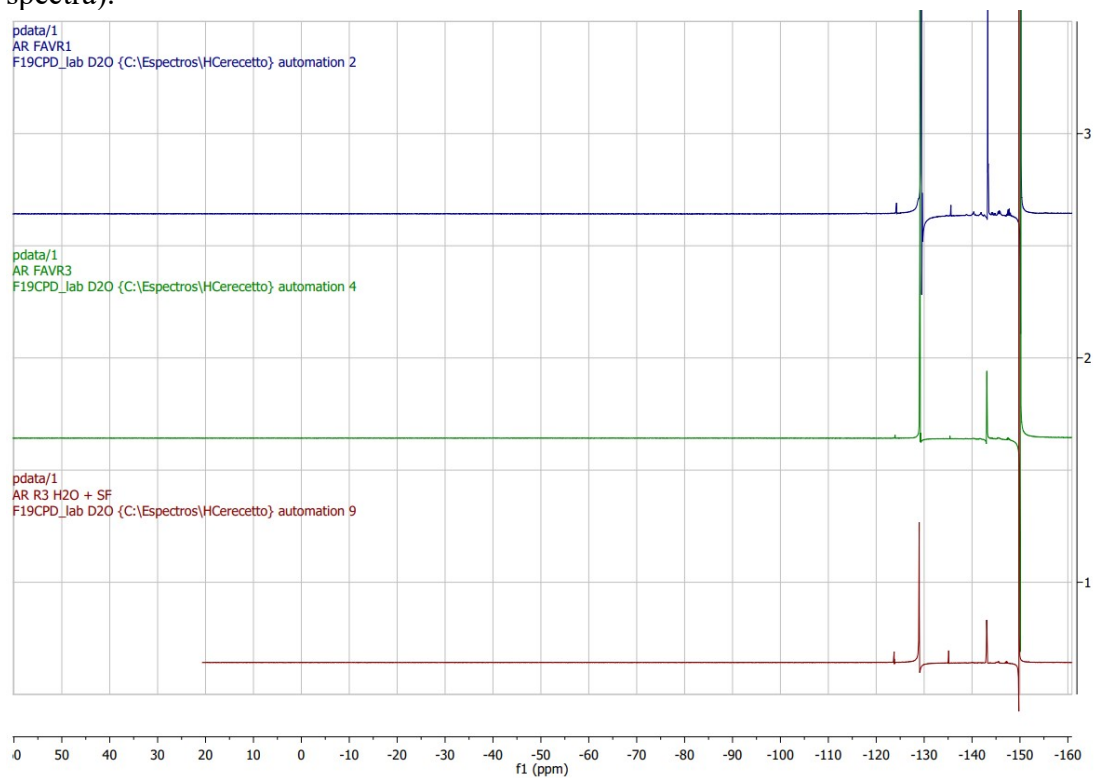


Figure S16. $^1\text{H-NMR}$ of favipiravir in reaction with Selectfluor $^{\text{®}}$ and H_2O : (A) at 80 $^{\circ}\text{C}$ (blue spectrum); (B) at 80 $^{\circ}\text{C}$ in $\text{BF}_4\text{-BMIM}$ (green spectrum) and, (C) at 25 $^{\circ}\text{C}$ (red spectrum).

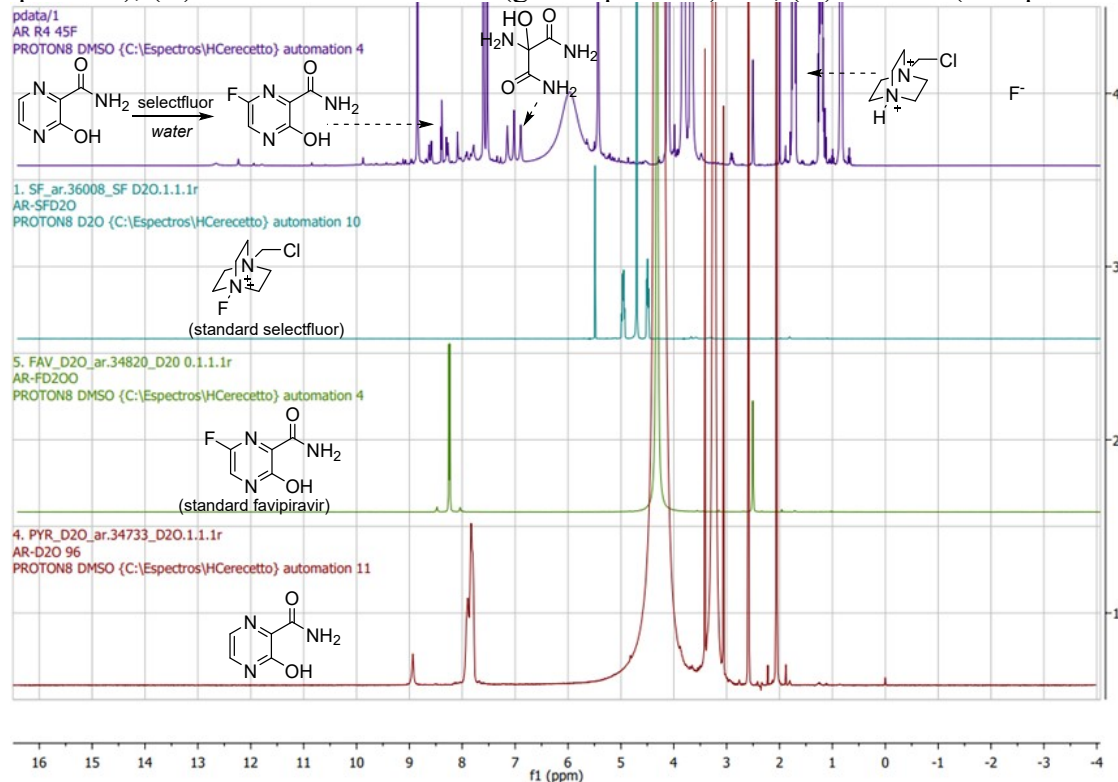


Figure S17. $^1\text{H-NMR}$ of starting pyrazine in presence of Selectfluor $^{\text{®}}$ and H_2O : reaction product (blue spectra); standard Selectfluor $^{\text{®}}$ (cyan), favipiravir (green) and starting pyrazine (red).

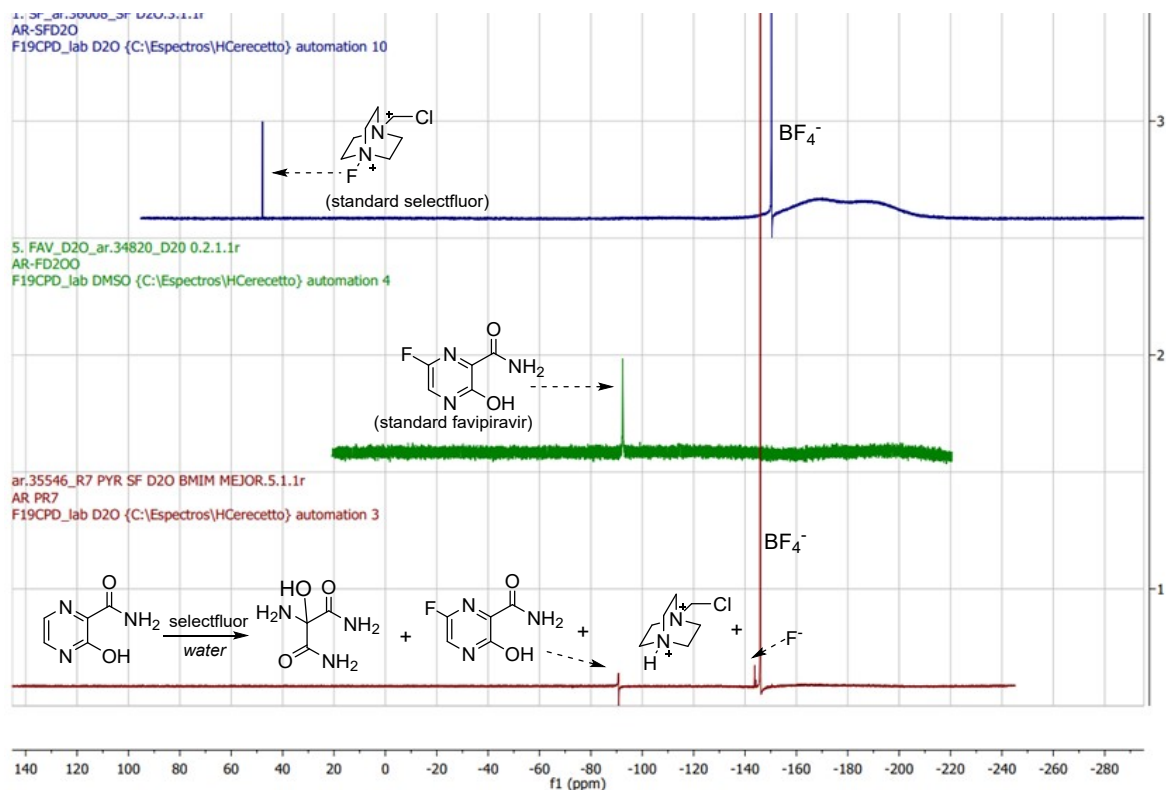


Figure S18. ¹⁹F-NMR of starting pyrazine in presence of Selectfluor® and H₂O: reaction product (blue spectra); standard Selectfluor® (blue), favipiravir (green) and starting pyrazine (red).
General spectra of reaction of starting pyrazine with Selectfluor® in water

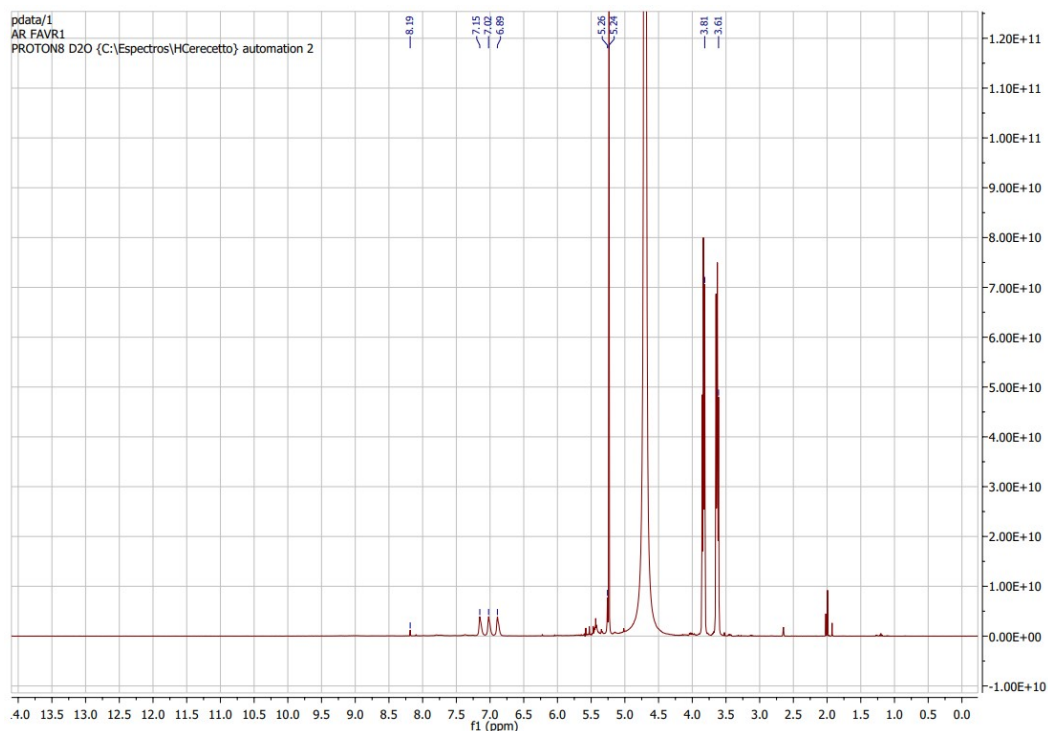


Figure S19. ¹H-NMR of starting pyrazine in presence of Selectfluor® and water.

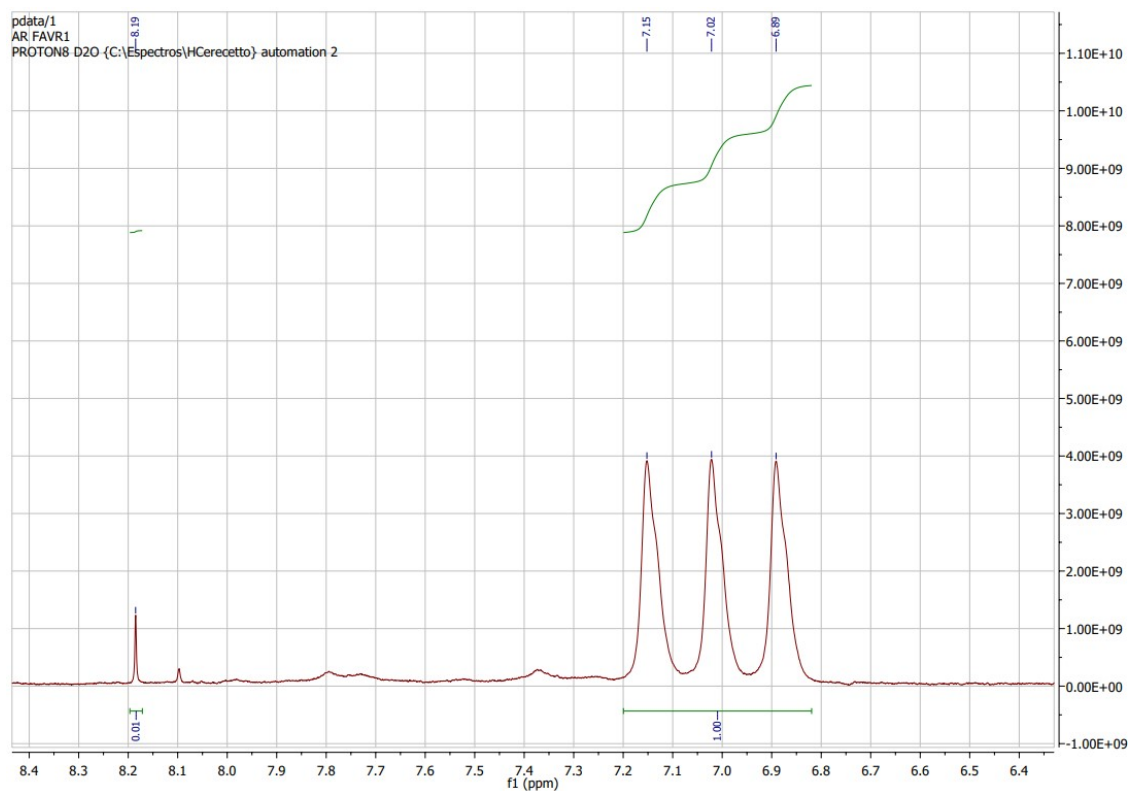


Figure S20. Ampliation of ^1H -NMR of starting pyrazine in presence of Selectfluor® and water.

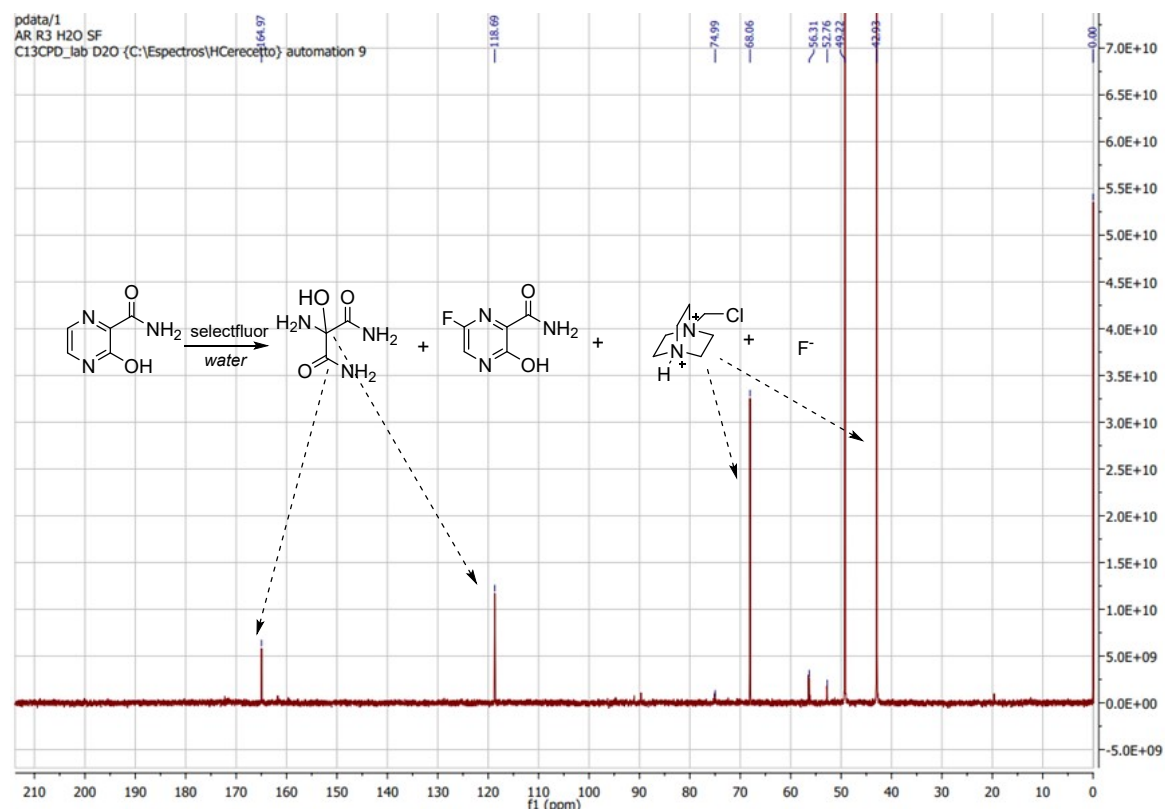


Figure S21. ^{13}C -NMR of starting pyrazine in presence of Selectfluor® and water.

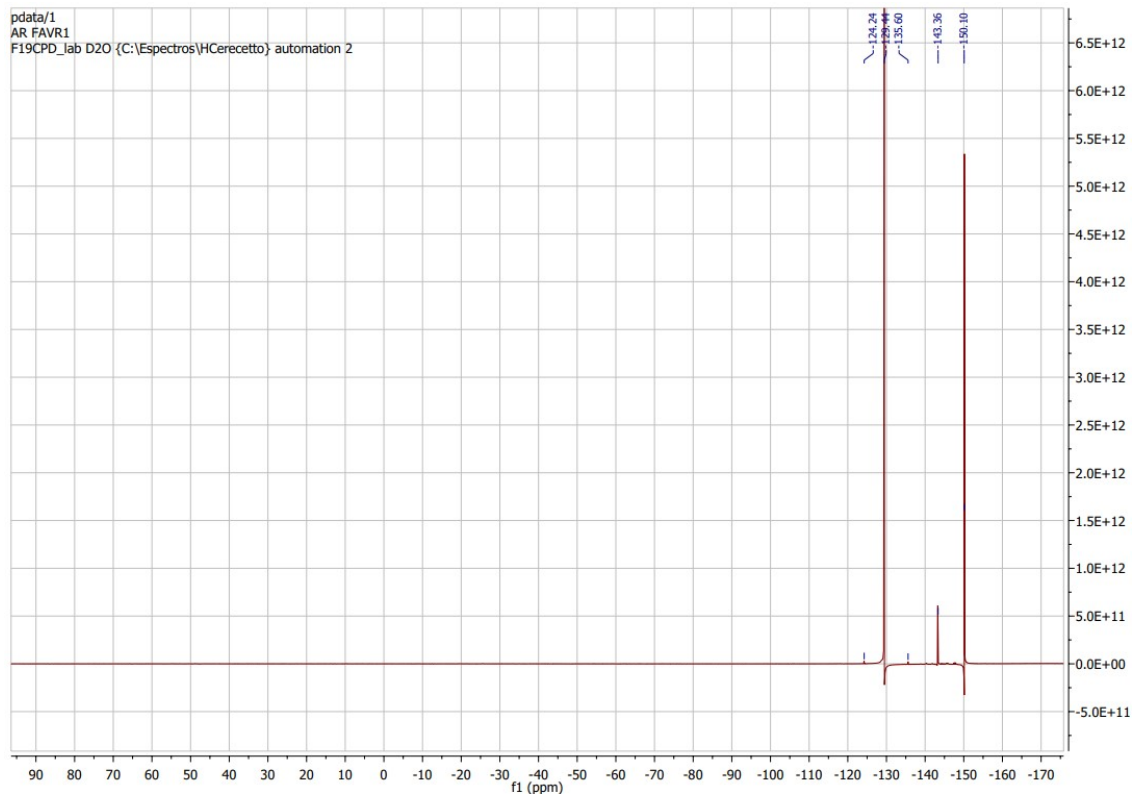


Figure S22. ^{19}F -NMR of starting pyrazine in presence of Selectfluor[®] and water.

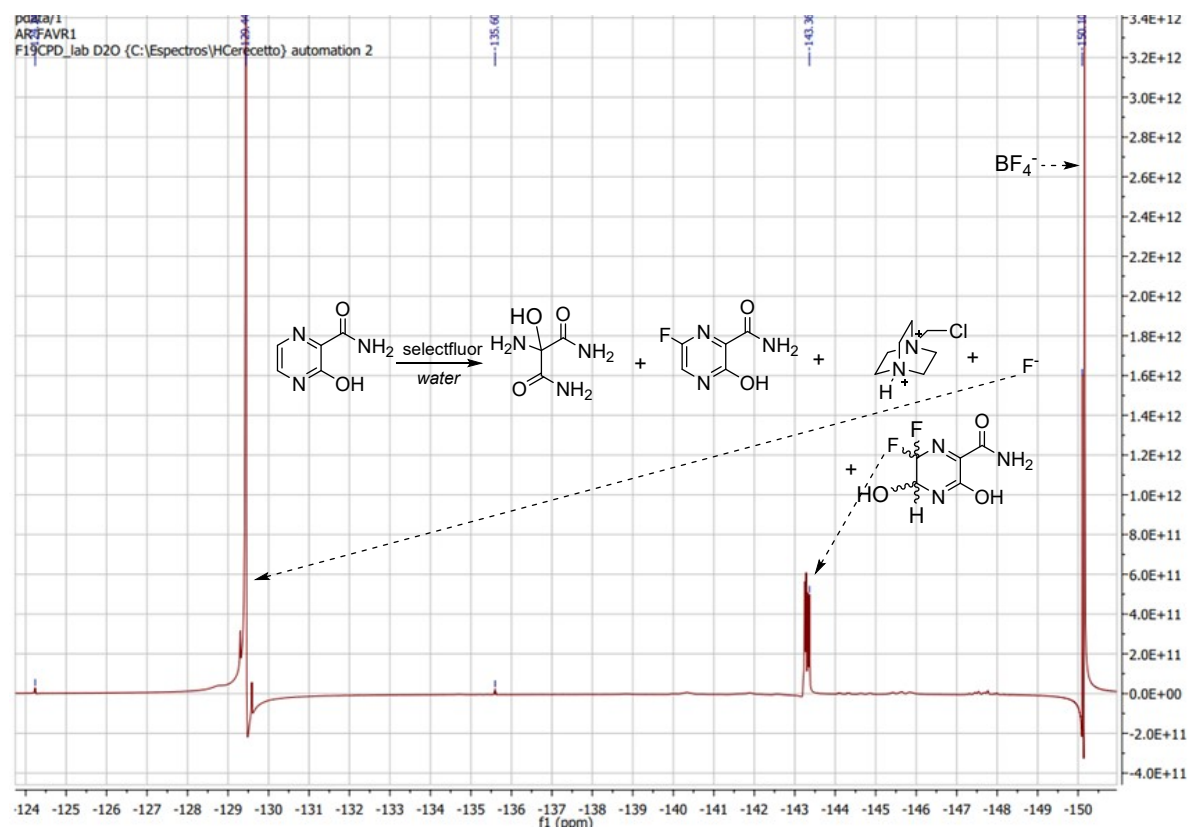


Figure S23. Ampliation of ^{19}F -NMR of starting pyrazine in presence of Selectfluor[®] and water.

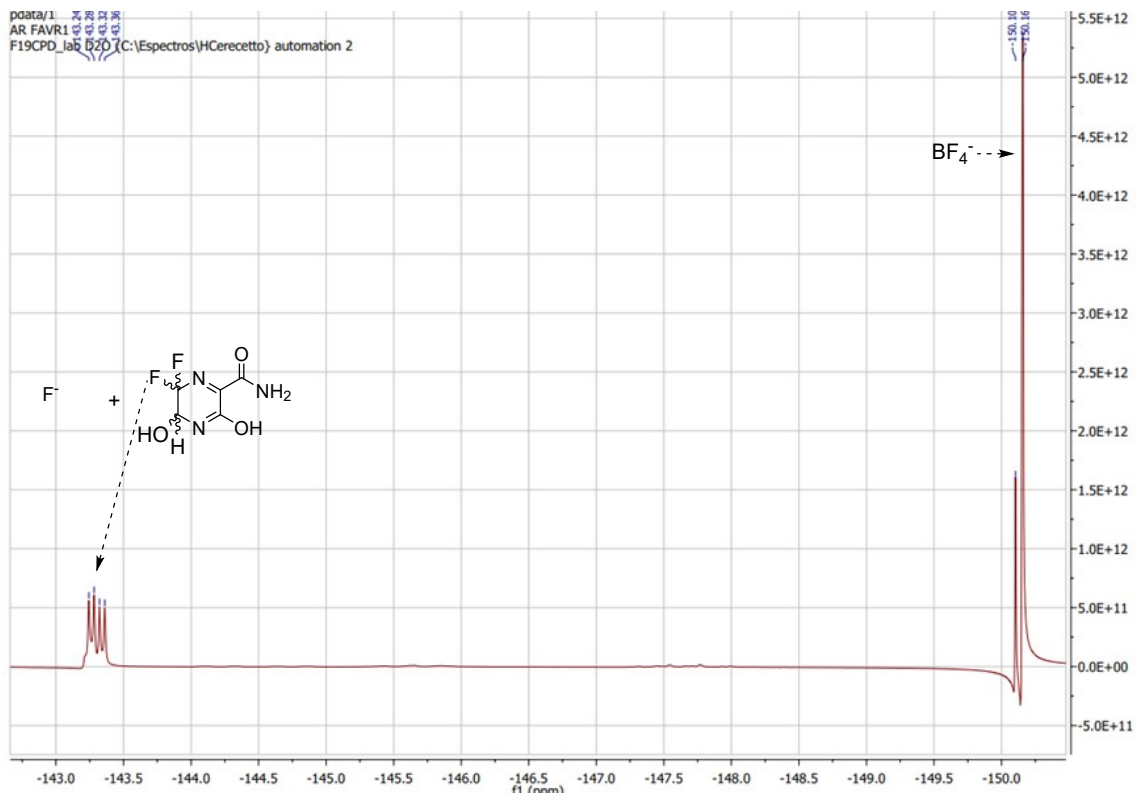


Figure S24. Ampliation 2 of ^{19}F -NMR of starting pyrazine in presence of Selectfluor® and water.

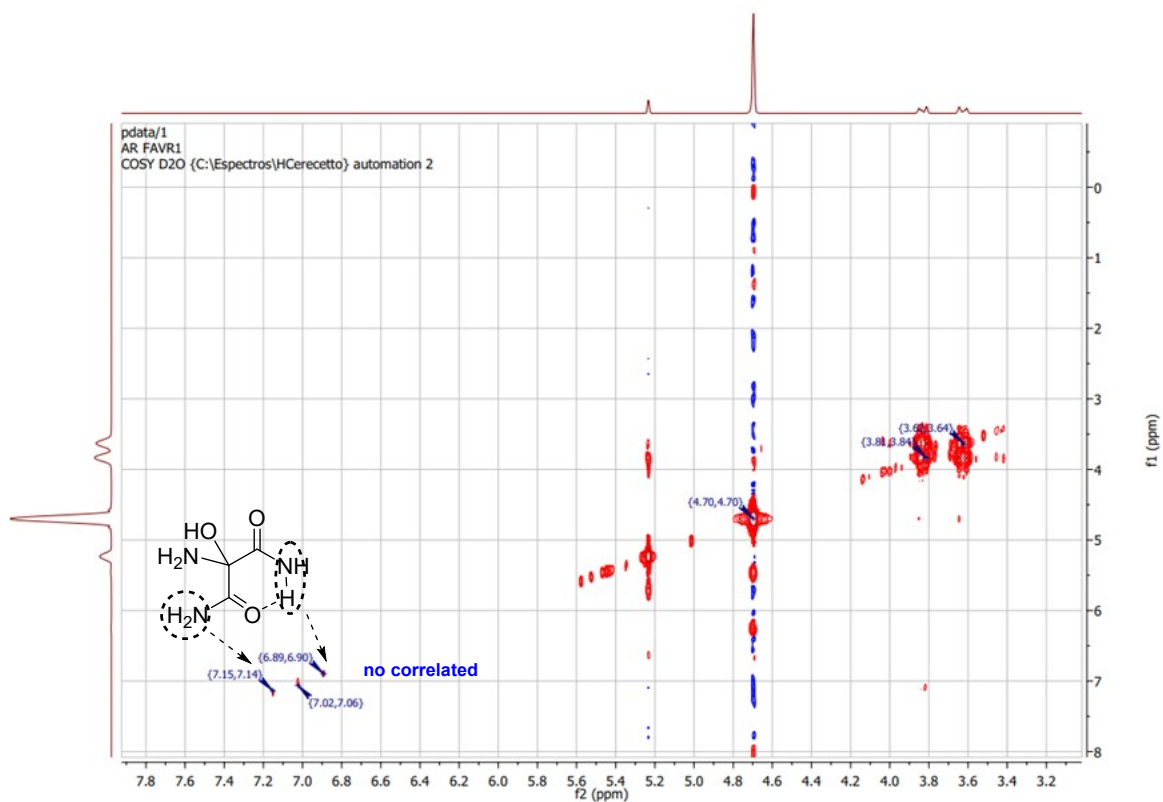


Figure S25. COSY of favipiravir in presence of Selectfluor® and water.

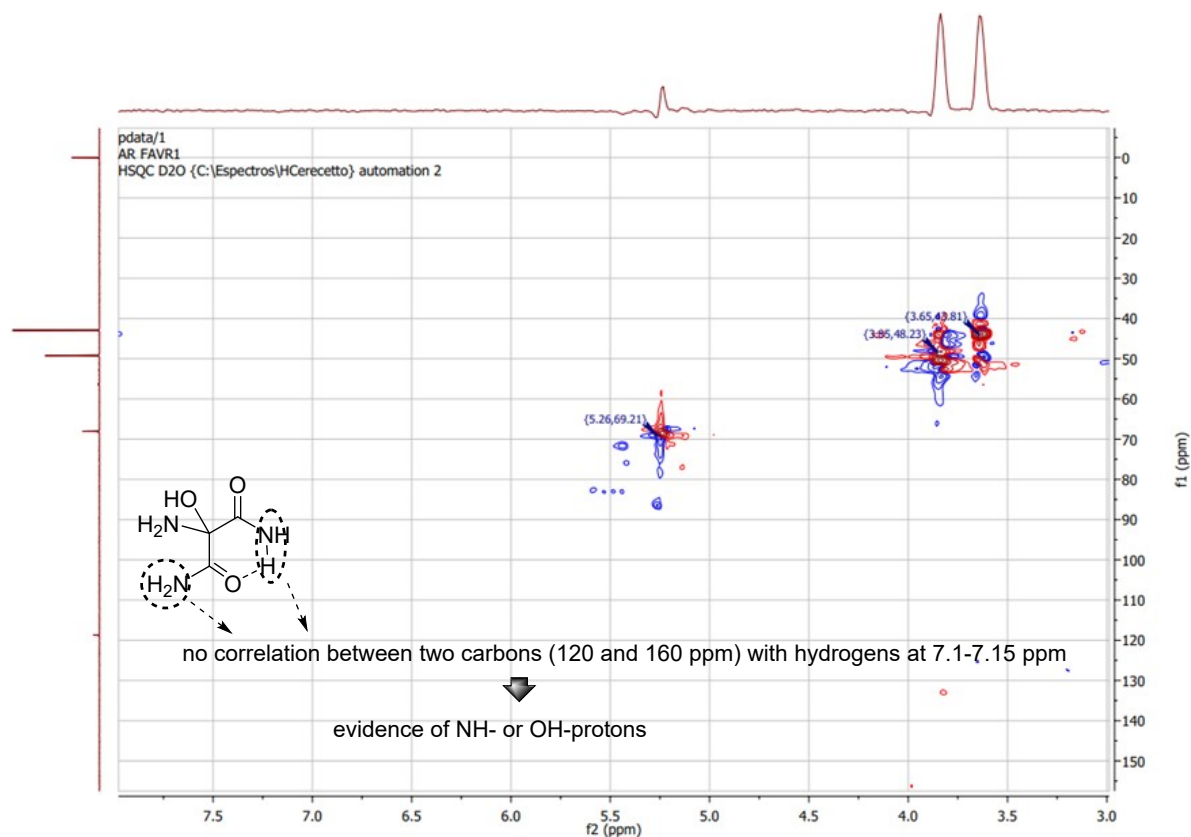


Figure S26. ^1H - ^{13}C -HSQC of starting pyrazine in presence of Selectfluor® and water.

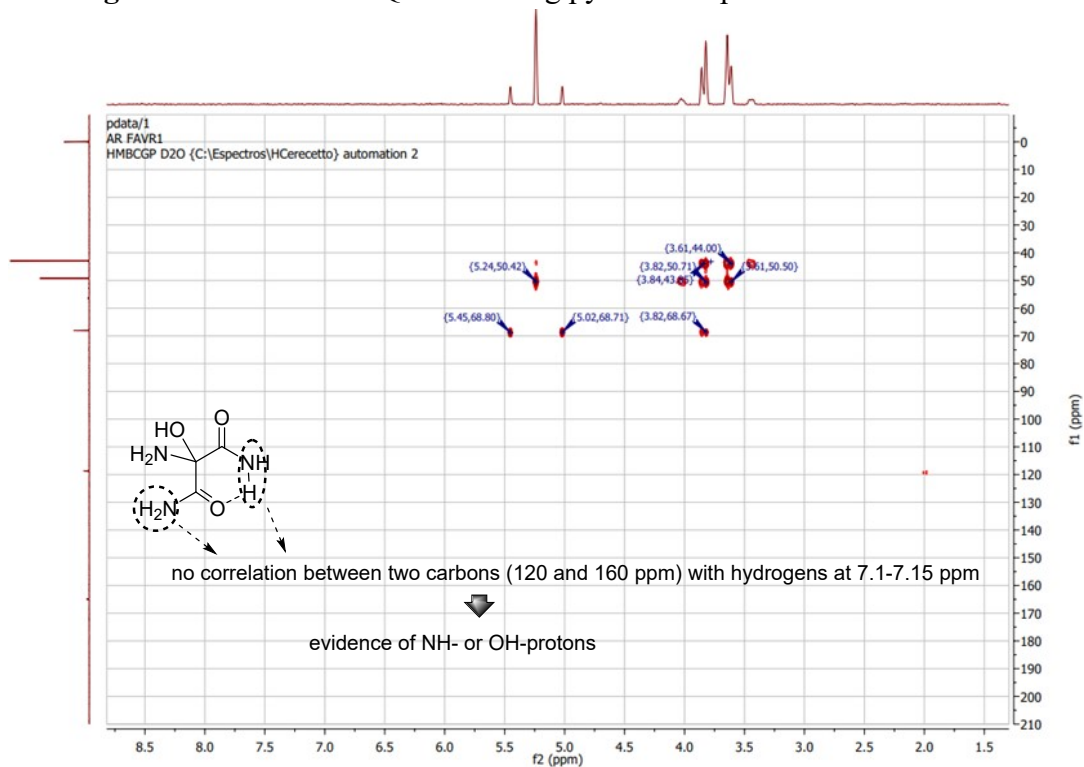


Figure S27. ^1H - ^{13}C -HMBC of starting pyrazine in presence of Selectfluor® and water.

2.5. Effect of Acid and Base in Aqueous Solution

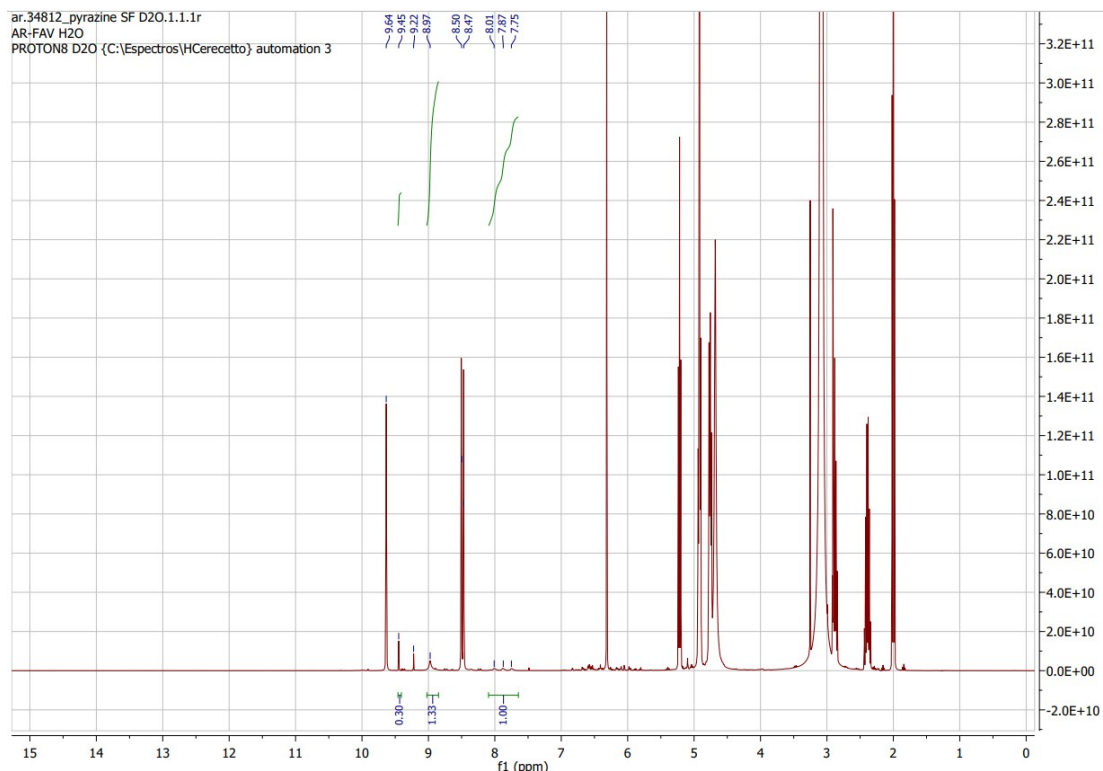


Figure S28. $^1\text{H-NMR}$ of starting pyrazine in presence of Selectfluor® and water.

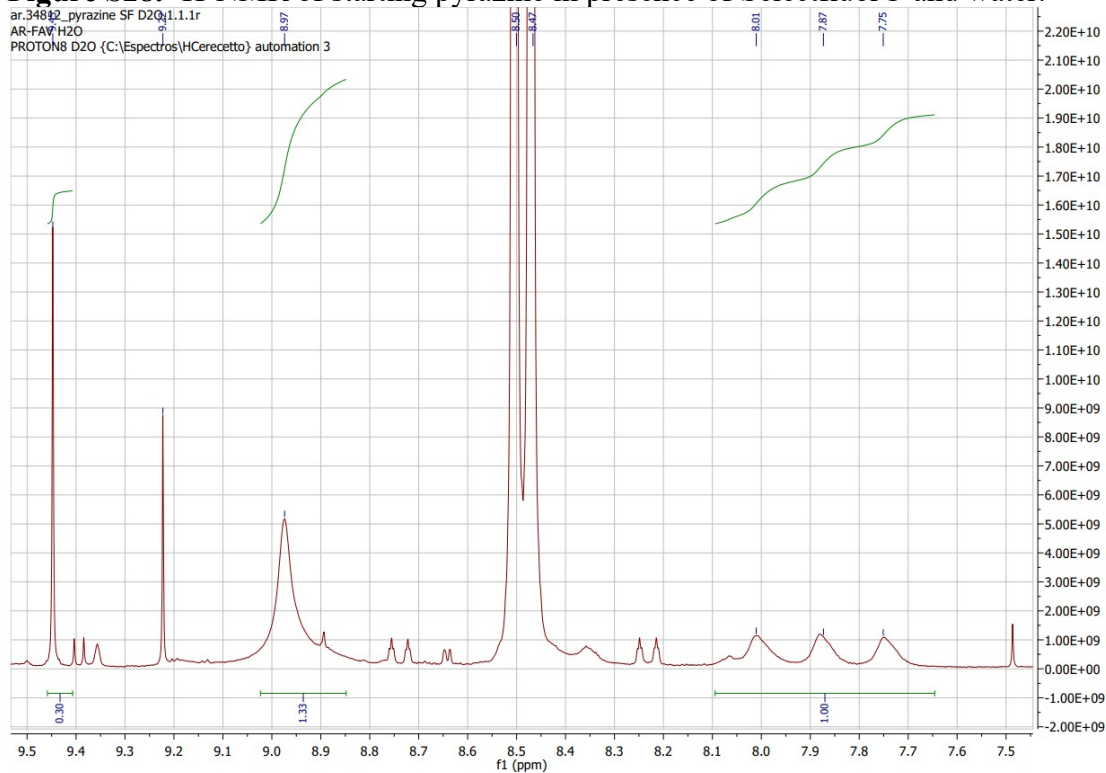


Figure S29. Ampliation of $^1\text{H-NMR}$ of starting pyrazine in presence of Selectfluor® and water.

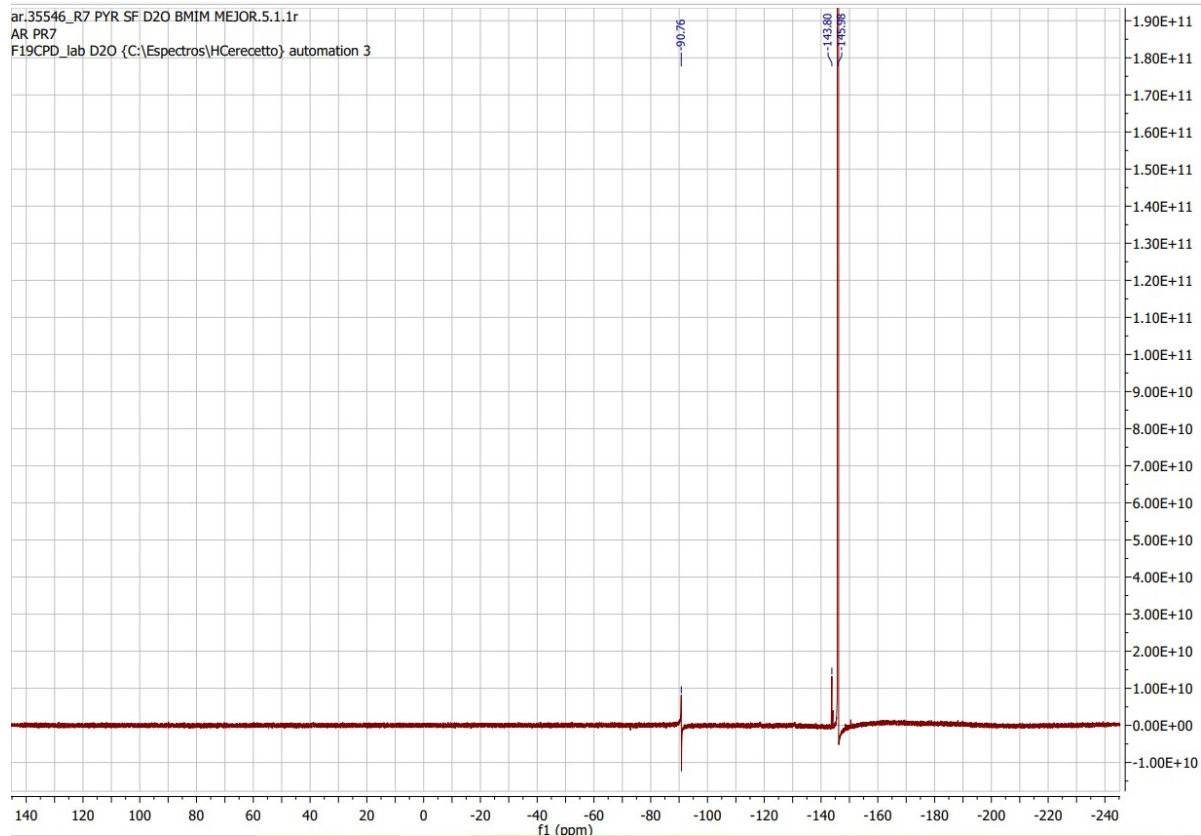


Figure S30. ^{19}F -NMR of starting pyrazine in presence of Selectfluor® and water.

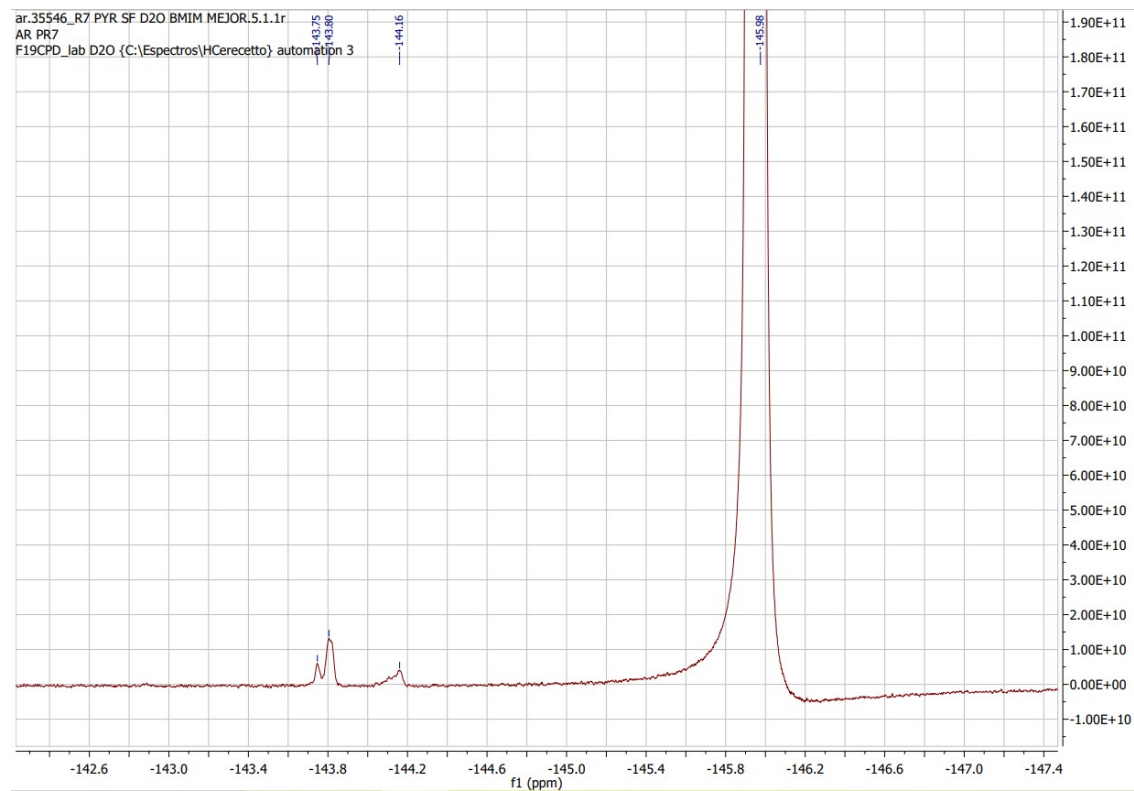


Figure S31. Ampliation of ^{19}F -NMR of starting pyrazine in presence of Selectfluor® and water.

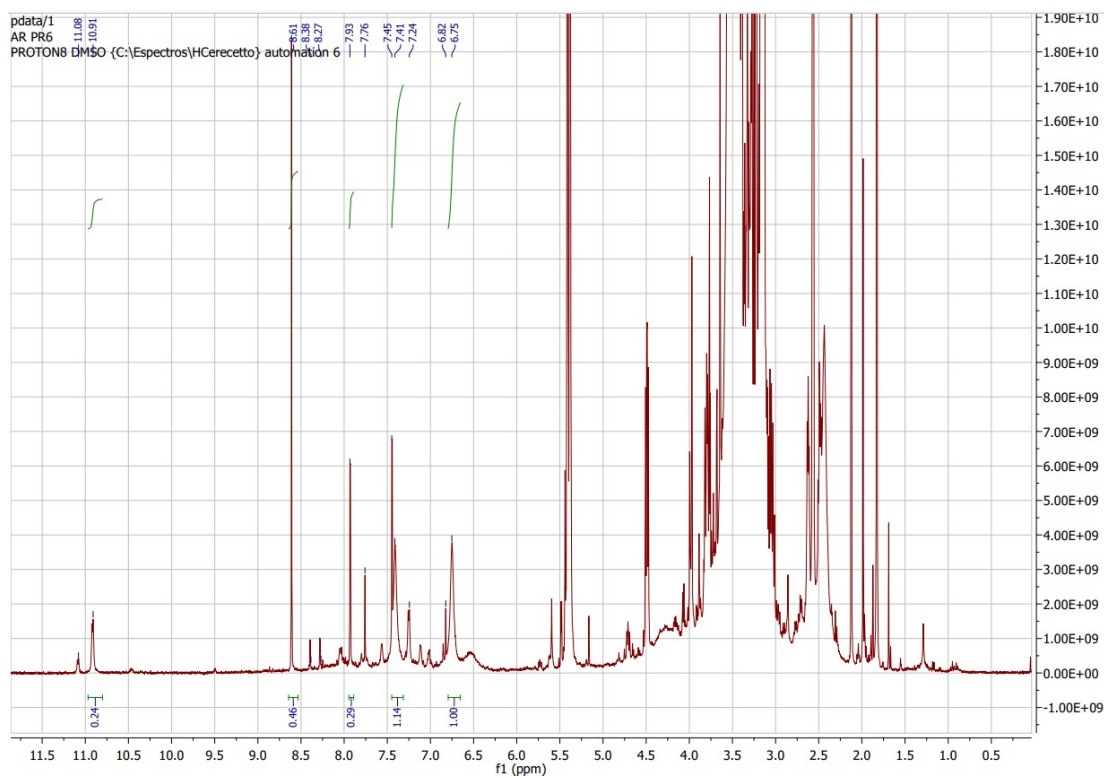


Figure S32. ^1H -NMR spectra of starting pyrazine with Selectfluor[®] in presence of K_2CO_3 .

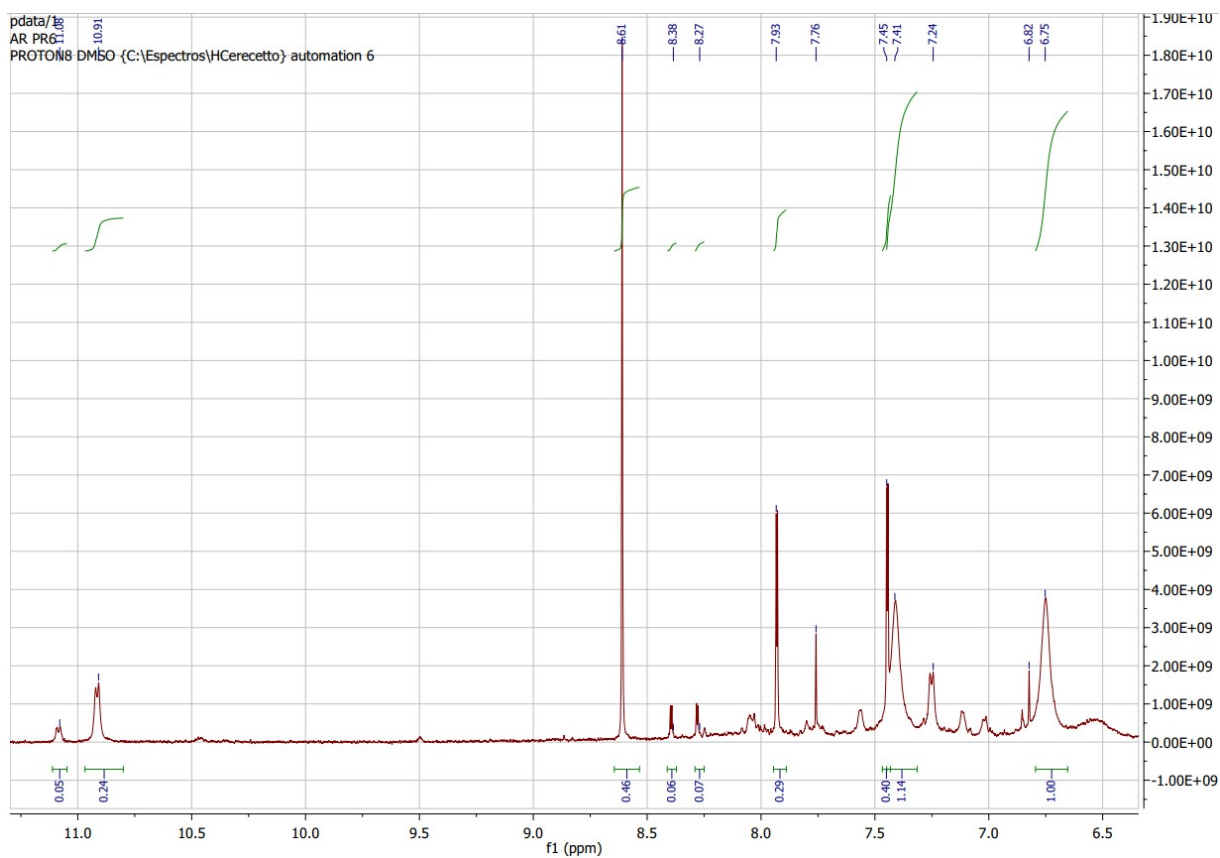
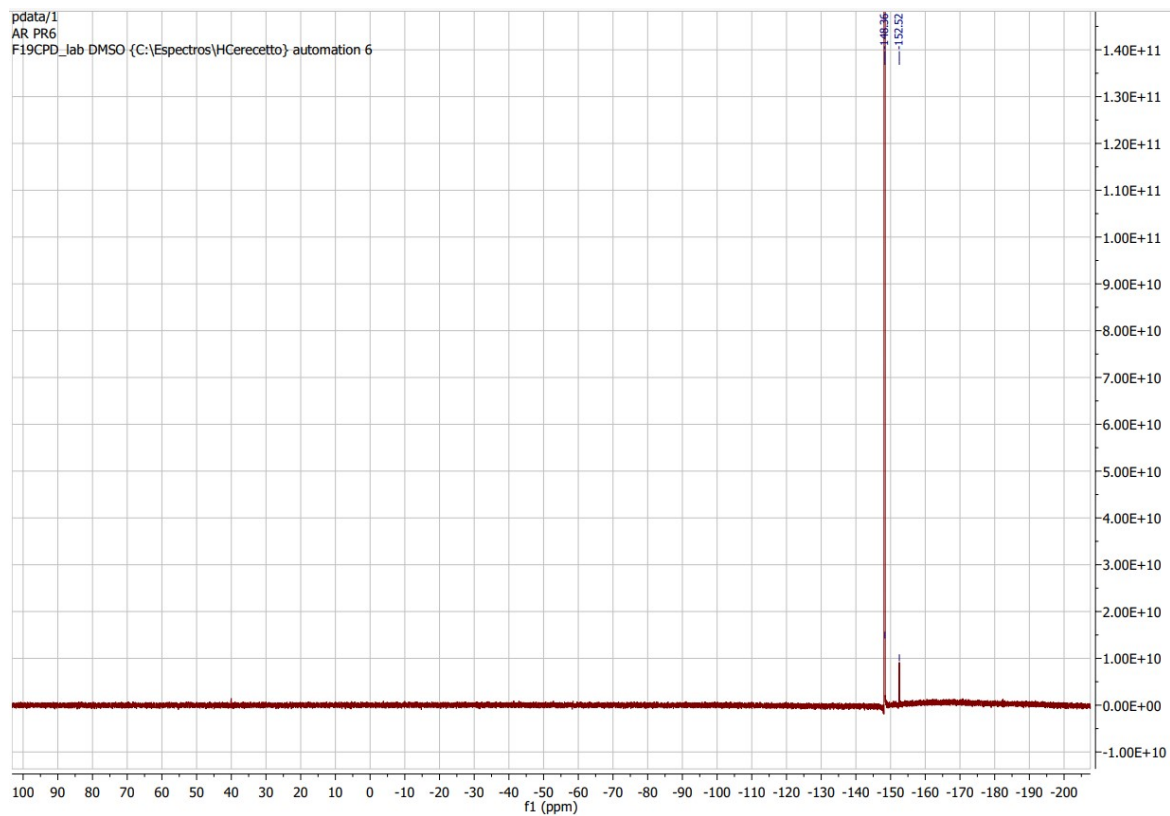


Figure S33. Ampliation of ^1H -NMR spectra of pyrazine with Selectfluor $^\circledR$ in presence of K_2CO_3 .



Figur

e S34. ^{19}F -NMR spectra of starting pyrazine with Selectfluor $^\circledR$ in presence of K_2CO_3 .

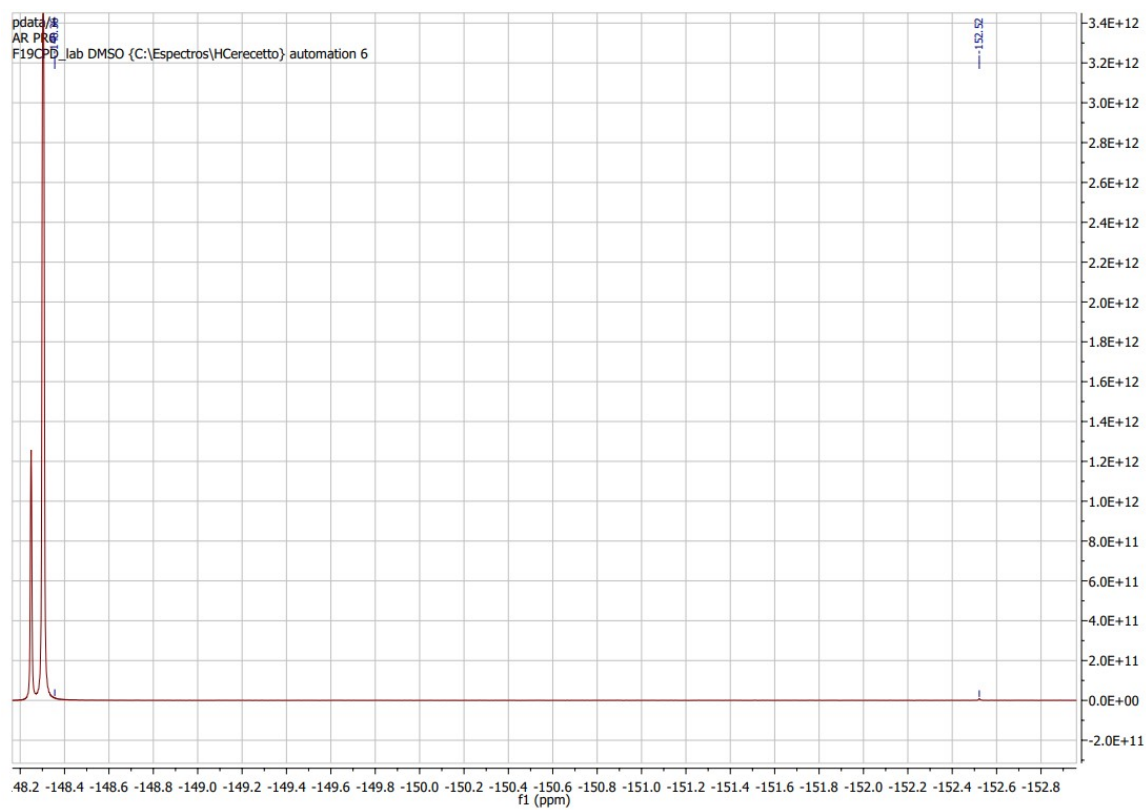


Figure S35. ^{19}F -NMR spectra of starting pyrazine with Selectfluor® in presence of K_2CO_3 .

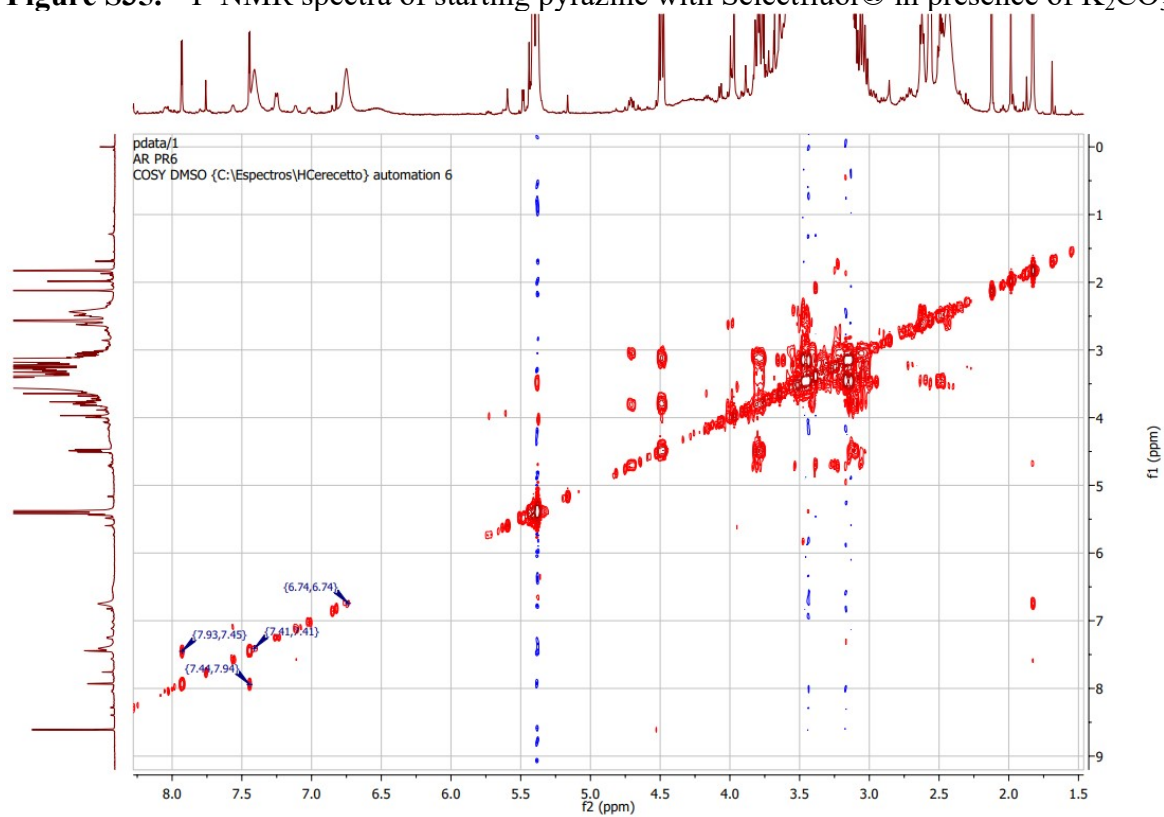


Figure S36. $^1\text{H}/^1\text{H}$ -COSY spectra of starting pyrazine with Selectfluor® in presence of K_2CO_3 .

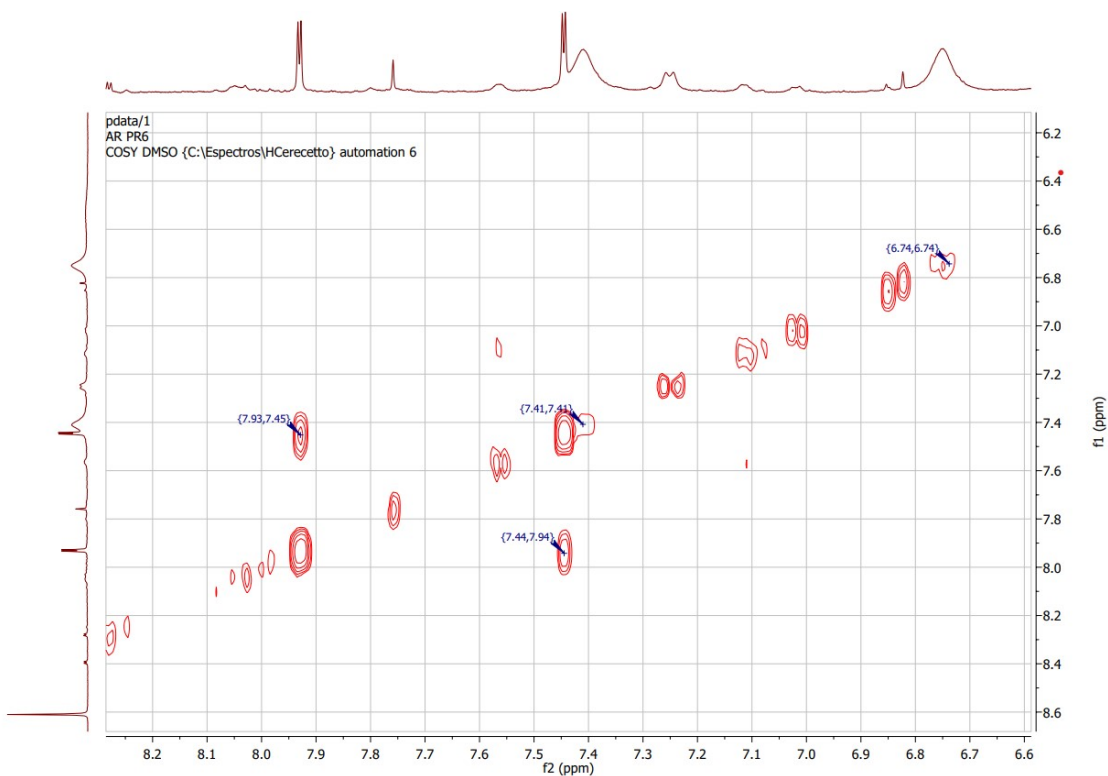


Figure S37. Ampliation of $^1\text{H}/^1\text{H}$ -COSY spectra of starting pyrazine with Selectfluor[®] in presence of K_2CO_3 .

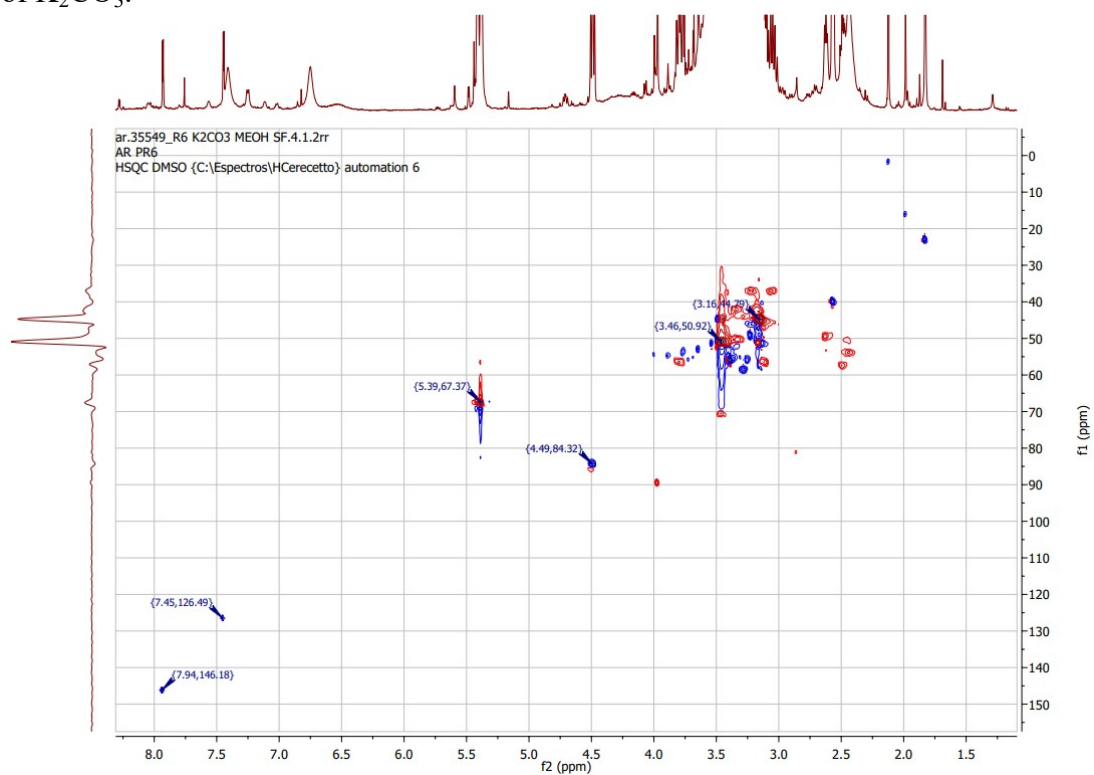


Figure S38. $^1\text{H}/^{13}\text{C}$ -HSQC spectra of starting pyrazine with Selectfluor[®] in presence of K_2CO_3 .

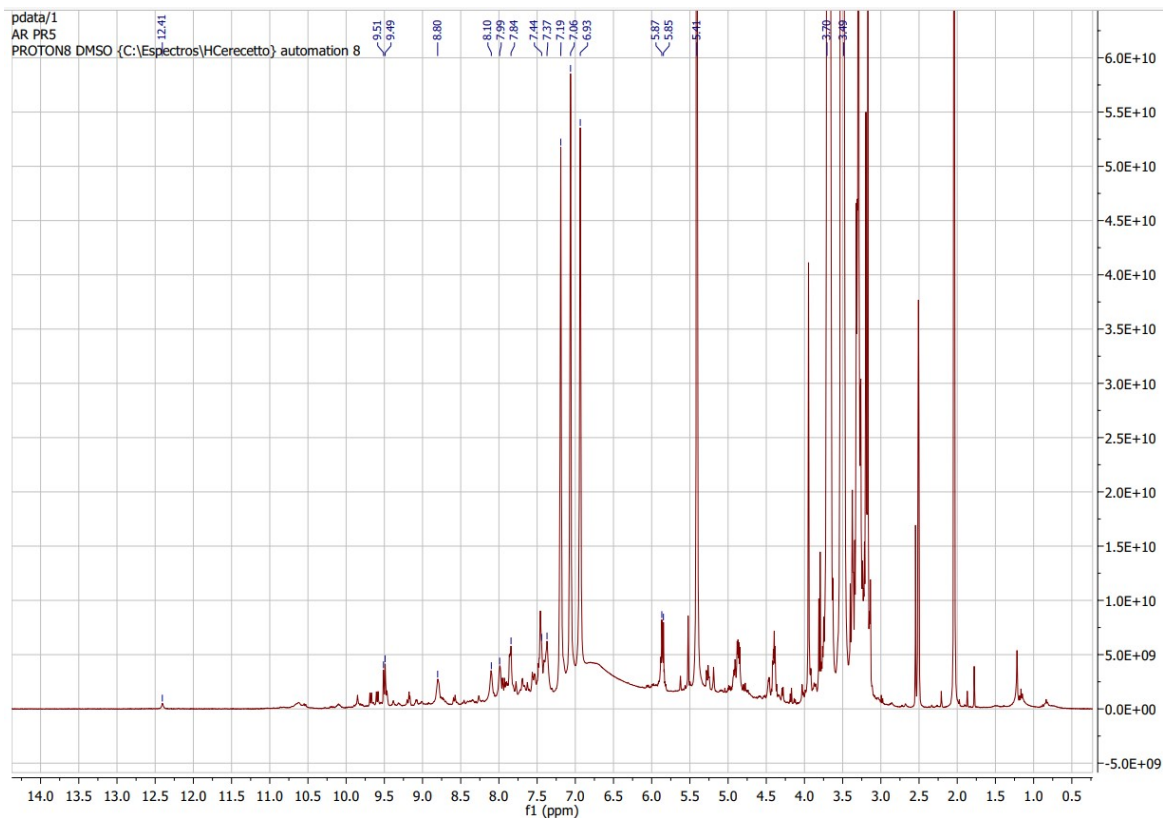


Figure S39. ^1H -NMR spectra of starting pyrazine with Selectfluor® in presence of TFA.

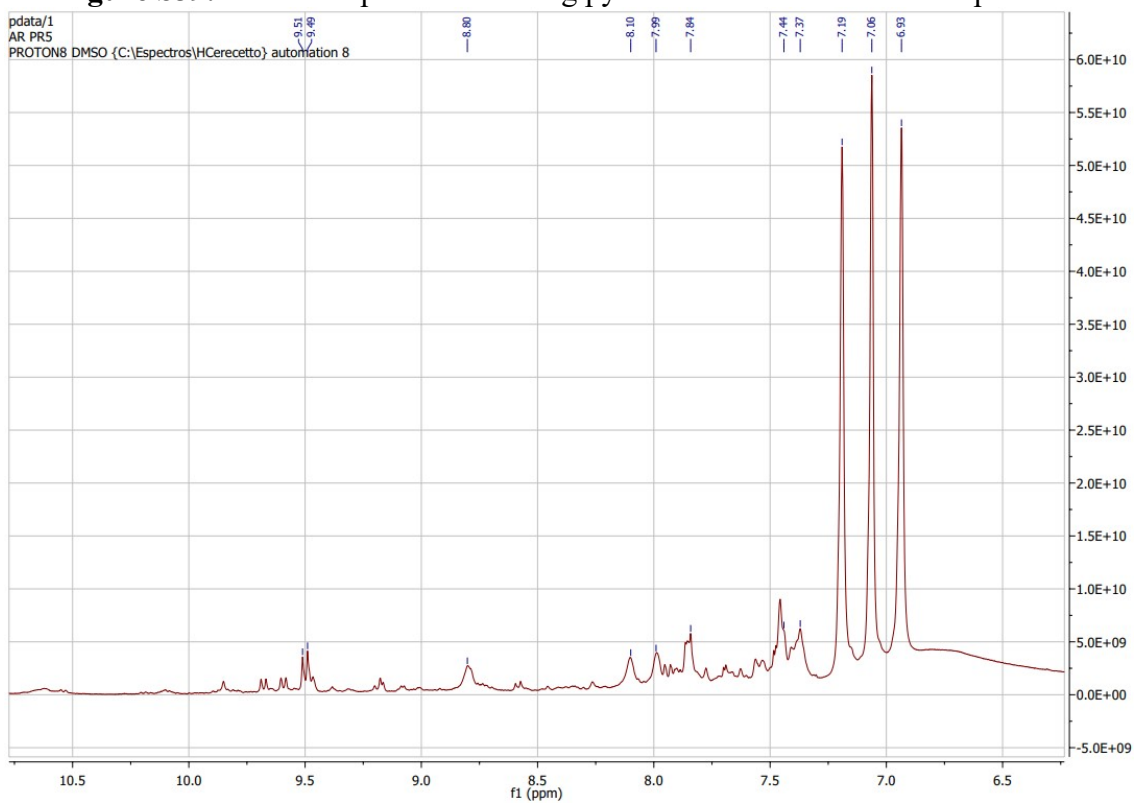


Figure S40. Ampliation of ^1H -NMR spectra of starting pyrazine with Selectfluor® in presence of TFA.

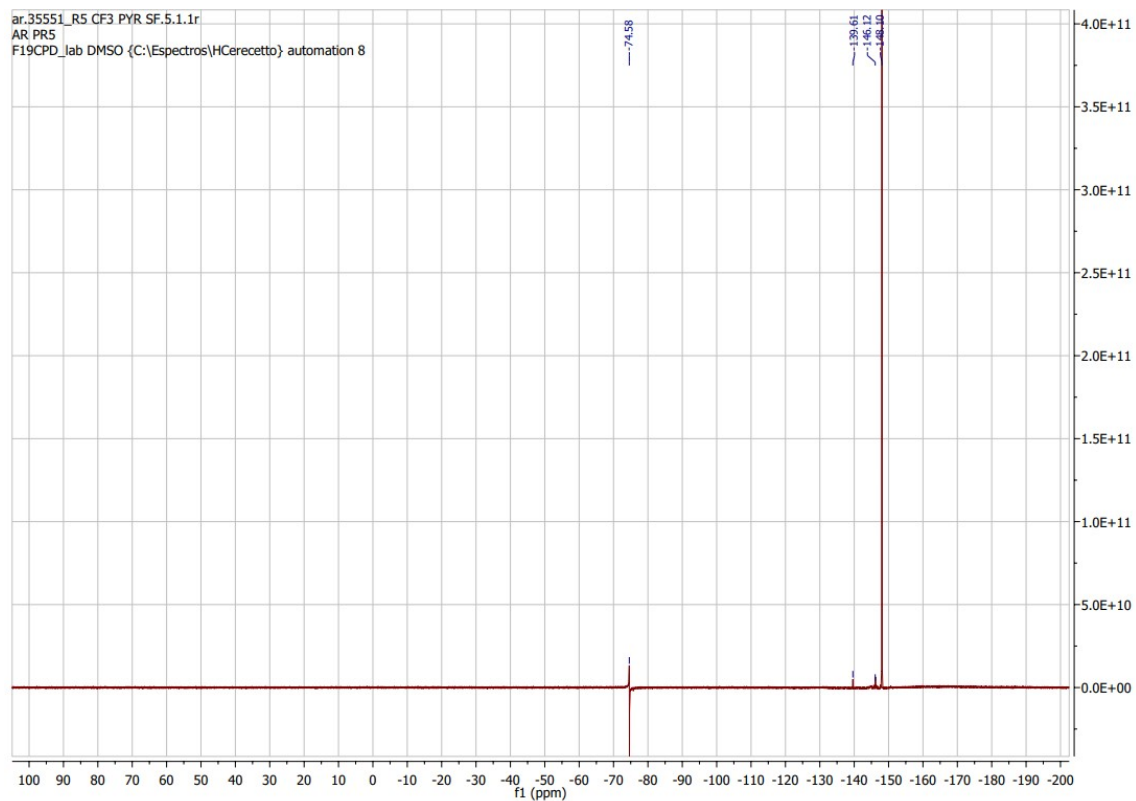


Figure S41. ^{19}F -NMR spectra of starting pyrazine with Selectfluor® in presence of TFA.

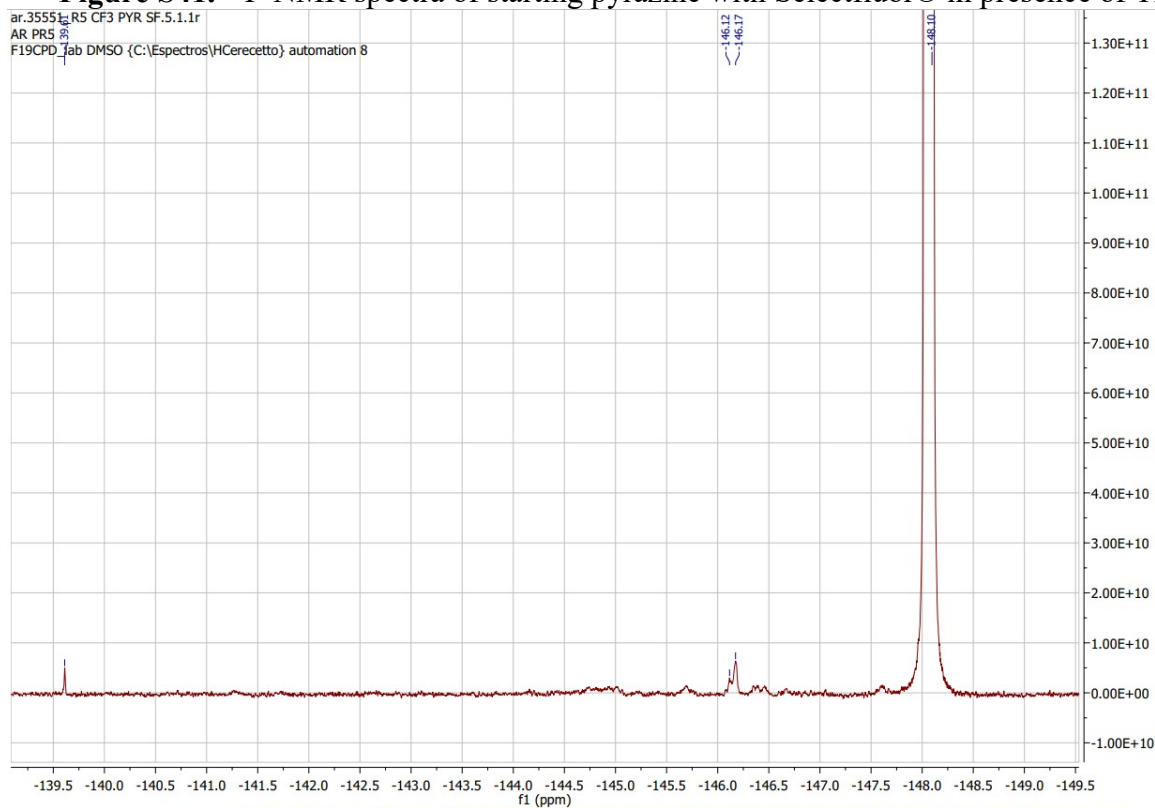


Figure S42. Ampliation of ^{19}F -NMR spectra of starting pyrazine with Selectfluor® in TFA.

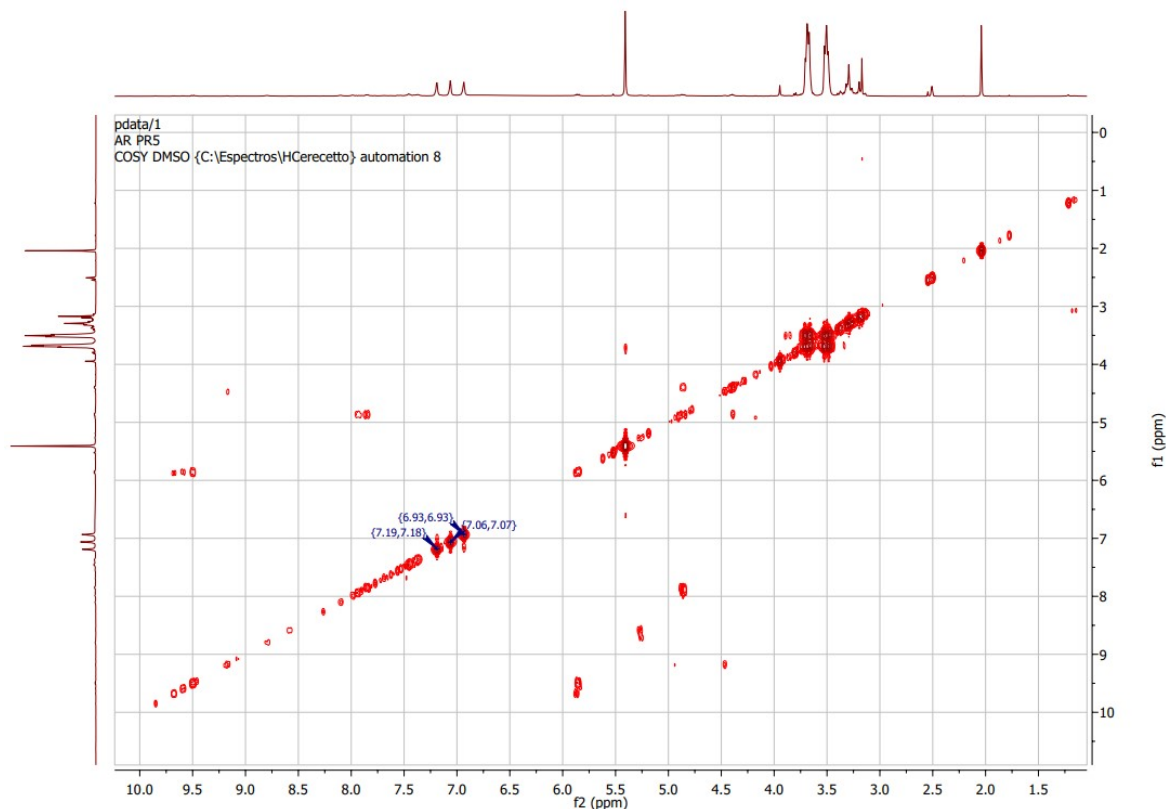
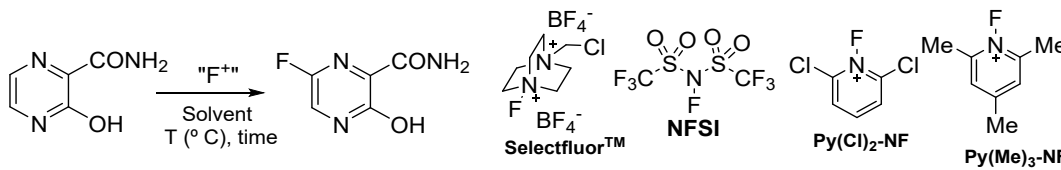


Figure S43. $^1\text{H}/^1\text{H}$ -COSY spectra of starting pyrazine with Selectfluor® in presence of TFA.

2.6. Effect of Fluorinating agent

The best conversion of 3-hydroxy-pyrazine-2-carboxamide to favipiravir was found by using Selectfluor® with a reaction yield (50.08%) in $\text{BF}_4\text{-BMIM}$ (entry 1, Table S1), which was improved by 1.7-fold more than reaction in acetonitrile (entry 2, Table S1). The rest of fluorinating agents showed so lower conversion than Selectfluor®, finding the best results for *N*-fluorosulphoimide (NFSI) (11.12 %) in $\text{BF}_4\text{-BMIM}$ (entry 3, Table S1). *N*-Fluoropyridiniums, *N*-fluoro-2,6-dochloropyridinium and *N*-fluoro-2,4,6-trimethylpyridinium, showed poor yields of 2.26 and 4.96 % (entries 7 and 11, Table S1), respectively, whereas only traces were detected from silver (II) difluoride as fluorinating agent (entries 15-17, Table S1). $\text{BF}_4\text{-BMIM}$ improved the fluorination with NFSI and *N*-fluoropyridiniums compared to those reaction performed in acetonitrile or water (entries 5-6, 9-10 and 13-14, Table S1), but the fluorination was limited. Increase of temperature did not improved the fluorination efficacy (entries 4, 8 and 12, Table S1). The poor reactivity of *N*-fluoropyridinium supposed that the fluorination of 3-hydroxy-pyrazine-2-carboxamide seems to be incompatible with ionic mechanism.

Table S1. Effect of fluorinating agent


Entries	Solvent ^a	Fluorinating agent	T (°C) ^b	Yield (%) ^c
1	BF ₄ -BMIM (20 eq.)	Selectfluor® (1.4)	80	50
2	MeCN	Selectfluor® (1.4)	80	30
3	BF ₄ -BMIM (20 eq.)	NFSI (1.4)	80	11
4	BF ₄ -BMIM (20 eq.)	NFSI (1.4)	100	11
5	MeCN	NFSI (1.4)	80	3
6	MeCN-H ₂ O (8 eq.)	NFSI (1.4)	80	6
7	BF ₄ -BMIM (20 eq.)	Py(Cl) ₂ NF (1.4)	80	2
8	BF ₄ -BMIM (20 eq.)	Py(Cl) ₂ NF (1.4)	100	2
9	MeCN	Py(Cl) ₂ NF (1.4)	80	1
10	MeCN-H ₂ O (8 eq.)	Py(Cl) ₂ NF (1.4)	80	3
11	BF ₄ -BMIM (20 eq.)	Py(Me) ₃ NF (1.4)	80	5
12	BF ₄ -BMIM (20 eq.)	Py(Me) ₃ NF (1.4)	100	4
13	MeCN	Py(Me) ₃ NF (1.4)	80	2
14	MeCN-H ₂ O (8 eq.)	Py(Me) ₃ NF (1.4)	80	5
15	MeCN	AgF ₂ (3.0)	25	Traces
16	THF	AgF ₂ (3.0)	25	Traces
17	MeCN	AgF ₂ -K ₂ S ₂ O ₈ (0.3)	25	Traces

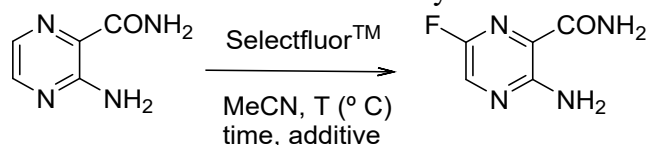
BMIM: *n*-butyl-methylimidazolium. ^aThe reactions in organic solvent were conducted at 0.1 M concentration. ^bReactions were performed for 24 h. ^cPurification yield was determined from HPLC/UV-Vis and fluorescence measurements.

2.7. Effect of Metallic Catalyst and Additives

We explored the effect of metallic catalyst, that typically are used for radical fluorination by using Selectfluor® such as AgNO₃ and CuSO₄ (entries 3 and 4, Table S2),^{13,14} some Lewis acids like Fe(II), AlCl₃, BF₃-THF, Pb(AcO)₂ and HgO (entries 5-14, Table S2), additives of ILs (entries 15-25, Table S2) and, a Brønsted acid (TFA) (entries 26-27, Table S2). The use of Lewis acids sought to activate the N---F bond in Selectfluor® by direct interaction M---F---N and, the reactions were performed in acetonitrile. ILs as additive were explored in order to develop a less-dependent IL protocol for a more suitable scalable purpose. From the catalysts, silver (I) was the most convenient giving a moderate reaction yield by about 46 %, followed by Pb(OAc)₂ (40 %) and Al(NO₃)₃ (38 %). Decrease in reaction yields were found for Cu (II) (17 %), Fe (II) (22 %), Hg (II) (24 %) and more for BF₃ (6 %). Lower reaction yields were obtained with decrease of reaction temperature to percentages from 18 to 21 for the better catalyst of Ag (I), Pb (II) and Al (III) (entries 10-12, Table S2). Use of pyridine as convenient radical initiator in presence of silver (I)¹⁴ affected the fluorination compared to silver (I) as sole catalyst (entries 14-15, Table S2). With the

IL as additive, BF₄-BMIM provided improvements in reaction yield compared to reaction in absence of the IL (entry 15 vs. entry 1, Table S2). PF₆-BMIM did not provided improvements (entry 16, Table S2). Change of solvent did not provide improvements in reaction yields (entries 17-20, Table S2). Reduction of yield from 42 to 38 % was obtained with decrease of BF₄-BMIM quantity (entry 21, Table S2) and, interestingly, large amount of the IL (10 eq.) in acetonitrile lead a significant decrease of reaction yield from 42 to 26 % (entry 22, Table S2). Regarding to equivalent of Selectfluor®, 1.4 and 1.7 equivalent of Selectfluor® were appropriated for the highest yields, whereas 2.0 equivalent did not provide improvements (entries 23-24, Table S2). TFA as Lewis acid catalyst or additive increased barely the reaction yields compared to reaction in without acid (entries 26-27, Table S2).

Table S2. Effect of metallic catalysts and additives



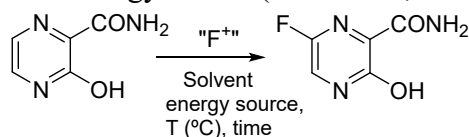
Entries	Solvent ^a	Catalysts/additive	Eq. SF	T (°C)	t (h)	Yield (%) ^b
1	MeCN	None	1.7	80	24	31
2	BF ₄ -BMIM (20 eq.)	None	1.7	80	24	50
3	MeCN	AgNO ₃ (0.12 eq.)	1.4	80	24	46
4	MeCN	CuSO ₄ (0.30 eq.)	1.4	80	24	17
5	MeCN	BF ₃ (0.6 eq.)	1.4	80	24	6
6	MeCN	Al(NO ₃) ₃ (0.14 eq.)	1.4	80	24	38
7	MeCN	HgO (0.30 eq.)	1.4	80	24	24
8	MeCN	Pb(OAc) ₂ (0.14 eq.)	1.4	80	24	39
9	MeCN	FeSO ₄ (0.3 eq.)	1.4	80	24	24
10	MeCN	AgNO ₃ (0.12 eq.)	1.4	65	48	22
11	MeCN	Al(NO ₃) ₃ (0.13 eq.)	1.4	65	48	19
12	MeCN	Pb(OAc) ₂ (0.14 eq.)	1.4	65	48	17
13	MeCN	AgNO ₃ (0.12 eq.)-Py	1.4	80	24	22
14	MeCN	AgNO ₃ (0.12 eq.)-4DAMP	1.4	80	24	19
15	MeCN	BF ₄ -BMIM (2.0 eq.)	1.4	80	24	43
16	MeCN	PF ₆ -BMIM (0.48 eq.)	1.4	80	24	32
17	DCE:DMF (10:1)	BF ₄ -BMIM (2.0 eq.)	1.4	80	24	5
18	THF	BF ₄ -BMIM (2.0 eq.)	1.4	80	24	9
19	Dioxane	BF ₄ -BMIM (2.0 eq.)	1.4	80	24	22
20	DMF	BF ₄ -BMIM (2.0 eq.)	1.4	80	24	21
21	MeCN	BF ₄ -BMIM (0.68 eq.)	1.4	80	24	38
22	MeCN	BF ₄ -BMIM (10 eq.)	1.4	80	24	26
23	MeCN	BF ₄ -BMIM (2.0 eq.)	1.7	80	24	42
24	MeCN	BF ₄ -BMIM (2.0 eq.)	2.0	80	24	35
25	MeCN	BF ₄ -BMIM (2.0 eq.)	1.4	65	48	23
26	MeCN	TFA (0.39 eq.)	1.4	80	24	36
27	MeCN	TFA (1.2 eq.)	1.4	80	24	36

BMIM: *n*-butyl-methylimidazolium; Py: pyridine, 4DAMP: *N,N'*-dimethylaminopyridine. ^aThe reactions in organic solvent were conducted at 0.1 M concentration. ^bPurification yield was determined from HPLC/UV-Vis and fluorescence measurements.

2.8. Effect of Energy Source

Other energy source such as ultrasound, microwave and UV light were proven; however, not improvements were found with respect to standard condition (entries 1-2, Table S3). Reaction upon excitation under different conditions of temperature, solvent or fluorinating agent (Selectfluor® or NFSI) did not lead improvements in reaction yields (entries 3-10, Table S3). Ultrasound provided good results, more approximated to standard condition with reaction yield of 38 and 42% for acetonitrile-BF₄-BMIM (2 eq.) and BF₄-BMIM (20 eq.), respectively, but it is not an accurate solution regard to standard condition (50 %, entry 1, Table S3). Microwave tool provided conversion of 20 % in 10 minutes, which was an improvement compared to the prolonged times needed for conventional heating, but it is not represent an alternative for obtaining accurate reaction yields (> 50 %). High energy and prolongation in times induced decomposition of IL.

Table S3. Effect of energy source (ultrasound, MW and UV light)



Entry	Solvent ^a	F ⁺ -source (eq.)	Eq. SF	T (°C)	t (h)	Yield (%) ^b
1	MeCN	SF (1.7)	1.7	80	24	31
2	BF ₄ BMIM (20 eq.)	SF (1.7)	1.7	80	24	50
3	BF ₄ BMIM (20 eq.)	SF (1.7 eq.)	UV	70	12	29
4	BF ₄ BMIM (20 eq.):40 eq H ₂ O	SF (1.7 eq.)	UV	70	12	31
5	BF ₄ BMIM (20 eq.):40 eq H ₂ O	SF (1.7 eq.)	UV	50	12	19
6	DCE	SF (1.7 eq.)	UV	70	12	5
7	MeCN	SF (1.7 eq.)	UV	70	12	8
8	DMF	SF (1.7 eq.)	UV	70	12	6
9	BF ₄ -BMIM (20 eq.)	NFSI (1.5)	UV	80	12	7
10	BF ₄ -BMIM (20 eq.)	NFSI (1.5)	UV	70	24	6
11	BF ₄ -BMIM (20 eq.)	SF (1.7 eq.)	Ultrasound	80	12	42
12	MeCN-BF ₄ -BMIM (2 eq.)	SF (1.7 eq.)	Ultrasound	80	12	38
13	BF ₄ -BMIM (20 eq.)	SF (1.7 eq.)	MW	80	10 min	desc. IL
14	MeCN + BF ₄ -BMIM (0.4 eq.)	SF (1.7 eq.)	MW	80	10 min	20
15	MeCN + BF ₄ -BMIM (0.4 eq.)	SF (1.7 eq.)	MW	80	20 min.	15
16	MeCN	SF (1.7 eq.)	MW	80	10 min	4
17	MeCN-BF ₄ -BMIM (0.4 eq.)	NFSI (1.5)	MW	80	10 min	Traces

BMIM: *n*-butyl-methylimidazolium. ^aThe reactions in organic solvent were conducted at 0.1 M concentration. ^bPurification yield was determined from HPLC/UV-Vis and fluorescence measurements.

2.9. Fluorination Comparison Under Different Selectfluor® Quantities

From spectra S44 to S46, it should be noted that the efficacy of the reaction was clearly dependent on the amount of Selectfluor®. The best conversion to favipiravir was appreciated to 1.7 equivalent of Selectfluor®, followed by 1.5 and lowest ratio of favipiravir was observed by using 0.8 equivalent of fluorinating agent.

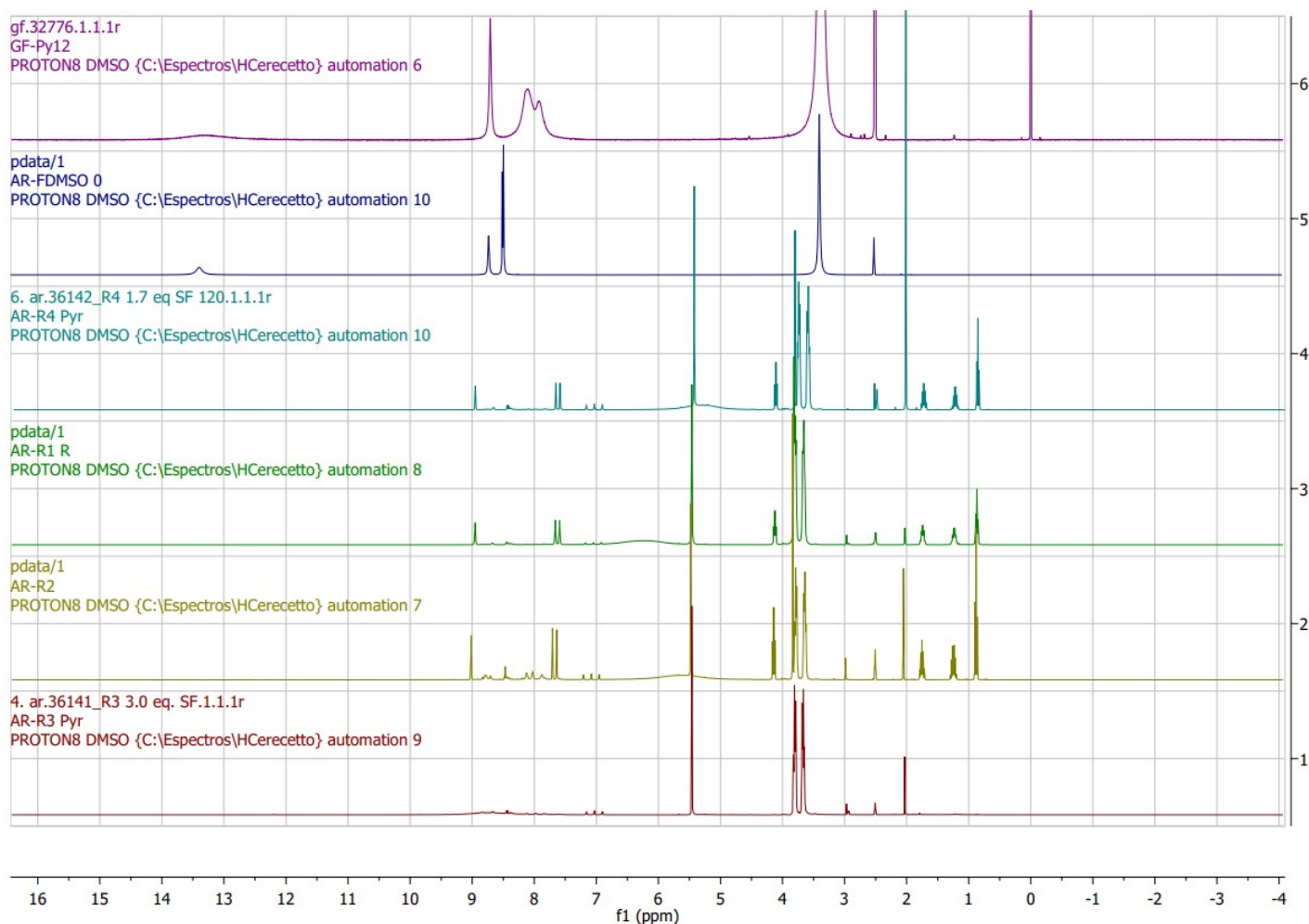


Figure S44. Reaction of starting pyrazine with Selectfluor® (S.F.) in acetonitrile: standard starting pyrazine (purple), favipiravir (blue), starting pyrazine + SF (1.7 eq.) (cyan), SF (1.4 eq.) (green), SF (0.8 eq.) (gold), SF (1.4 eq.) at 120 °C (red).

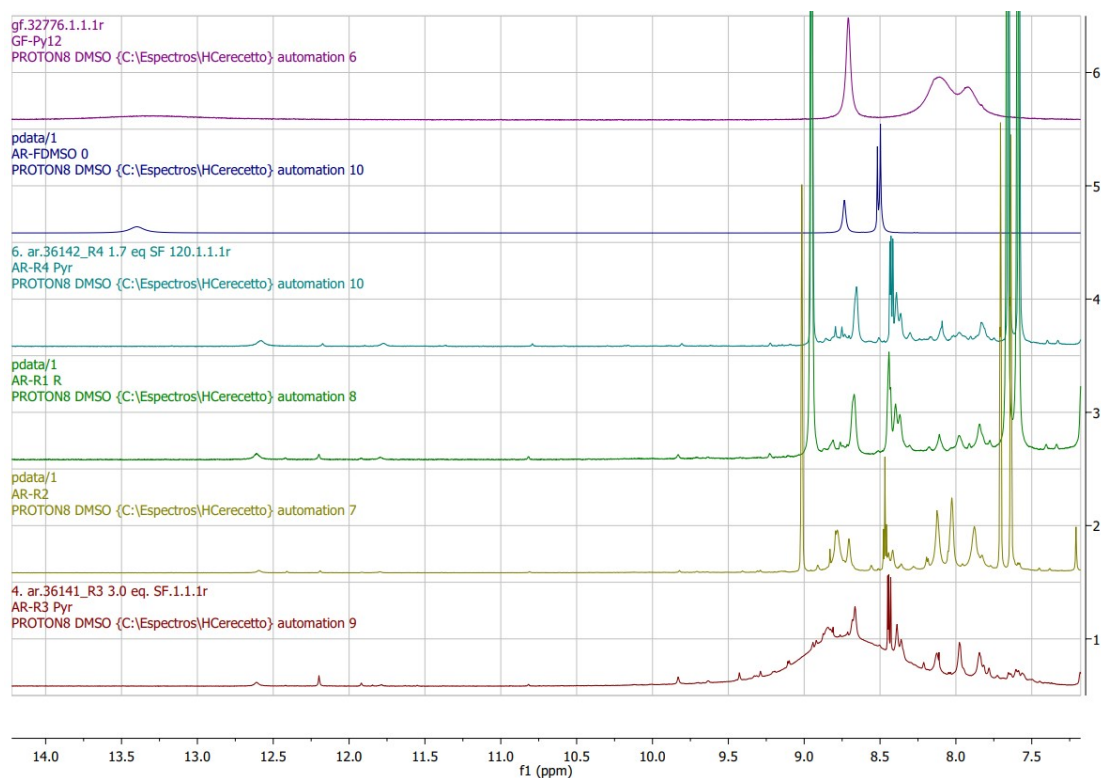


Figure S45. Standard starting pyrazine (purple), favipiravir (blue), starting pyrazine + SF (1.7 eq.) (cyan), SF (1.4 eq.) (green), SF (0.8 eq.) (gold), SF (1.4 eq.) at 120 °C (red).

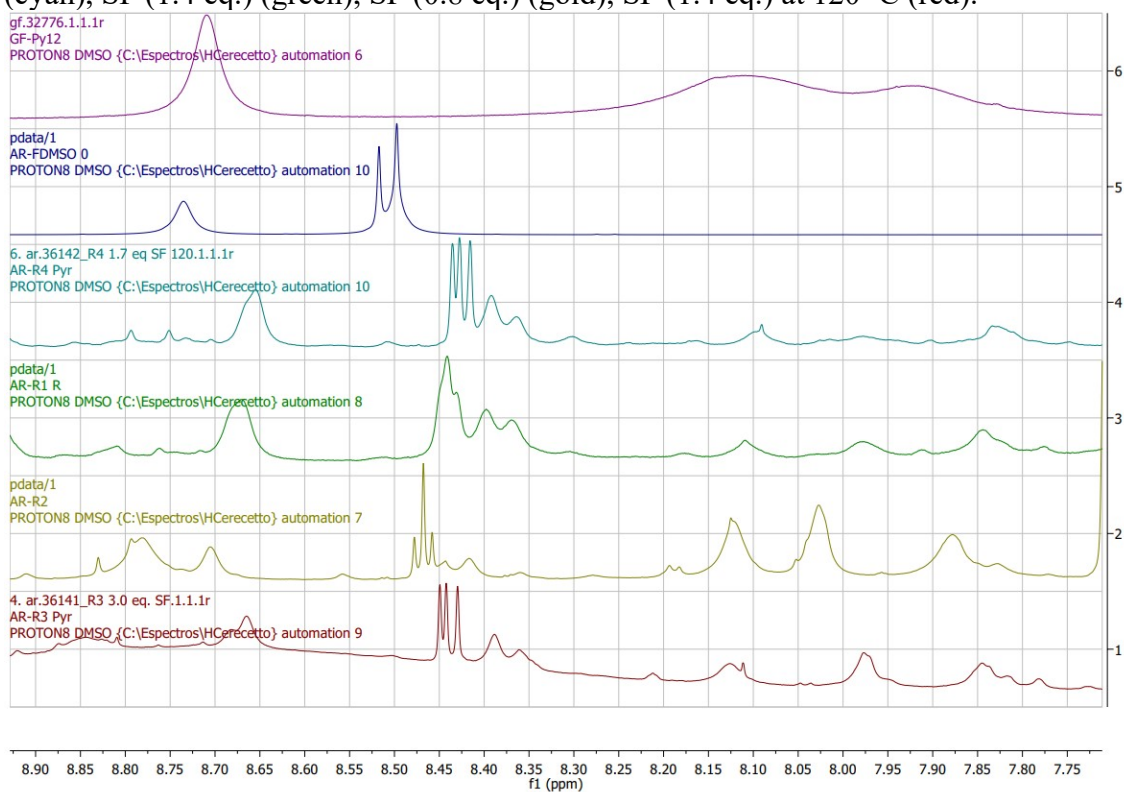
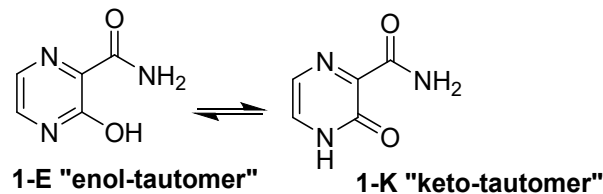


Figure S46. Standard starting pyrazine (purple), favipiravir (blue), starting pyrazine + SF (1.7 eq.) (cyan), SF (1.4 eq.) (green), SF (0.8 eq.) (gold), SF (1.4 eq.) at 120 °C (red).

2.10. Tautomeric studies (preliminary view)

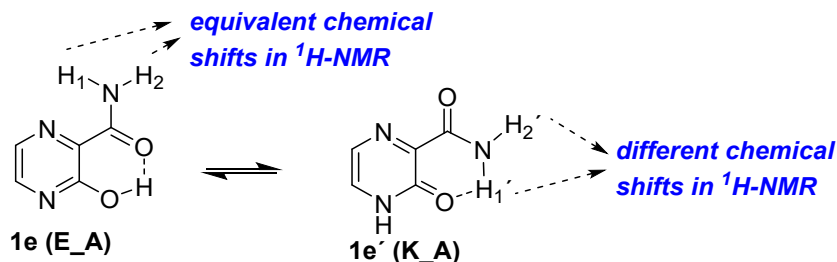
Table S4A. Keto-enol proportion for the 3-hydroxy-2-pyrazinecarboxamide **1** under different solvents.



	λ_{abs} (nm) (enol-keto ratio) ^a						AcOH
	Gas phase ^b	H ₂ O	MeOH	MeCN	DMSO	DMSO/BF ₄ -BMIM	
1	279.4/320.0	310/348 (0.0)	312/346 (1.2)	302/348 (4.8)	308/356 (1.9)	308/356 (1.6)	344 (0.0)

^aEnol-keto ratio was estimated from a mean between the total areas of the absorption enol- (lower band) and keto- (higher band) wavelengths as follow: A_{enol}/A_{keto} . ^bTheoretical absorption wavelengths calculated in gas phase (B3LYP/6-31G(d,p)).

Table S4B. Chemical shift differences between carboxamide (NH)-protons in ¹H-NMR spectra for the 3-hydroxy-2-pyrazinecarboxamide **1e** under different solvents at 25 °C.



	$\Delta\delta$ (ppm) (range)				
	H ₂ O	MeOH	MeCN	DMSO	DMSO/BF ₄ -BMIM
1e	1.04 (8.93-7.89)	0.82 (8.86-8.04)	0.65 (8.74-8.09)	0.58 (8.70-8.12)	0.64 (8.82-8.18)

Details can be found in our next publication about the tautomerism of 3-hydroxy-2-pyrazinecarboxamide in solid and solution states. In general, from Tables S4a and S4b, it should be noted that that keto-tautomer is dominant in protic solvent like water and acetic acid and dominance of the enol-tautomer under no protic solvent like acetonitrile and DMSO. It suggested that the 3-hydroxy-2-pyrazinecarboxamide was found under enol-tautomer for reaction, which were performed in acetonitrile in most of the case. The addition of BF₄-BMIM in DMSO increased barely the keto-tautomerism, which was evidenced by higher differences in chemical shifts of carboxamide-protons. The latter reflects the potential of the BF₄-BMIM for favoring the keto-tautomerism, although further investigation are needed for a higher keto-tautomerization.

3. Mechanistic Experiments

3.1. Reactions with Radical Scavengers

General procedure: In determining whether or not our reaction occurred via a radical pathway, (2,2,6,6-Tetramethylpiperidin-1-yl)oxyl (TEMPO, 24 mg, 0.16 mmol, 1.2 equiv.) or 2,6-di(*t*-butyl)-4-hydroxytoluene (BHT, 37 mg, 0.17 mmol, 1.2 equiv.) was added to reactions and observed how it affected the product yields. NMR spectra were then obtained. From TEMPO experiment, only 3-hydroxy-pyrazine-2-carboxamide, H-TEDA-BF₄ and different forms of TEMPO were appreciated from ¹H-NMR, ¹³C-NMR and ¹H/¹H-COSY (Figure S47-S50). Then, the no detection of product suggested that a radical mechanism could be involved. A tentative mechanism was proposed for the disruption of the radical fluorination, where the radical forms of pyrazine and Selectfluor® derived from pyrazine-Selectfluor® interaction were trapped by TEMPO as electron-donor regenerating the starting pyrazine and H-TEDA-BF₄ (Figure S51). It generated two molecules of oxidized form of TEMPO.

Meanwhile, from reactions in presence of BHT, a chemical specie derived from coupling between 3-hydroxy-pyrazine-2-carboxamide and BHT was identified (Figure S53), where the oxygen of pyrazine is covalently connected with benzylic carbon of BHT to form intermediate. From ¹H-NMR, no evidence of starting pyrazine and small amount of BHT was observed. Aromatic proton of pyrazine ring change from values by about 8.10-8.00 to 6.75 and 6.81 ppm (Figure S54-S55), which were correlated accordingly ¹H/¹H-COSY (Figure S56). ¹H/¹³C-HSQC confirmed the different CH aromatic protons (Figure S57). ¹H/¹³C-HMBC confirmed correlation between pyrazine proton with benzylic carbon and CH aromatic proton of BHT fragment (Figure S58). All these evidences suggested that the fluorination of the 3-hydroxy-pyrazine-2-carboxamide by Selectfluor® is mediated by a radical pathway, which involves the formation of a radical derived from Selectfluor® and a radical from starting pyrazine also is formed. Mechanism radical pathway for the fluorination was proposed in the main manuscript (Scheme 5).

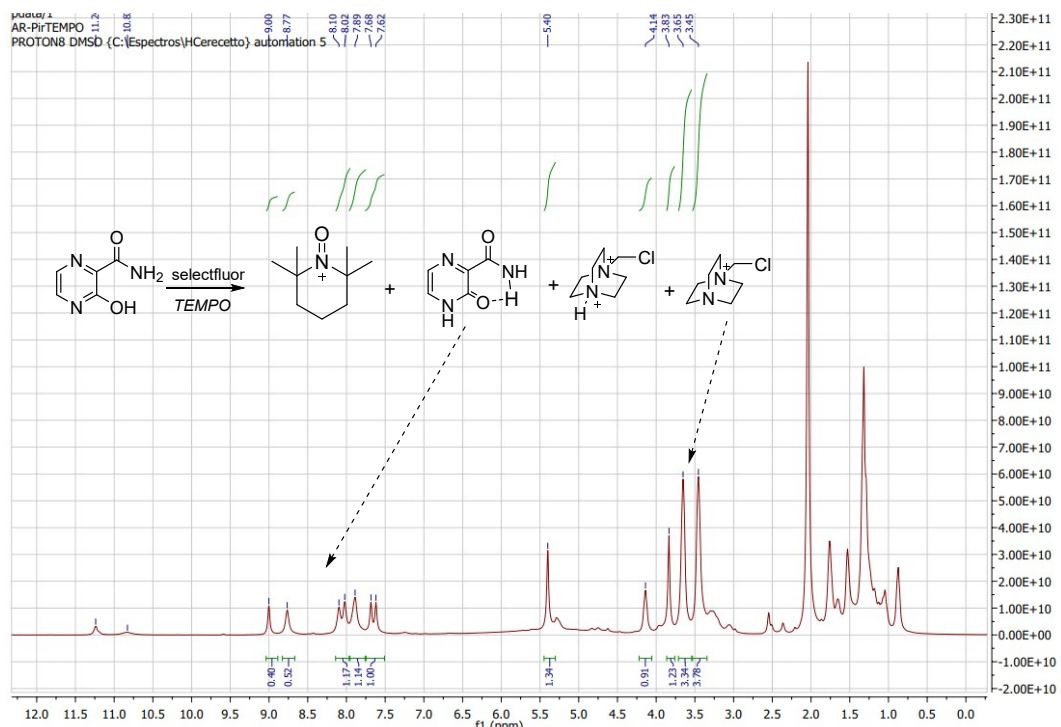


Figure S47. ^1H -NMR of 3-hydroxy-pyrazine-2-carboxamide in $\text{BF}_4\text{-BMIM}$ in presence of Selectfluor[®] and TEMPO.

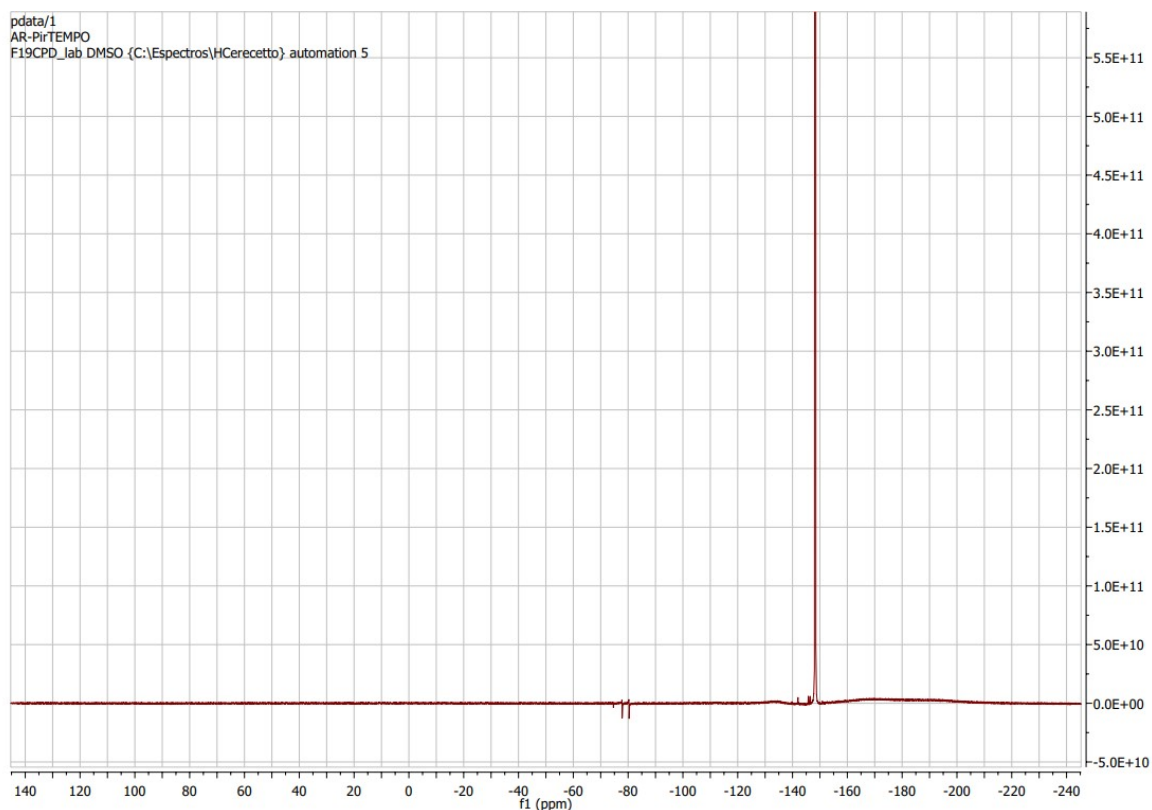


Figure S48. ^{19}F -NMR of 3-hydroxy-pyrazine-2-carboxamide in $\text{BF}_4\text{-BMIM}$ in presence of Selectfluor[®] and TEMPO.

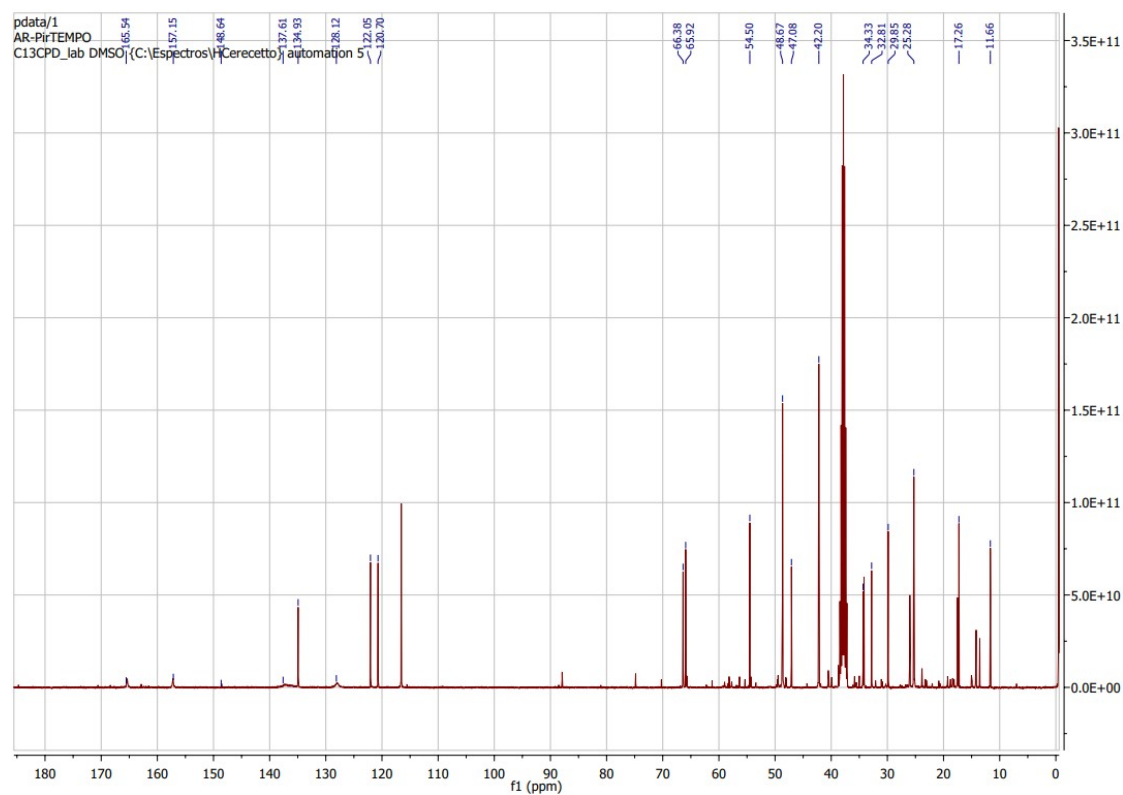


Figure S49. ^{13}C -NMR of 3-hydroxy-pyrazine-2-carboxamide in $\text{BF}_4\text{-BMIM}$ in presence of Selectfluor® and TEMPO.

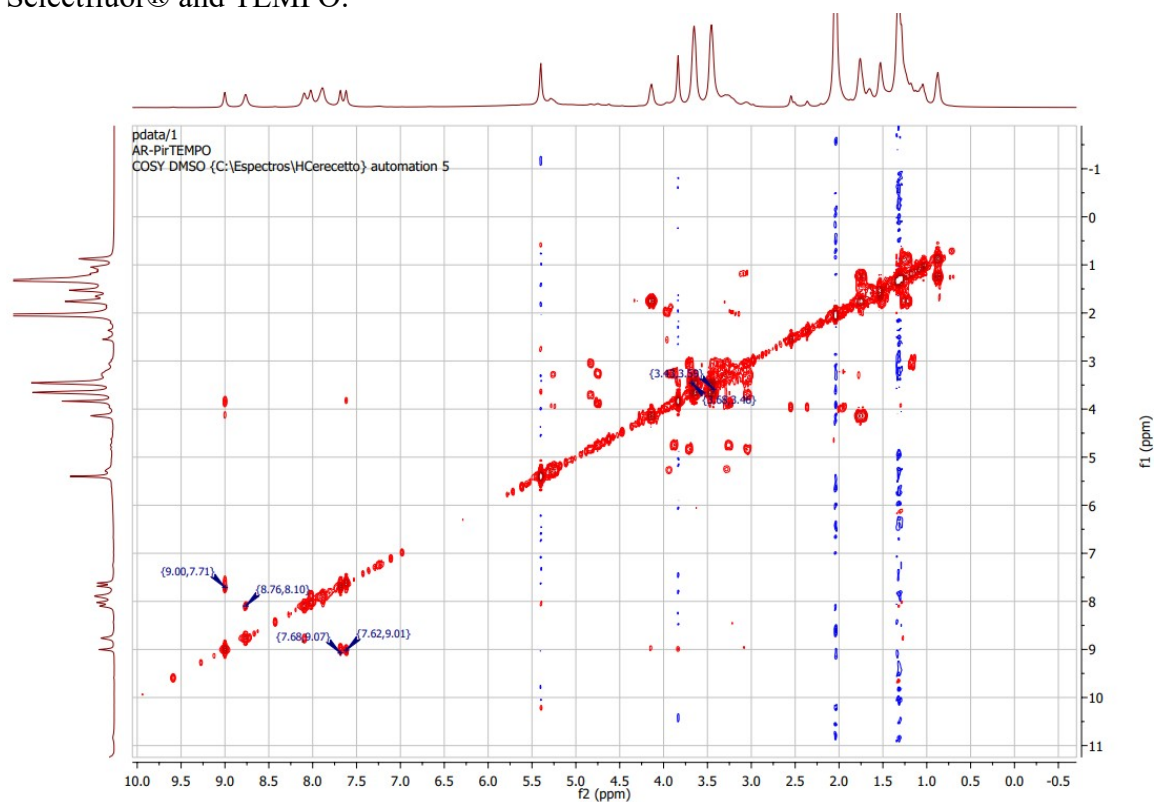


Figure S50. $^1\text{H}/^1\text{H}$ -COSY of 3-hydroxy-pyrazine-2-carboxamide in $\text{BF}_4\text{-BMIM}$ in presence of Selectfluor® and TEMPO.

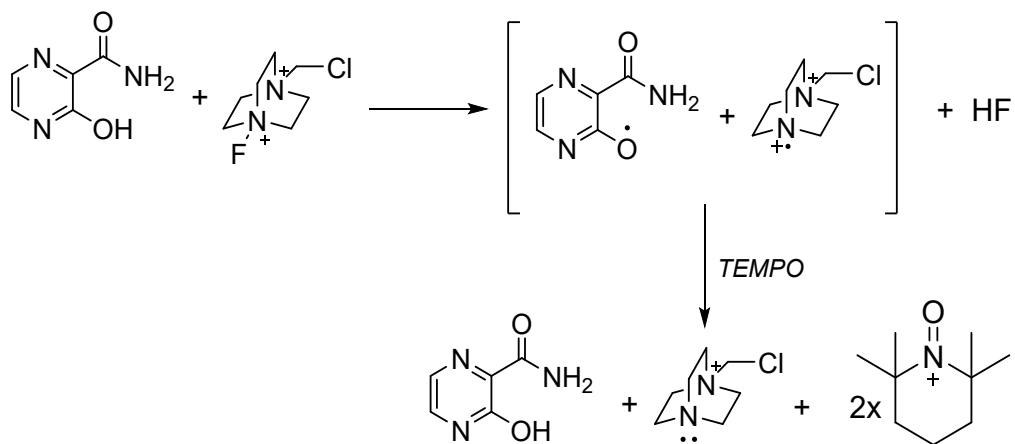


Figure S51. Tentative disruption of radical fluorination of 3-hydroxy-pyrazine-2-carboxamide by TEMPO.

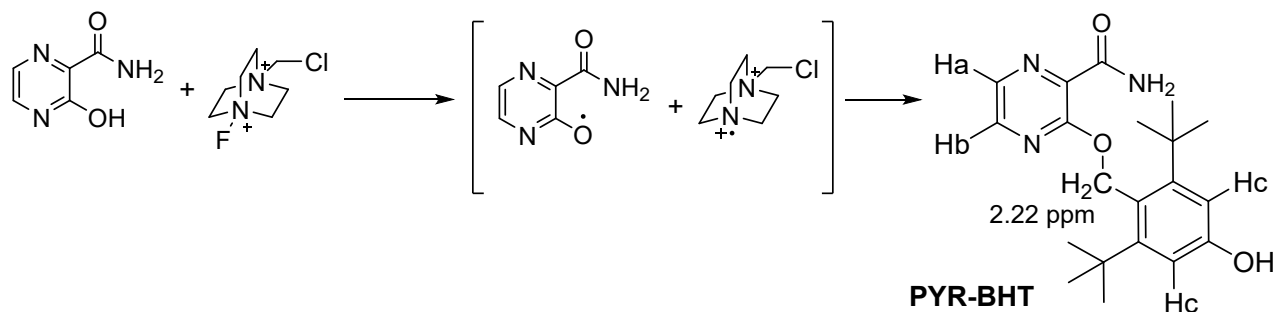


Figure S52. Tentative disruption of radical fluorination of 3-hydroxy-pyrazine-2-carboxamide by BHT through formation of PYR-BHT.

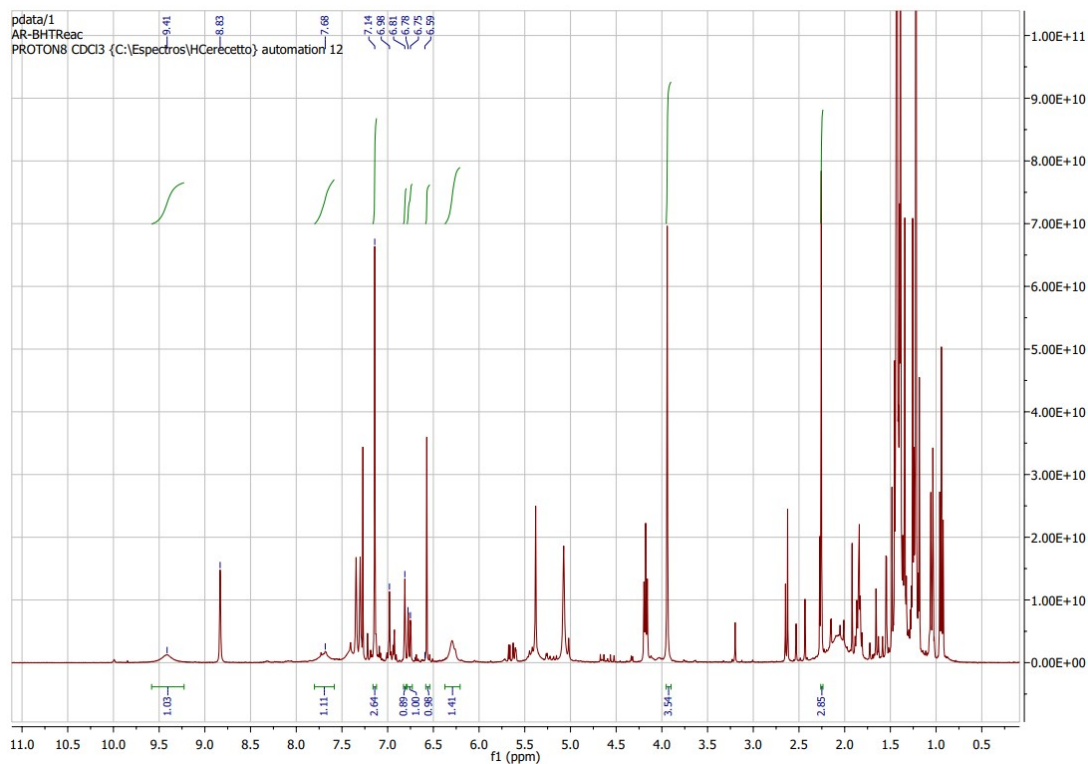


Figure S53. $^1\text{H-NMR}$ of 3-hydroxy-pyrazine-2-carboxamide in $\text{BF}_4\text{-BMIM}$ in presence of Selectfluor® and BHT.

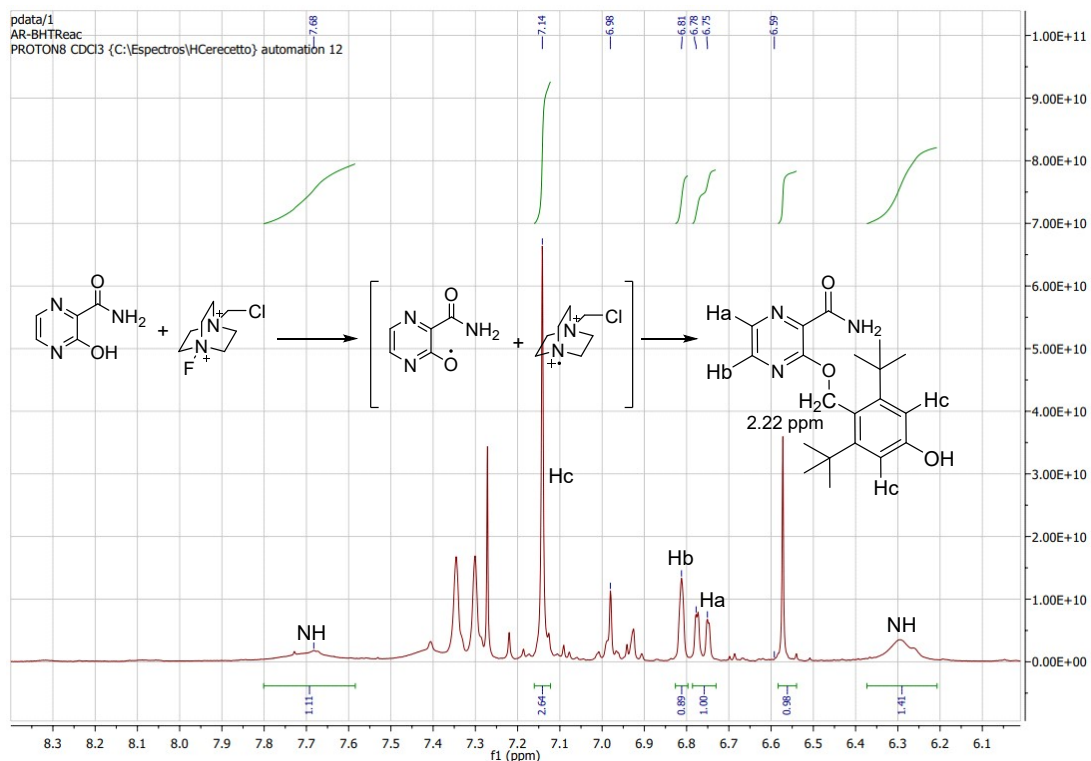


Figure S54. Amplification of $^1\text{H-NMR}$ of 3-hydroxy-pyrazine-2-carboxamide in $\text{BF}_4\text{-BMIM}$ in presence of Selectfluor® and BHT.

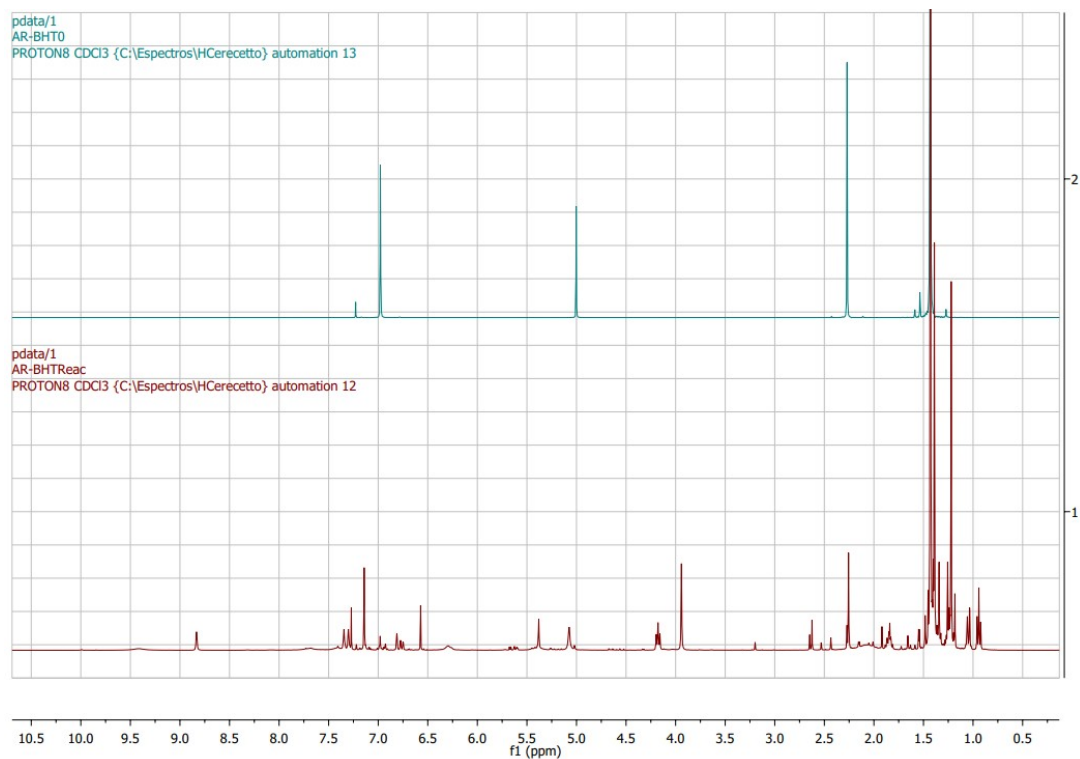


Figure S55. Superposition between ^1H -NMR spectra of 3-hydroxy-pyrazine-2-carboxamide in $\text{BF}_4\text{-BMIM}$ in presence of Selectfluor® and BHT (red spectrum) and sole BHT (blue spectrum).

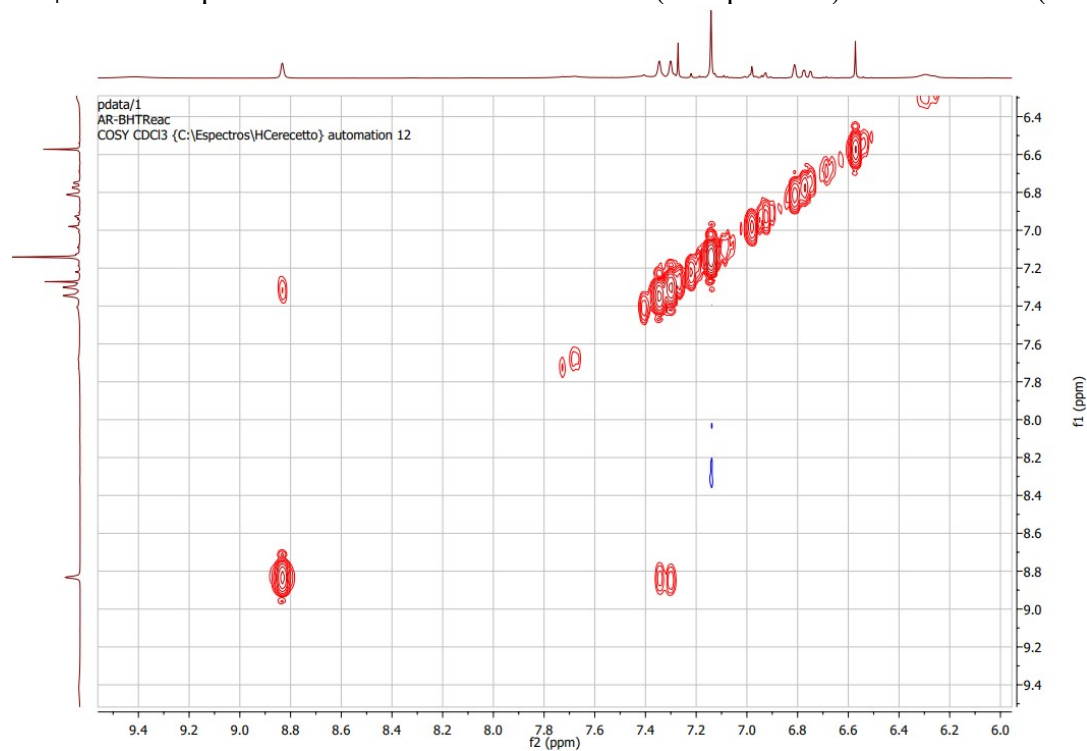


Figure S56. $^1\text{H}/^1\text{H}$ -COSY of 3-hydroxy-pyrazine-2-carboxamide in $\text{BF}_4\text{-BMIM}$ in presence of Selectfluor® and BHT.

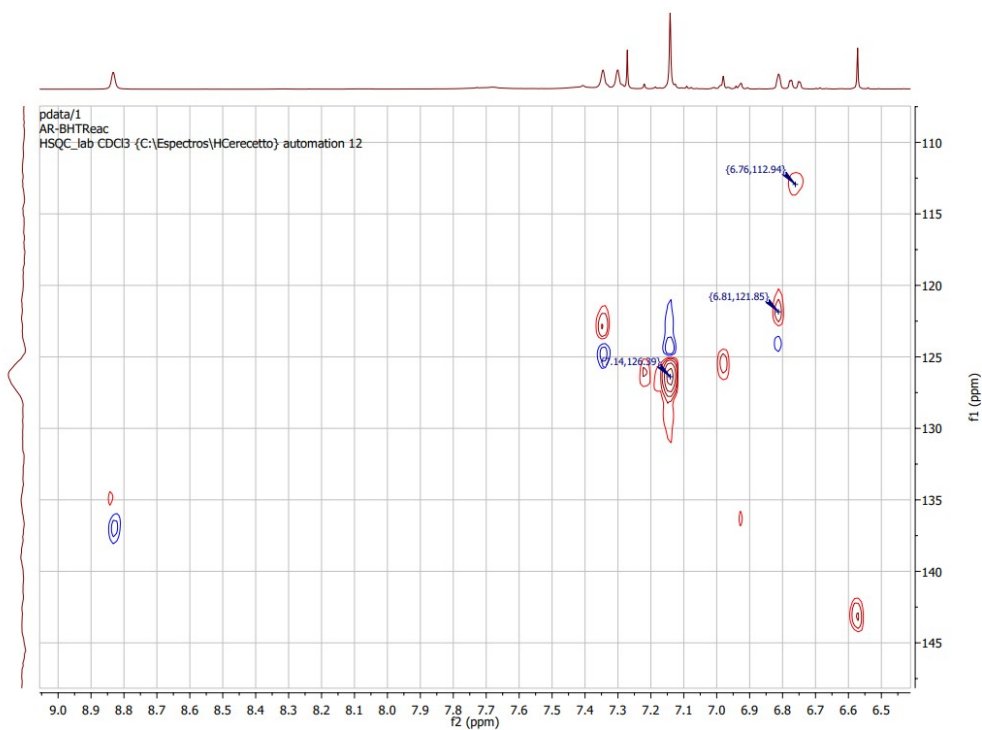


Figure S57. $^1\text{H}/^{13}\text{C}$ -HSQC of 3-hydroxy-pyrazine-2-carboxamide in $\text{BF}_4\text{-BMIM}$ in presence of Selectfluor® and BHT.

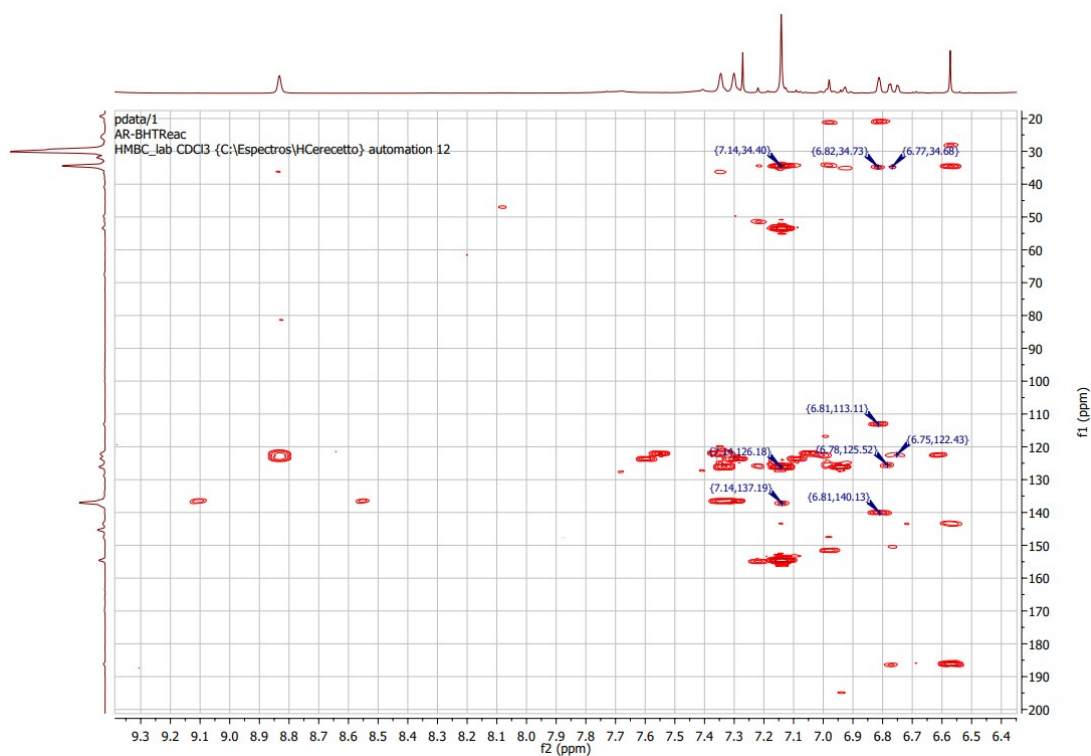


Figure S58. $^1\text{H}/^{13}\text{C}$ -HMBC of 3-hydroxy-pyrazine-2-carboxamide in $\text{BF}_4\text{-BMIM}$ in presence of Selectfluor® and BHT.

4. Mini-Scalable and Gram-scalable Synthesis of Favipiravir

4.1. General Procedure: 3-Hydroxy-pyrazine-2-carboxamide (200 mg, 1 eq., 1.44 mmol) and fluorinating agent (866-561 mg, 1.7-1.1 eq., 2.45-1.58 mmol) were added in a bottom-round flask in presence of the corresponding solvent (MeCN at 0.15 M, MeCN at 0.15 M in combination with BF₄-BMIM (2 eq.) or BF₄-BMIM (20 eq.)). Then, the reaction mixture was stirred at 80 °C for 24 h. Reactions were monitored by TLC with a solvent *n*-hexane/ethyl acetate (7/3). After 24 h, the reaction mixture was cooled at room temperature and an isolation procedure was applied depending on the nature of the solvent. For acetonitrile, solvent was evaporated through vacuum and, the resulting solid was treated with water and successive extractions with ethyl acetate (5x20 mL) were performed to obtain organic product. The solvent was evaporated to obtain a yellow solid product.

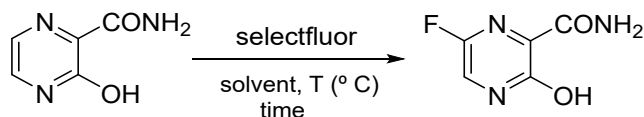
For reaction in pure BF₄-BMIM, the reaction mixture was treated with ethyl acetate (5x20 mL) to extract the favipiravir product. Solvent was evaporated through vacuum to obtain a yellow solid. The resulting solution of BF₄-BMIM was treated with chloroform to extract the IL, giving: (i) an organic phase that was evaporated to obtain the pure IL and, (ii) a solid precipitate corresponding to H-TEDA-BF₄ and “self-addition subproduct” **9** (Scheme 4A).

For acetonitrile in combination with BF₄-BMIM, first acetonitrile was evaporated and the resulting mixture was treated following the previous isolation procedure for pure BF₄-BMIM.

Finally, the resulting yellow solid for each reaction was purified through a flash chromatographic column using silice gel and *n*-hexane/ethyl acetate (7/3) to give a beige solid (0.095 g, 42.2 %). The reaction yield was reported from two separated experiments for isolated product (Table S4). The IL from chloroform phase was purified through a flash chromatographic column using alumina and chloroform as eluent obtaining a pure BF₄-BMIM (Figure S87 to S93). IL was used at least eight time without negative effect in reaction yield. Reaction was repeated at 1g-scale using 3-hydroxy-2-pyrazinecarboxamide (1.0023 g; 7.2 mmol), Selectfluor (4.3321 g; 1.7 eq.) and BF₄-BMIM (30.23 g; ~ 20 eq.), giving the desired favipiravir in a 39.6 % yield. Data for isolated product: Rf.: 0.59 (AcOEt). M.p.: 247-250 °C (dec.) (Lit.¹ 251-253 °C). ¹H-NMR (400 MHz, DMSO-*d*₆): δ

8.50-8.52 (m, 2H); 8.74 (s, 1H); 13.39 (s, 1H). ^{13}C -NMR (100 MHz, $\text{DMSO-}d_6$): δ 169.2; 160.2; 154.1-151.7 ($J = 242.0$ Hz, 1C); 136.2-135.9 ($J = 35.0$ Hz, 1C), 122.7 ($J = 7.0$ Hz, 1C). ^{19}F -NMR (500 MHz, CDCl_3): δ -92.73. EI-MS ($[\text{M}]^+$): 157.03. Found: 157.05. Spectra from Figure S83 to S86.

Table S5. Scalable synthesis of favipiravir



Entry	Solvent	Eq. Selectfluor®	T (°C) (time, h)	Yields (%) ^a
1	MeCN	1.7	80 (24)	25.28 ± 1.01 ^b
2	MeCN-BF ₄ -BMIM (2 eq.)	1.7	80 (24)	31.45 ± 1.41 ^b
3	BF ₄ -BMIM (20 eq.)	1.7	80 (24)	42.51 ± 2.12 ^b
4	BF ₄ -BMIM (20 eq.)	1.4	80 (24)	37.07 ± 2.04 ^b
5	BF ₄ -BMIM (20 eq.)	1.1	80 (24)	30.34 ± 2.10 ^b
6	BF ₄ -BMIM (20 eq.)	1.7	80 (24)	39.6 ^c

^aPurification yield was from isolated product. ^bYield percentage derived from three independent experiments. ^cReaction yield derived from a gram-scale experiment, 1 g (7.2 mmol).

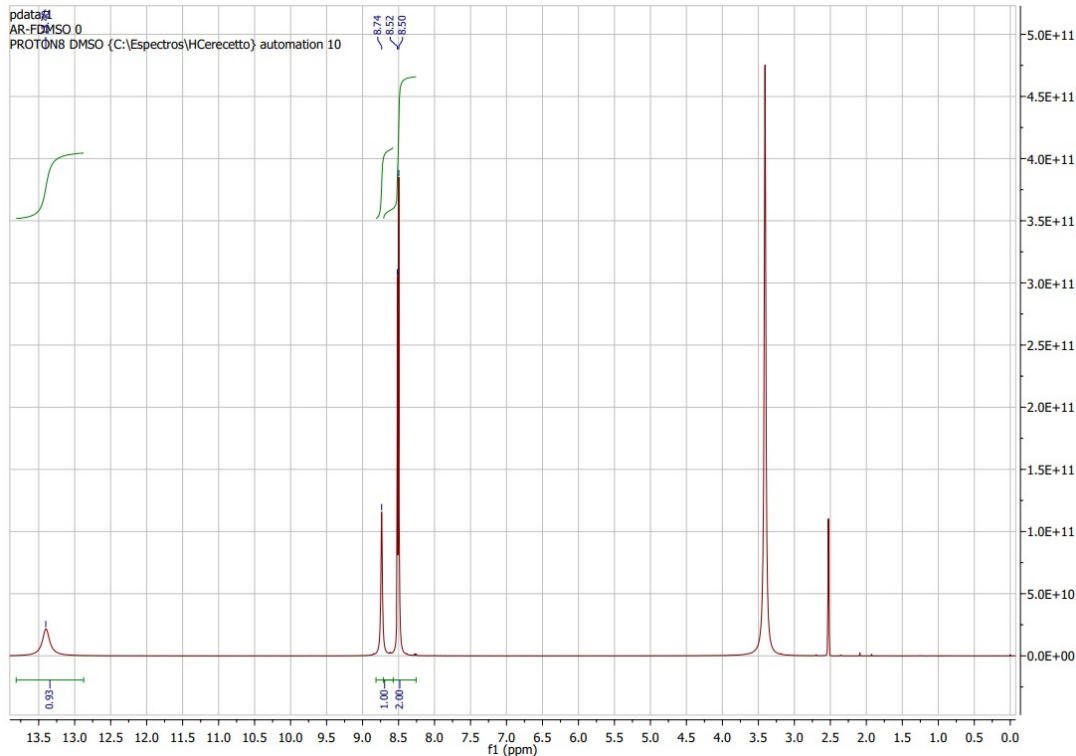


Figure S59. ^1H -NMR spectrum of favipiravir derived from fluorination of 3-hydroxypyrazine-2-carboxamide.

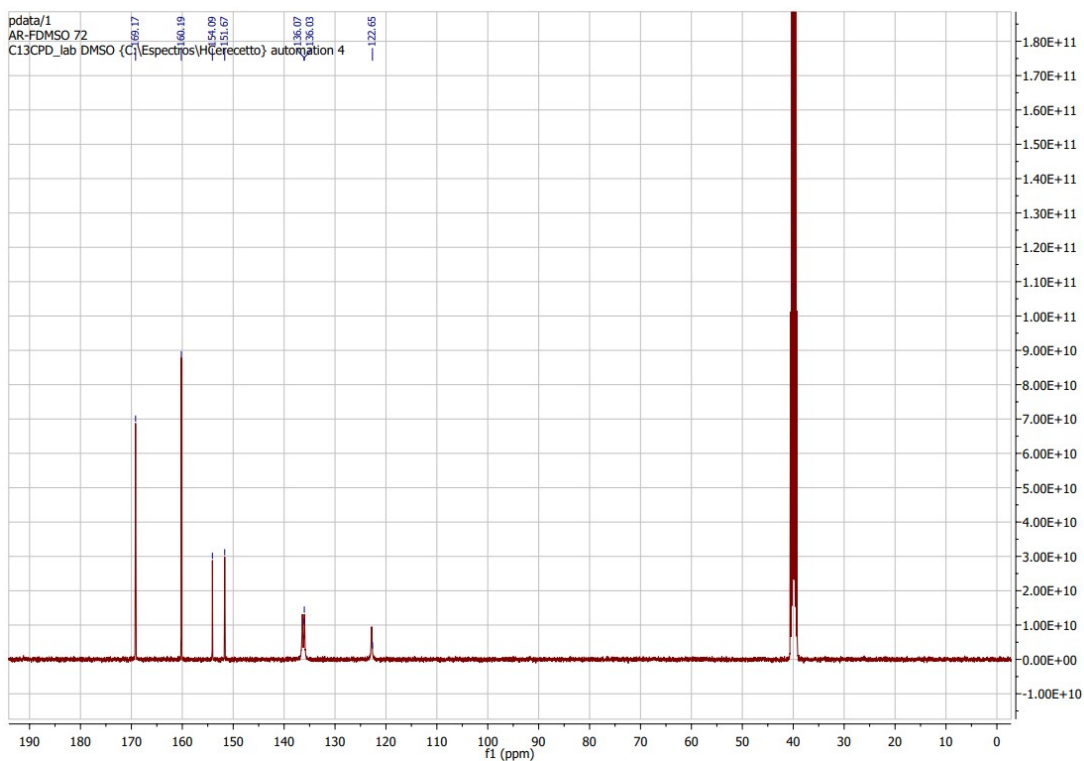


Figure S60. ^{13}C -NMR spectrum of favipiravir derived from fluorination of 3-hydroxypyrazine-2-carboxamide.

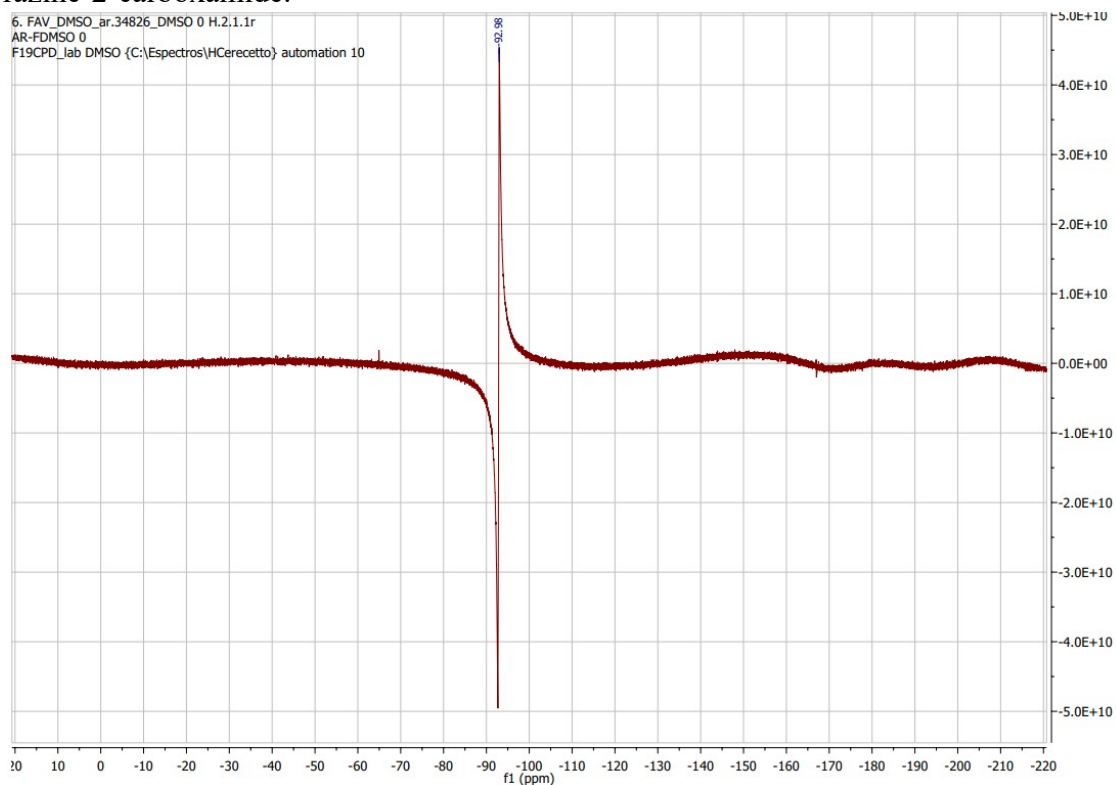
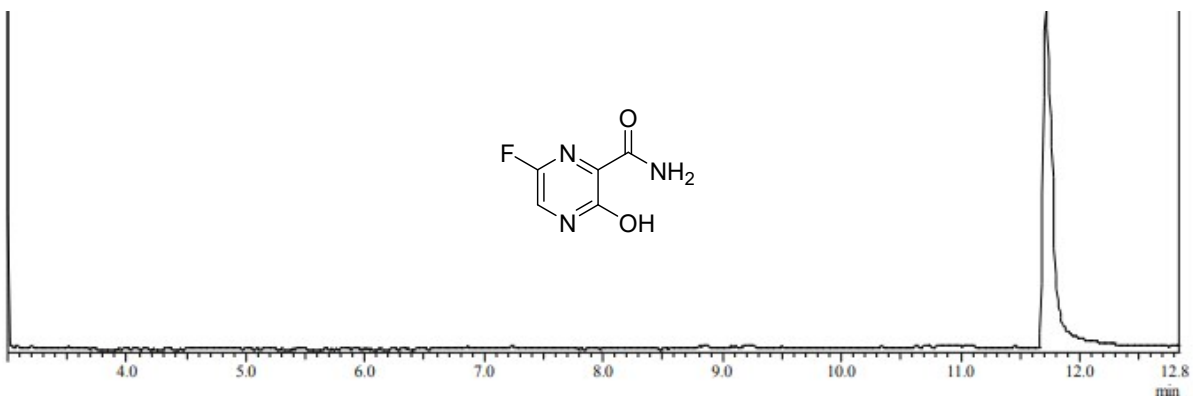
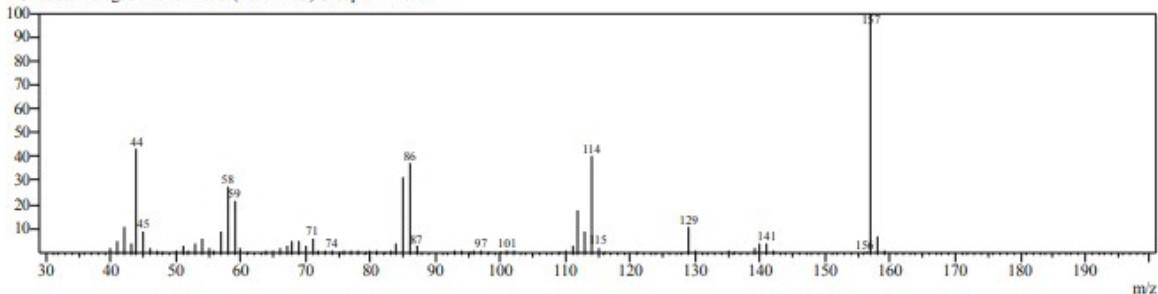


Figure S61. ^{19}F -NMR spectrum of favipiravir derived from fluorination of 3-hydroxypyrazine-2-carboxamide.



Spectrum

Line#:1 R.Time:11.717(Scan#:1047)
 MassPeaks:75
 RawMode:Averaged 11.558-12.033(1028-1085) BasePeak:157(27940)
 BG Mode:Averaged 11.925-12.767(1072-1173) Group 1 - Event 1



Mass Table
 Line#:1 R.Time:11.717(Scan#:1047)
 MassPeaks:75

RawMode:Averaged 11.558-12.033(1028-1085) BasePeak:157(27940)
 BG Mode:Averaged 11.925-12.767(1072-1173) Group 1 - Event 1

#	m/z	Abs. Int.	Rel. Int.	#	m/z	Abs. Int.	Rel. Int.	#	m/z	Abs. Int.	Rel. Int.
1	40.00	517	1.85	22	64.00	108	0.39	43	85.00	8841	31.64
2	41.00	1212	4.34	23	64.95	260	0.93	44	86.00	10458	37.43
3	42.00	2862	10.24	24	66.00	362	1.30	45	87.00	629	2.25
4	43.00	1081	3.87	25	67.00	741	2.65	46	93.00	57	0.20
5	44.00	12023	43.03	26	68.00	1243	4.45	47	94.00	73	0.26
6	45.00	2435	8.72	27	68.95	1337	4.79	48	95.00	28	0.10
7	46.00	566	2.03	28	70.00	747	2.67	49	96.00	109	0.39
8	47.00	213	0.76	29	71.00	1554	5.56	50	97.00	121	0.43
9	48.00	36	0.13	30	72.00	100	0.36	51	98.00	31	0.11
10	50.05	172	0.62	31	73.00	279	1.00	52	100.00	28	0.10
11	51.00	630	2.25	32	74.00	295	1.06	53	101.00	172	0.62
12	52.00	260	0.93	33	75.00	33	0.12	54	102.00	118	0.42
13	53.00	1002	3.59	34	76.00	58	0.21	55	109.00	29	0.10
14	54.00	1632	5.84	35	77.00	294	1.05	56	110.05	52	0.19
15	55.00	452	1.62	36	78.00	191	0.68	57	111.00	786	2.81
16	56.05	116	0.42	37	79.00	31	0.11	58	112.00	4998	17.89
17	57.00	2522	9.03	38	80.00	90	0.32	59	113.00	2363	8.46
18	58.00	7666	27.44	39	81.00	58	0.21	60	114.00	11126	39.82
19	59.00	6053	21.66	40	82.00	41	0.15	61	115.00	589	2.11
20	59.95	556	1.99	41	83.00	252	0.90	62	116.00	41	0.15
21	61.00	39	0.14	42	84.00	972	3.48	63	121.00	40	0.14
#	m/z	Abs. Int.	Rel. Int.	#	m/z	Abs. Int.	Rel. Int.	#	m/z	Abs. Int.	Rel. Int.
64	129.00	2831	10.13	68	139.05	384	1.37	72	156.05	42	0.15
65	130.05	164	0.59	69	140.00	999	3.58	73	157.05	27940	100.00
66	135.05	53	0.19	70	141.00	1030	3.69	74	158.05	1969	7.05
67	136.00	29	0.10	71	142.00	110	0.39	75	159.00	170	0.61

Figure S62. Chromatogram, EI-MS spectrum of favipiravir derived from fluorination.

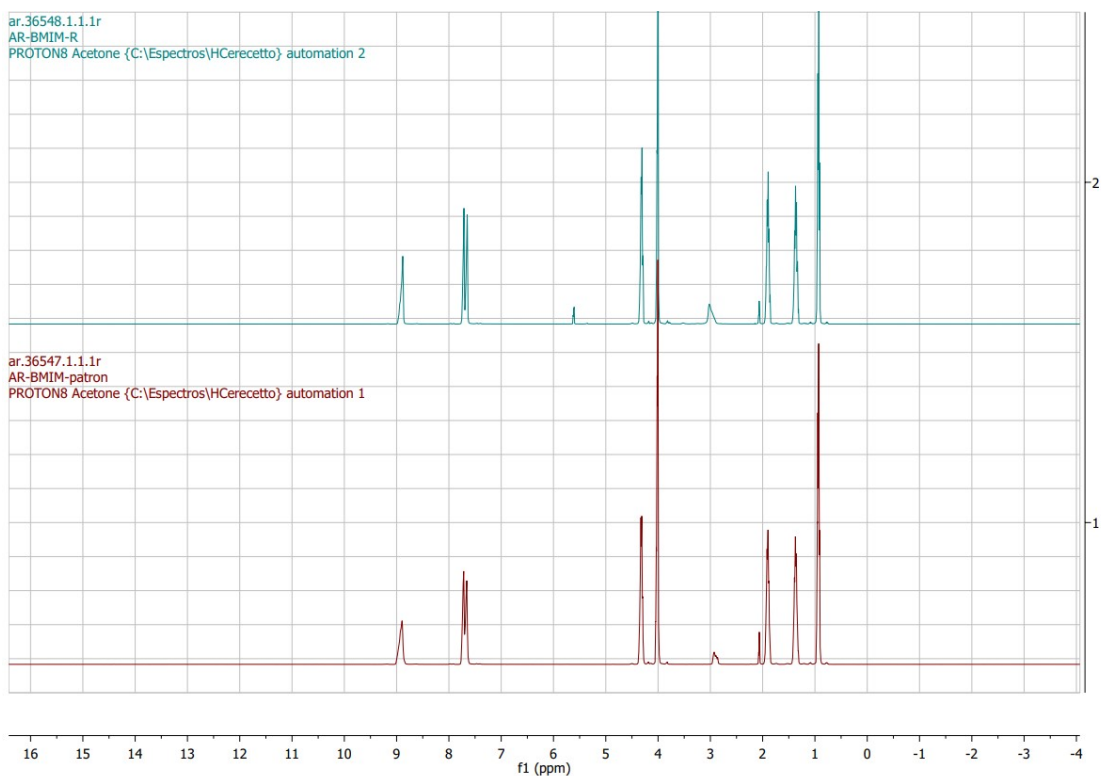


Figure S62. Superposition of ^1H -NMR spectra of commercial $\text{BF}_4\text{-BMIM}$ (red spectrum) with that derived from the reaction after two reactions (blue spectrum).

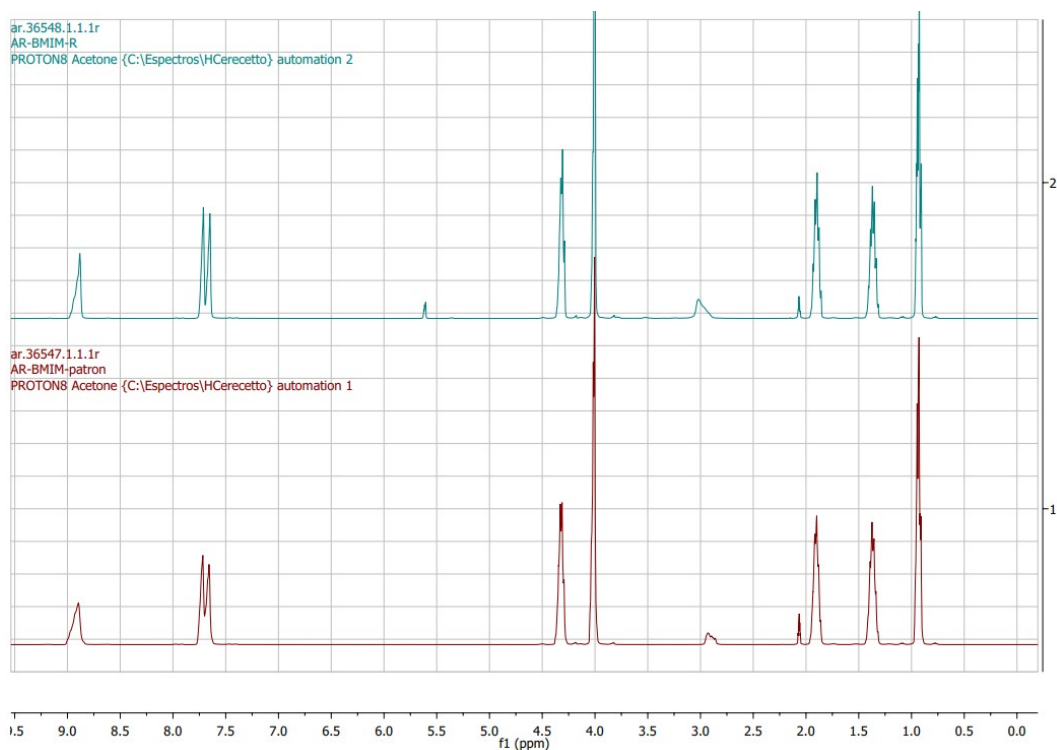


Figure S63. Amplification of superposed ^1H -NMR spectra of commercial $\text{BF}_4\text{-BMIM}$ (red spectrum) with that derived from the reaction after two reactions (blue spectrum).

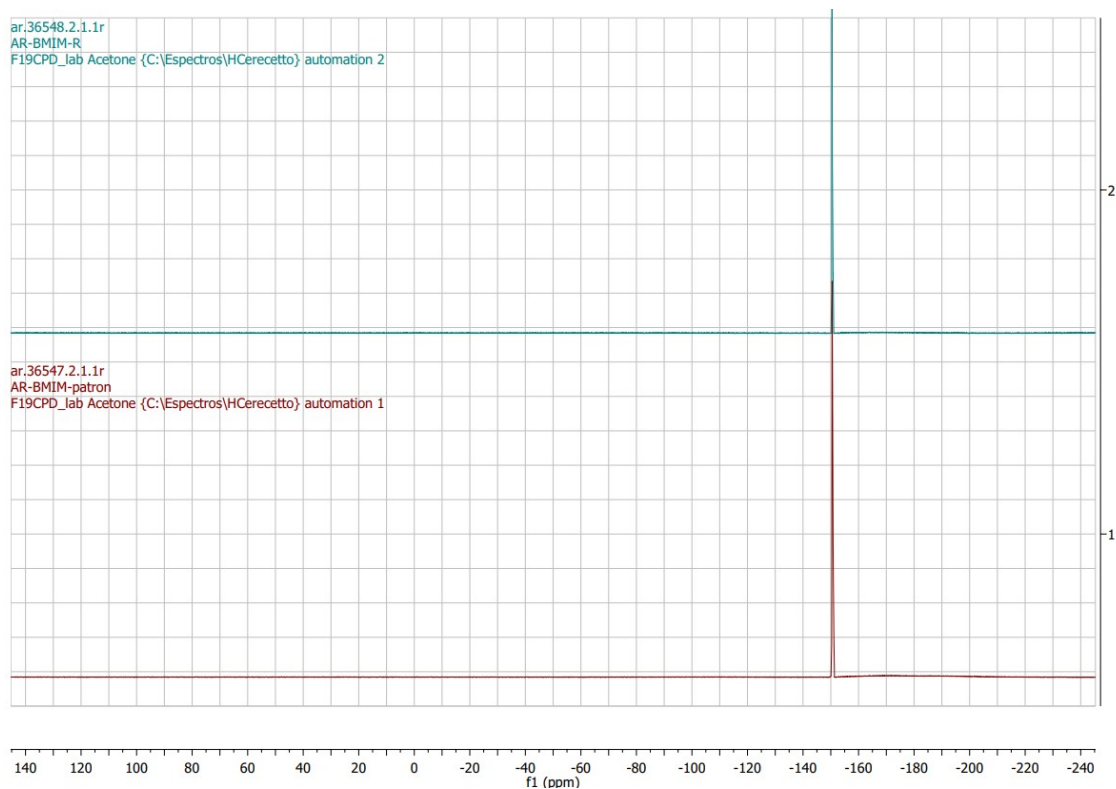


Figure S64. Superposition of ^{19}F -NMR spectra of commercial $\text{BF}_4\text{-BMIM}$ (red spectrum) with that derived from the reaction after two reactions (blue spectrum).

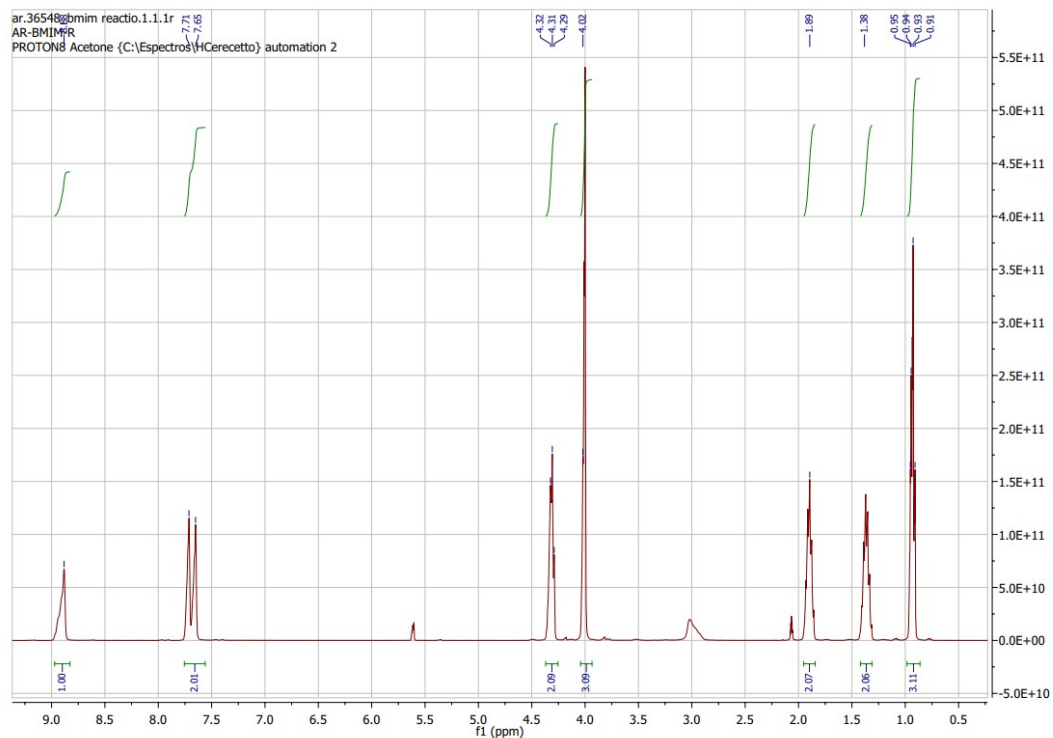


Figure S65. Complete ^1H -NMR spectrum of $\text{BF}_4\text{-BMIM}$ derived from the reaction after two reactions.

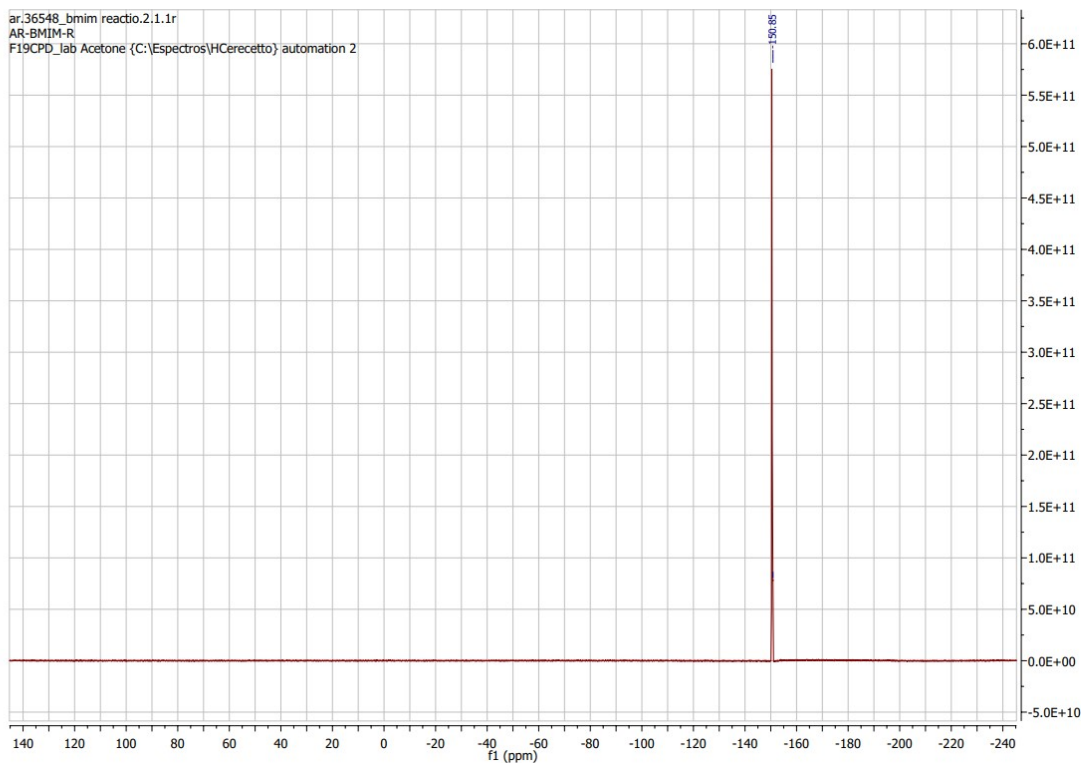


Figure S66. Complete ^{19}F -NMR spectrum of $\text{BF}_4\text{-BMIM}$ derived from the reaction after two reactions.

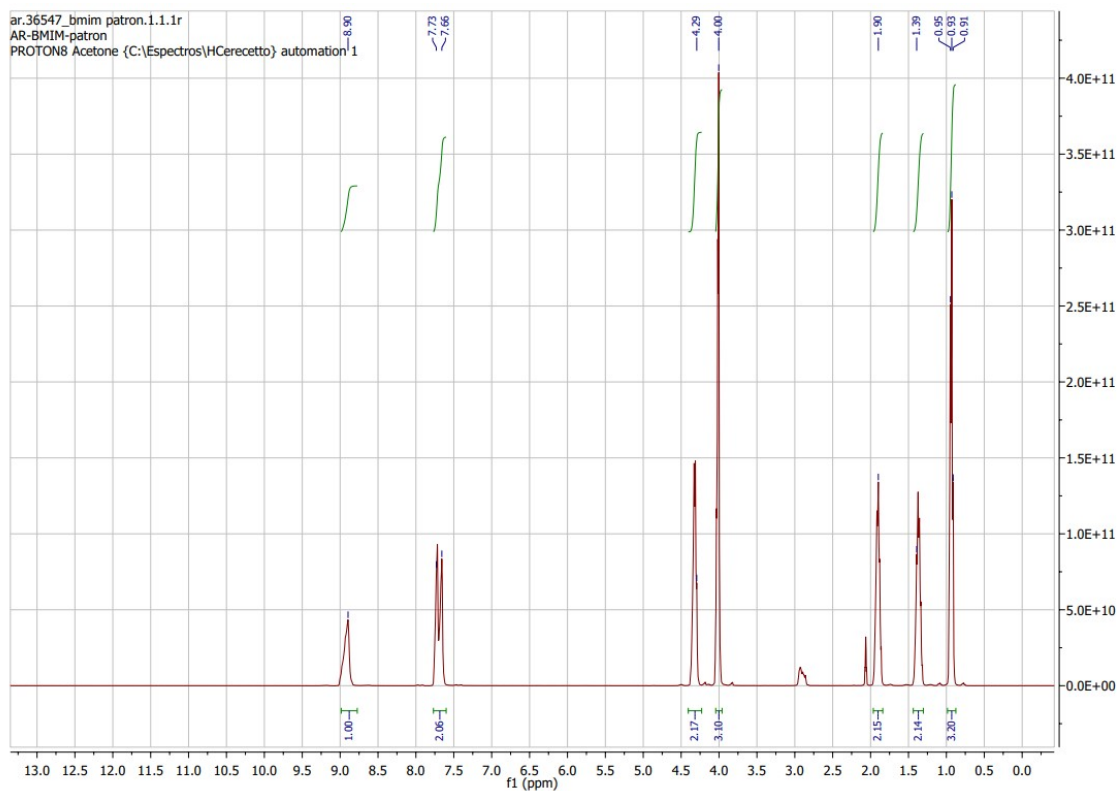


Figure S67. Complete ^1H -NMR spectrum of commercial $\text{BF}_4\text{-BMIM}$.

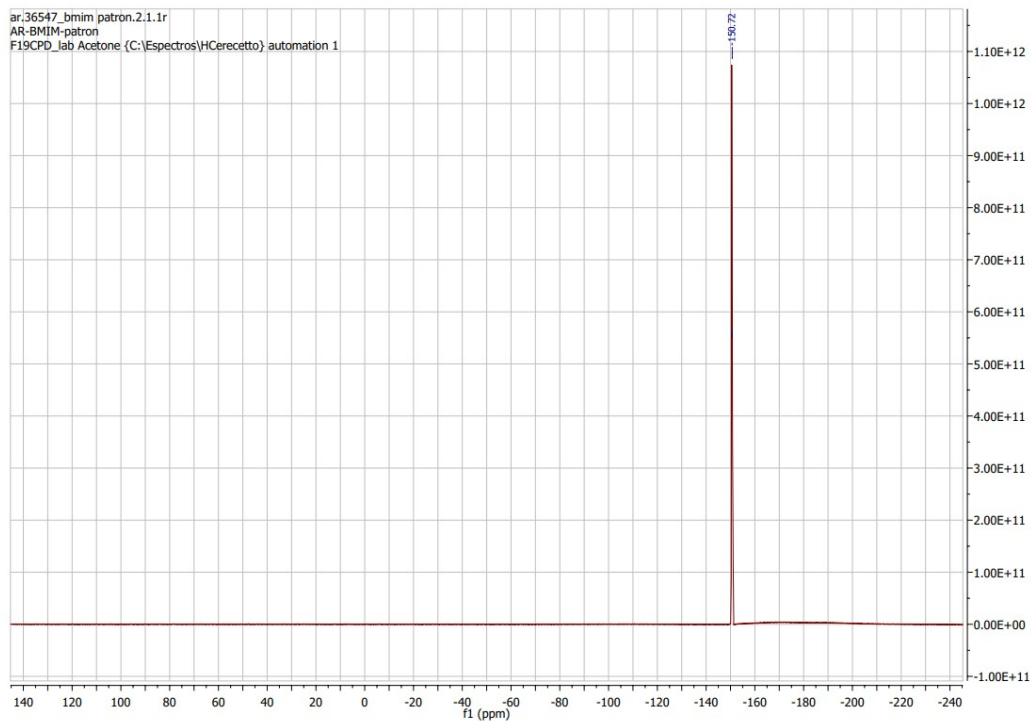


Figure S68. Complete ^{19}F -NMR spectrum of commercial $\text{BF}_4\text{-BMIM}$.

Sub-product self-addition 9

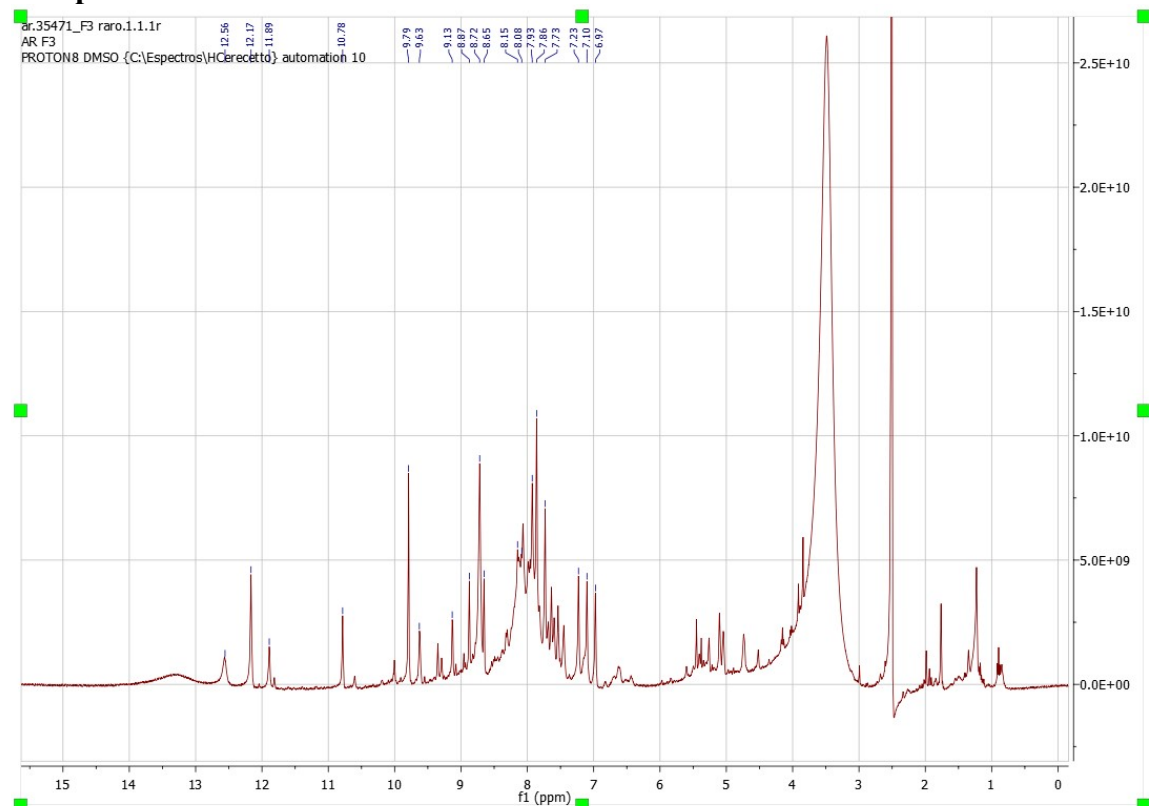


Figure S69. ^1H -NMR spectrum for “self-addition sub-product” **9** (Scheme 4A), collected after purification as last insoluble fraction derived from reaction.

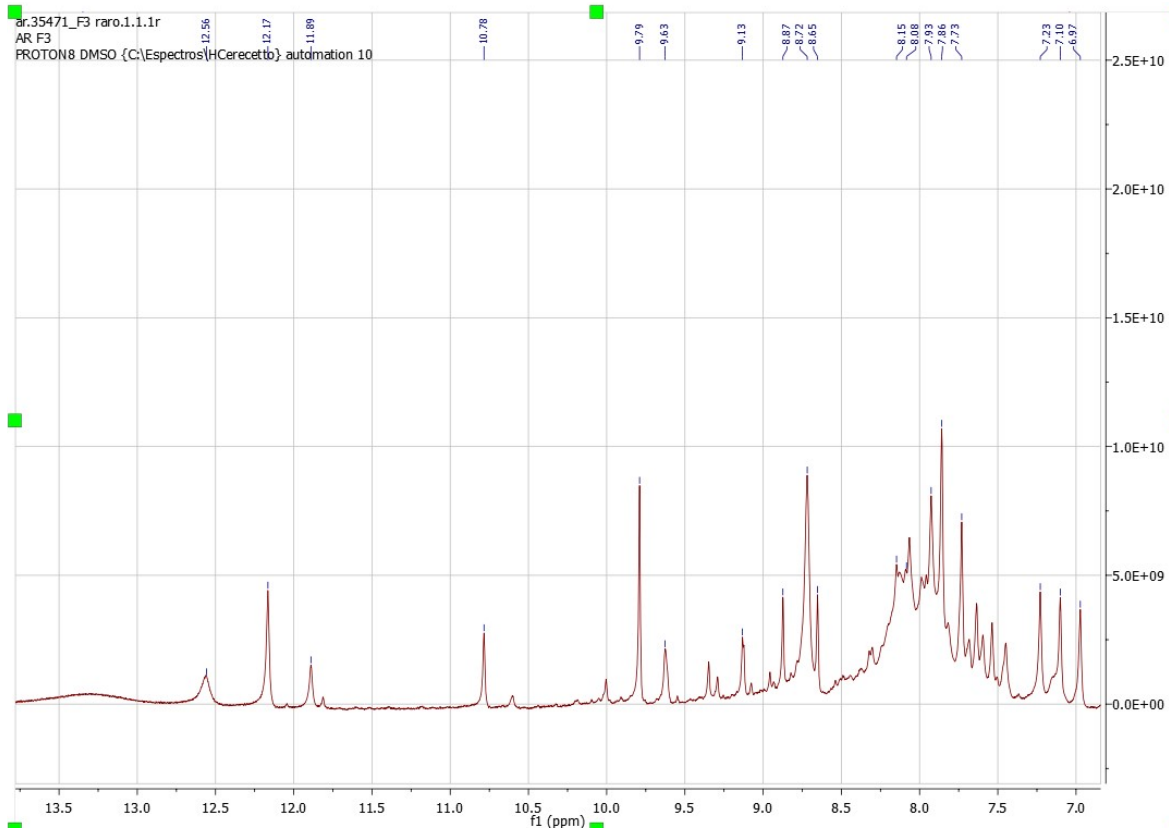


Figure S70. ^1H -NMR spectrum for “self-addition sub-product” **9** (Scheme 4A), collected after purification as last insoluble fraction derived from reaction (Ampliation aromatic zone).

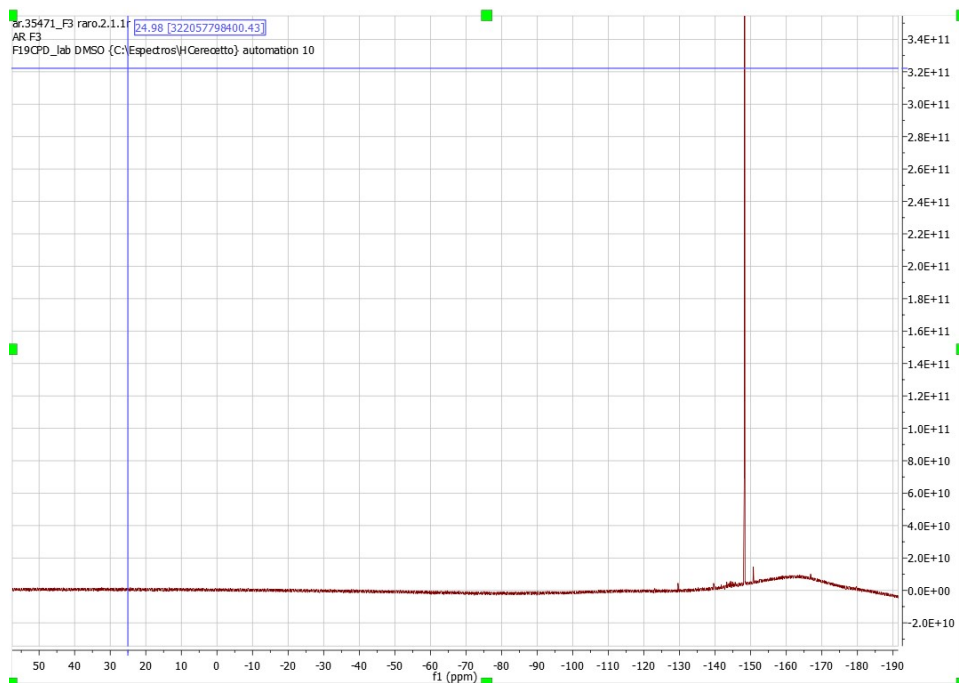


Figure S71. ^{19}F -NMR spectrum fluoride anion (-124 ppm) and “HF” (-168 ppm), collected after purification as last insoluble fraction derived from reaction.

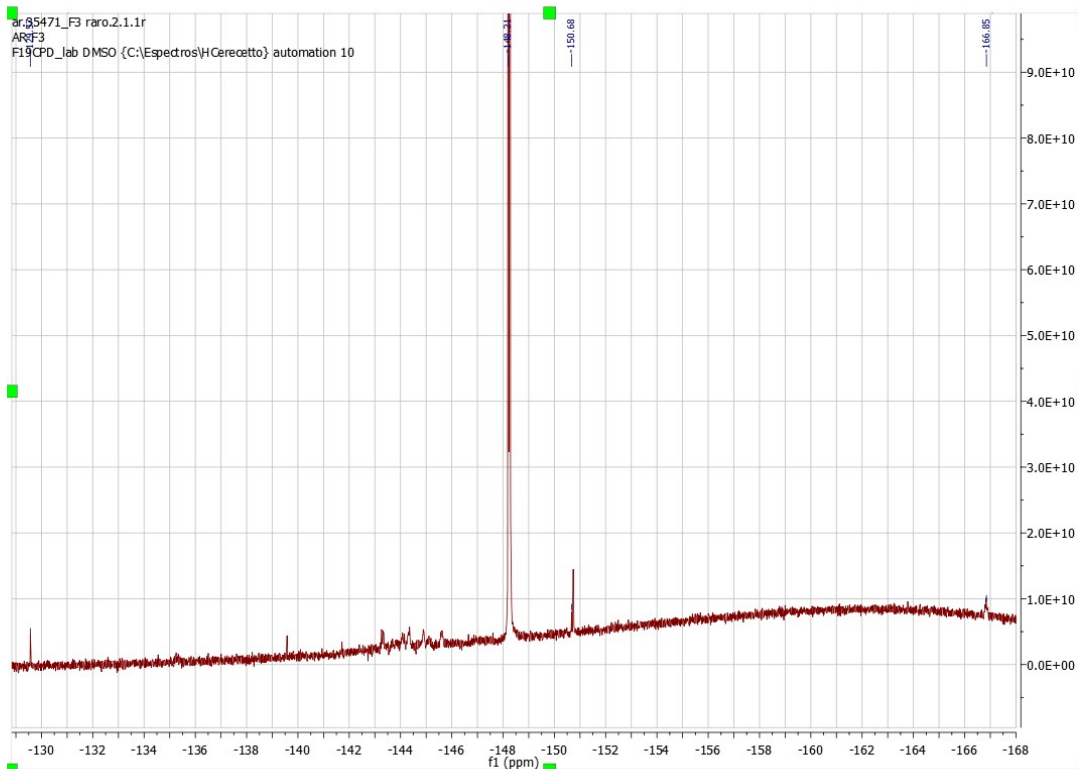


Figure S72. Ampliation of ^{19}F -NMR spectrum for “self-addition sub-product” **9** (Scheme 4A), collected after purification as last insoluble fraction derived from reaction. Traces of fluoride at -129 ppm and other fluorinated sub-product in traces (-143 to -145 ppm). The self-addition sub-product containing fluorine, that can be derived from **9**, are found in traces.

5. References

- [1] De Savi, C.; Hughes, D.L.; Kvaerno, L. Quest for a COVID-19 Cure by Repurposing Small-Molecule Drugs: Mechanism of Action, Clinical Development, Synthesis at Scale, and Outlook for Supply. *Org. Process Res. Dev.* **2020**, *24*, 940-976.
- [2] Furuta, Y.; Egawa, H. Nitrogenous Heterocyclic Carboxamide Derivatives or Salts Thereof and Antiviral Agents Containing Both. WO 2000/010569, March 2, 2000.
- [3] Furuta, Y.; Hiroyuki, E.; Nomura, N. Nitrogen-Containing Heterocyclic Carboxamide Derivatives or Salts Thereof and Antiviral Agents Comprising the Same. US 2002/0013316 A1, January 31, 2002.
- [4] Furuta, Y.; Hiroyuki, E.; Nomura, N. Nitrogen-Containing Heterocyclic Carboxamide Derivatives or Salts Thereof and Antiviral Agents Comprising the Same. US 6,787,544 B2, September 7, 2004.
- [5] Egawa, H.; Furuta, Y.; Sugita, J.; Uehara, S.; Hamamoto, S.; Yonezawa, K. Novel Pyrazine Derivatives or Salts Thereof, Pharmaceutical Compositions Containing the Derivatives or the Salts and Intermediates for the Preparation of Both. WO 2001/060834, August 23, 2001.

- [6] Hara, H.; Norimatsu, N.; Kurushima, H.; Kano, T. Method for Producing Dichloropyrazine Derivative. US 2011/0275817 A1, November 10, 2011.
- [7] Zheng, J.; Zhang, T.; Liu, C.; Feng, B.; Li, Z. Preparation of 6-Fluoro-3-hydroxy-2-pyrazinamide. CN 102775358, November 14, 2012.
- [8] Zhang, T.; Kong, L.; Li, Z.; Yuan, H.; Xu, W. Synthesis of Favipiravir. *Chin. J. Pharm.* **2013**, *44*, 841-844.
- [9] Guo, Q.; Xu, M.; Guo, S.; Zhu, F.; Xie, Y.; Shen, J. The Complete Synthesis of Favipiravir from 2-Aminopyrazine. *Chem. Pap.* **2019**, *73*, 1043-1051.
- [10] S.M. Megahed, A.A. Habib, S.F. Hammad, A.H. Kamal, *Spectrochimica Acta Part A: Molecular and Biomolecular Spectroscopy*, **2021**, *249*, 119241.
- [11] Method for producing 3-hydroxy-2-pyrazinecarboxamide, JP 5739618 B2, 2015.6.24, Toyama Chemical Co Ltd.
- [12] Moorthy, J.N.; Singhal, N. Facile and Highly Selective Conversion of Nitriles to Amides via Indirect Acid-Catalyzed Hydration Using TFA or AcOH-H₂SO₄. *J. Org. Chem.* **2005**, *70*, 1926-1929.
- [13] Dong, T.; Tsui, G.C. Construction of Carbon-Fluorine Bonds via Copper-Catalyzed/-Mediated Fluorination Reactions. *Chem. Rec.* **2021**, *21*, 4015-4031.
- [14] Hua, A.M.; Bidwell, S.L.; Baker, S.I.; Hratchian, H.P.; Baxter, R.D. Experimental and Theoretical Evidence for Nitrogen-Fluorine 2 Halogen Bonding in Silver-Initiated Radical Fluorinations. *ACS Catal.* **2019**, *9*, 3322-3326.
- [15] Lal, G.S.; Pastore, W.; Pesaresi, R. A Convenient Synthesis of 5-Fluoropyrimidines Using 1-(Chloromethyl)-4-fluoro-1,4-diazabicyclo[2.2.2]octane Bis(tetrafluoroborate)-SELECTFLUOR® Reagent. *J. Org. Chem.* **1995**, *60*, 7340-7342.
- [16] Price, D.A.; James, K.; Osborne, S.; Harbottle, G.W. Selective fluorination of 1-hydroxyisoquinolines using Selectfluor®. *Tetrahedron Lett.* **2007**, *48*, 7371-7373.
- [17] Vincent, S.P.; Burkart, M.D.; Tsai, C.Y.; Zhang, Z.; Wong, C.Y. Electrophilic Fluorination-Nucleophilic Addition Reaction Mediated by Selectfluor®: Mechanistic Studies and New Applications. *J. Org. Chem.* **1999**, *64*, 5264-5279.
- [18] Unpublished results, which are currently under revision.